Chair of Hydrology

University of Freiburg

INFLUENCE OF VEGETATION ON PRECIPITATION PARTITIONING AND ISOTOPIC COMPOSITION IN NORTHERN UPLAND CATCHMENTS

Hannah Braun

Master's Thesis

Supervisor: Prof. Dr. Markus Weiler

Co-Supervisor: Prof. Dr. Doerthe Tetzlaff

Aberdeen, December 2015

DECLARATION/ EHRENWÖRTLICHE ERKLÄRUNG

This master's thesis is the result of my own work and I hereby confirm that I worked independently and only with the use of aids indicated.

Hiermit versichere ich ehrenwörtlich, dass die folgende Arbeit selbstständig und nur unter Verwendung der angegebenen Hilfsmittel erstellt wurde.

Place, Date: Aberdeen, December 2015 Signed: _____________________

Hannah Braun

ABSTRACT

In this study field experiments in a northern high latitude headwater catchment in the Scottish Highlands were undertaken to investigate the importance of vegetation cover on water partitioning and isotopic composition. A total of 75 throughfall (TF) collectors and 10 stemflow (SF) collectors were established to guaranty a dense TF monitoring at four sub-sites under varying vegetation and aspect. Differences in both, quantity and isotopic composition of TF and SF under two Scots pine (*Pinus sylvestris*) plantations and two heather (*Calluna vulgaris*) sites were investigated and a direct comparison between the north and south facing slopes and within the sites was presented. During the field season, weekly TF samples were taken (>1100) and analysed for stable isotopes $\delta^{18}O$ and $\delta^{2}H$. Interception losses were 38% under heather and up to 47% for the plantation sites. Both TF and SF amounts were found to be highly variable and were mostly governed by gross rainfall (GR), canopy coverage and wind speed. TF was the dominant canopy pathway and SF only accounted for 1.0% to 2.5% of GR inputs. The isotopic signal was found to be complex and variable between the sites, however, the mainly influencing factor was the isotopic composition of GR.

Keywords: precipitation partitioning, throughfall, stemflow, vegetation effects, forest hydrology, variability in throughfall and stemflow, Bruntland Burn, Interception loss, net rainfall

EXTENDED ABSTRACT

Diese Studie befasst sich mit den Auswirkungen von Vegetationsbedeckung (Kronenschluss) auf die räumlich-zeitliche Variabilität von Bestandesniederschlag (TF) und Stammabfluss (SF) sowohl in Quantität als auch in der Isotopenzusammensetzung. Die Geländearbeit wurde in einem Kopfeinzugsgebiet der Schottischen Highlands durchgeführt. Insgesamt wurden 75 Bestandesniederschlagssammler und 10 Stammabflussbehälter auf vier, sich in Vegetationstyp und Exposition unterscheidenden Untersuchungsflächen im Einzugsgebiet installiert. Somit konnten die direkten Unterschiede in TF und SF zwischen zwei Waldkieferplantagen (*Pinus sylvestris*) und zwei Heidekraut Flächen (*Calluna vulgaris*) über einen Zeitraum von vier Monaten untersucht werden. Bestandesniederschlag und SF wurden während des gesamten Zeitraums wöchentlich gemessen und es wurden insgesamt über 1100 Isotopenproben entnommen, welche auf die stabilen Isotope $\delta^{18}O$ und $\delta^{2}H$ untersucht wurden. Interzeptionsverluste waren mit bis zu 38% im Heidekraut und bis zu 47% in den Kiefernplantagen relativ hoch. Es konnte gezeigt werden, dass sowohl TF sowie SF räumlich und zeitlich sehr variabel sind und hauptsächlich von Nettoniederschlagsmenge, Windgeschwindigkeit und Kronenschluss beeinflusst wurden. Der gemessene SF lag, mit 1.0% bis 2.5%, im niedrigen Bereich. Unterschiede in der Isotopenzusammensetzung von TF, SF und Nettoniederschlag waren komplex und zeitlich sehr variabel und wurden vor allem durch die Isotopensignatur des ankommenden Nettoniederschlags geprägt.

Stichwörter: Wasserverteilung, Bestandesniederschlag, Stammabfluss, Einfluss von Vegetation, Forsthydrologie, Variabilität von Bestandesniederschlag und Stammabfluss, Bruntland Burn, Interzeptionsverluste, Nettoniederschlag

Acknowledgements

First of all, I would like to thank my supervisors Prof. Dr. Doerthe Tetzlaff and Prof. Dr. Markus Weiler as well as Prof. Dr. Chris Soulsby for providing this interesting research topic and their guidance and support throughout the study.

A special thanks to Dr. Marjolein van Huijgevoort for valuable assistance in planning and installing the field equipment as well as Dr. Jon Dick for his expertise and support in analysing the isotope samples.

I would also like to thank my fellow students Bernhard Scheliga, Claire Tunaley and Daniel Günther for discussions, encouragement and help with sampling on numerous field days. Lastly, I want to thank my family and friends for supporting me throughout my studies.

CONTENTS

LIST OF TABLES

LIST OF FIGURES

List of Abbreviations and Acronyms

Abbreviation	*Description*
^{o}	Degrees
°C	Grad Celsius
cm	Centimetre
EMMAH	Mediterranean Environment and Agro-Hydro System Modelisation
FAO	Food and agriculture organization
GMWL	Global meteoric water line
GPS	Global Positioning System
h	Hours
Heather North F.	Heather north facing
Heather Soutfh F.	Heather south facing
HNF	Heather north facing
HSF	Heather south facing
Inc.	Incorporated
km^2	Square kilometre
l	Litre
LGR1A	Standard 1 produced by Los Gatos
LGR2A	Standard 2 produced by Los Gatos
LGR3A	Standard 3 produced by Los Gatos
LGR4A	Standard 4 produced by Los Gatos
LGR5A	Standard 5 produced by Los Gatos
LiDAR	Light detection and ranging
LMWL	Local meteoric water line
LR	Linear regression
m	Meter
Max	Maximum
Min	Minimum
ml	Millilitre
MLRM	Multiple linear regression model
mm	Millimetre
Plant North F.	Plantation north facing
Plant South F.	Plantation south facing
PNF	Plantation north facing
PSF	Plantation south facing

PVC	Polyvinylchloride
RGB	Red Green Blue
UKCP09	United Kingdom climate projections, 2009
VSMOW	Vienna standard mean ocean water

LIST OF SYMBOLS

Symbol	**Unit**	**Description**
δ	[-]	Change, difference
Δ	[-]	Change, difference
Δ_s	[kPa °C^{-1}]	Slope vapour pressure curve
^{18}O	[-]	Oxygen 18
^2H/D	[-]	Deuterium
a	[-]	Coefficient of the LMWL
b	[-]	Coefficient of the LMWL
$b_{0,1,n}$	[-]	Regression coefficients
$b_{0,1,n}$	[-]	Intercept or constant term
$b_{1,x}$	[-]	Slope, regression coefficient
BA	[m²]	Basal area of the stem
BHD	[cm]	Breast height diameter
C	[mm]	Canopy interception loss
C	[cm]	Circumference of a tree
CL	[mm]	Canopy loss
CV	[-]	Coefficient of variation
e_a	[kPa]	Actual vapour pressure
e_s	[kPa]	Saturation vapour pressure
e_s-e_a	[kPa]	Saturation vapour pressure deficit
ET	[mm]	Evapotranspiration
ET.Mean	[mm]	Mean evapotranspiration (for the sample periods)
ET_0	[mm day^{-1}]	Reference evapotranspiration
f.SF. Mean	[%]	Mean SF fraction
f.SF.CV	[%]	Coefficience of variance of SF amount
f.TF. Mean	[%]	Mean TF fraction
f.TF.CV	[%]	Coefficience of variance of TF fraction
G	[MJ m^{-2} day^{-1}]	Soil heat flux density
GR	[mm]	Gross rainfall/ gross precipitation

GR $\delta^{18}O$	[‰]	$\delta^{18}O$ composition of GR
GR $\delta^{2}H$	[‰]	$\delta^{2}H$ composition of GR
GR.Hours	[h]	Hours of rainfall
GR.M.Int	[mm h^{-1}]	Maximum intensity of GR
GR.Sum	[mm]	Summarized rainfall (for the sample periods)
I	[mm]	Interception loss
lc-excess	[‰]	Line conditioned excess
N	[-]	Number of samples
NP	[mm]	Net precipitation
p	[-]	p-value
P_1	[mm]	Amount of first sample to be weighted
P_2	[mm]	Amount of second sample to be weighted
P_n	[mm]	Amount of sample to be weighted
P-value	[-]	Probability of obtaining a result
q.SF.CV	[%]	Coefficience of variance of SF amount
q.SF.Mean	[mm]	Quantity SF mean (mean SF amount)
q.TF.CV	[%]	Coefficience of variance of TF amount
q.TF.Mean	[mm]	Quantity TF mean (mean TF amount)
q.TF.mean	[mm]	mean TF fraction
q.TF.median	[mm]	median TF fraction
R	[-]	Correlation coefficient
R^2	[-]	Coefficient of determination
RH	[mm]	Humidity
RH.Mean	[%]	Mean humidity
Rn	[MJ m^{-2} day^{-1}]	Net radiation at the crop surface
s	[-]	Standard deviation of the samples
SF	[mm]	Stemflow/ Stammabfluss
Std.Dev.	[-]	Standard deviation
Std.Error	[%]	Standard error
T	[°C]	Mean daily air temperature at 2 m height
t	[-]	t-statistics, significance test of corresponding regressor
T.a	[°C]	Air temperature
T.a.Mean	[°C]	Mean air temperature
TF	[mm]	Throughfall /Bestandesniederschlag
TF fraction	[%]	TF as fraction of GR
TF.CV	[%]	Coefficient of variance of TF

TF.Mean	[mm]	Mean TF
TF.Median	[mm]	Median TF
U	[m s^{-1}]	Wind speed
U.D.Max	[m s^{-1}]	Maximum daily wind speed
U.Max	[m s^{-1}]	Maximum wind speed
U.Mean	[m s^{-1}]	Mean wind direction (for the sample periods)
u_2	[ms^{-1}]	Wind speed at 2 m height
WINDR	[°]	Wind direction (for the sample periods)
WINDR.Mean	[°]	Mean wind direction (for the sample periods)
$x_{1,2,n}$	[-]	Independent variables
y	[kPa $°C^{-1}$]	Psychrometric constant
Y	[-]	Dependent variable
α	[-]	fraction
$\delta^{18}O$ daily	[‰]	Daily $\delta^{18}O$ composition
$\delta^{18}O$ weighted	[‰]	Weighted $\delta^{18}O$
$\delta^{18}O$.TF.CV	[‰]	CV TF fraction
$\delta^{18}O$.TF.Mean	[‰]	Mean TF fraction
$\delta^{18}O$.TF.Median	[‰]	Median TF fraction
$\delta^{2}H$ daily	[‰]	Daily $\delta^{2}H$ composition
$\delta^{2}H$ weighted	[‰]	Weighted $\delta^{2}H$
δ2H.TF.CV	[%]	CV TF fraction
δ2H.TF.Mean	[‰]	Mean TF fraction
δ2H.TF.Median	[‰]	Median TF fraction
δX	[‰]	$\delta^{2}H$ or $d^{18}O$ of GR, TF or SF
δX1	[‰]	Isotopic composition of the first sample to be weighted
δX2	[‰]	Isotopic composition of the second sample to be weighted
δXn	[‰]	Isotopic composition of the last sample to be weighted

1 INTRODUCTION

Climate change is predicted to have far reaching implications for northern high latitude regions in the coming decades, including changing precipitation regimes and temperatures (Kundzewicz et al., 2007; Rennermalm et al., 2010; Capell et al., 2013). As vegetation communities are very responsive to those changes, they may adjust in composition, distribution and species which will lead to changing hydrological processes, e.g. release, storage and mixing of water in a catchment (Wookey et al., 2009). Many northern landscapes are already responding and experiencing those shifts with an expansion of shrub and tree cover (Tetzlaff et al., 2014). For example, in the Scottish Highlands, forest cover is increasing as a result of adaptive management and increased biofuel production (The Scottish Forest Strategy, 2006). In the wet, windy Scottish hydroclimate this has the potential to significantly increase interception losses, reduce net precipitation and affect the spatial and temporal distribution of soil moisture (Kundzewicz et al., 2007; Tetzlaff et al., 2013; Capell et al., 2013). Recent studies have also shown that such processes may also change the isotopic signature of throughfall and stemflow with implications for using isotopes as hydrological tracers. Such effects may be exacerbated by projected higher temperatures and reduced summer precipitation.

1.1 Literature Review

1.1.1 Vegetation Influences on Water Partitioning

Precipitation (incident rainfall or gross rainfall, GR) falling above a forest reaches the forest floor in various ways (Allen et al., 2015). It can either be intercepted by the canopy cover, evaporate (interception loss) or fall through gaps without interacting with the crown cover at all (Levia et al., 2011; Allen et al., 2014). Forest canopies can intercept high amounts of precipitation and are therefore not just changing the amount of water reaching the ground, but also the precipitation pattern, both spatially and temporally. These interactions have great influences on the hydrology and ecology of a catchment (Allen et al. 2014).

Interception is defined as the process where GR is delayed by the vegetation from where it is then redistributed, either as canopy drip, free throughfall, stemflow (SF), or evaporation (ET), (Figure 1-1) (Rowe and Hendrix, 1951; Levia et al., 2011). Throughfall (TF) is often considered as the sum of drip and free throughfall (David et al., 2005) and is defined as the amount of precipitation that falls through or drips from the canopy after interception or interaction with vegetation above the ground and diffusely reaches the forest floor (Levia et al., 2011). Free throughfall is the part of GR falling through gaps and open areas, reaching the ground without interacting with the canopy cover (Rutter et al., 1971; David et al., 2005). Stemflow is the amount of GR that is funnelled down to the bole or stem of a plant after interception by leaves and branches (Levia et al., 2011); it reaches the ground as a point input (further described under *Stemflow*) (Bialkowsky and Buttle, 2015).

TF and SF together usually form about 70 to 90% of the GR and are highly important in forest environments. The remaining 10% to 30% are lost via interception. Intercepted rainfall is temporarily stored in the canopy from where it is either evaporated or sublimated, depending if the input precipitation is falling as rain or as snow (Levia and Frost, 2003). Interception can cause a major reduction in GR (Molina and del Campo, 2011) and it is a well-researched process depending on several variables that are related to forest type, structure and the climatic conditions (Crockford and Richardson, 2000; David et al., 2011). Several studies investigated this topic over recent years e.g. Bosch and Hewlett (1982); Brown et al. (2005); Llorens and Domingo (2007); Molina and del Campo (2011). These studies have shown that interception losses of liquid precipitation can vary widely ranging from about 6% to 60% (Crockford and Richardson, 2000; David et al., 2011). The amount of rain that actually reaches the floor is called net precipitation (NP) and is the sum of TF and SF (Crockford and Richardson, 2000).

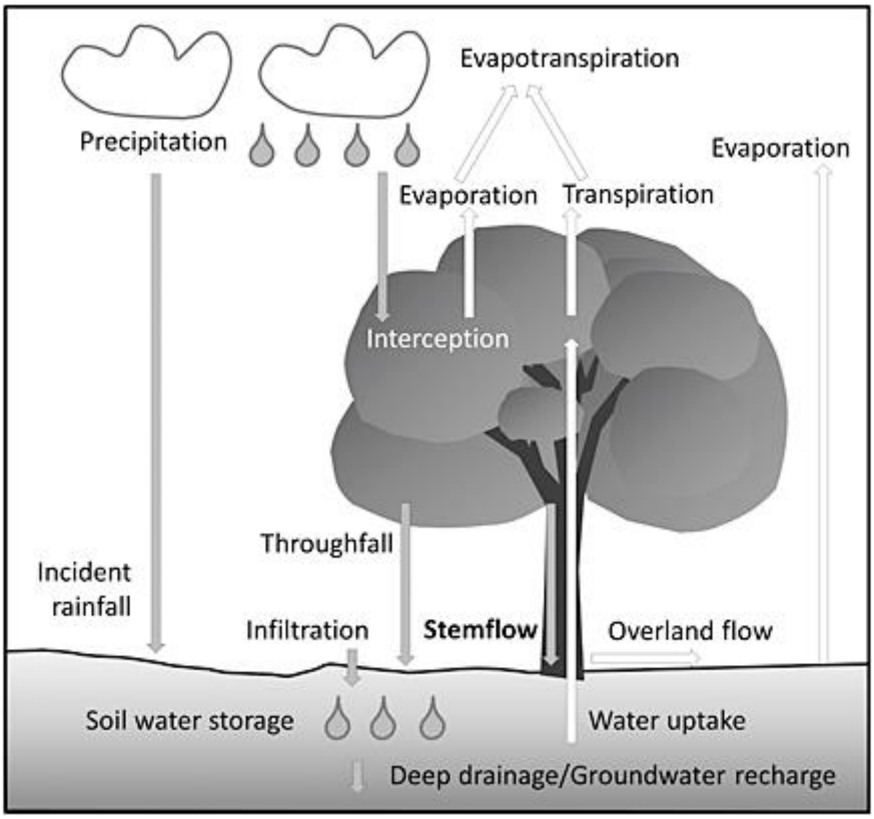

Figure 1-1: The hydrologic cycle of a wooded ecosystems (Levia & Germer, 2015). Precipitation can interact with the canopy cover (interception) where it either evaporates or reaches the ground as throughfall or stemflow.

The canopy cover is defined by the area of forest floor covered by a tree's crown, foliage and branches and, if measured for a distinct sample point, refers to the area vertically above (Jennings et al., 1999). Due to its importance on water partitioning, various environmental applications are dependent on canopy cover and density measurements. These parameters can be either derived by airborn Light Detection and Ranging (LiDAR) data, where the ratio of vegetation versus ground cover is estimated, or through hemispherical photography (Moeser et al., 2014). The amount of water that is temporarily stored on the external surfaces is referred to as the canopy storage.

Throughfall

Precipitation redistribution over wooded ecosystems is affected by different factors. Due to its effects on interception loads, canopy storage, evaporation fluxes and distinct geometries the vegetation type can profoundly influence the ecosystems water balance, soil moisture dynamics and recharge pattern. Climatic factors also influence fluxes like interception and TF (Crockford and Richardson, 2000). Altitude and exposure to wind and precipitation are strongly correlated with topography. In a study of Hofhansl et al. (2011), topography affected TF rate as it increased in higher elevations.

Studies from Perry (1994) and Parker (1995) showed that the structure of the canopy – accounting for tree branches, boles and foliage – has a great influence on ecological and biophysical processes. Thus, TF quantities are mainly dependent on GR amounts (Rutter, 1963), the ecosystem's canopy cover and existence of foliage (Reynolds and Henderson, 1967). Rutter et al. (1971) stated, that free throughfall is the most important component in small storm events. Canopy drip becomes more important when GR amount and intensity increase and the canopy is fully saturated (Rutter et al., 1971). The heterogeneity and spatial variability of TF can affect the soil wetting pattern, soil water distribution and the recharge (R) (Guswa and Spence, 2012). Some studies found that overland flow and surface erosion were also affected by the spatiotemporal variability of TF (Nanko et al., 2008; Mizugaki et al., 2010). The heterogeneity of TF amount decreases with increasing GR (Bouten et al., 1992). Staelens et al. (2006) stated that there is a higher variability in TF distribution for precipitation events with low intensities due to the initial interception loss in the canopy cover. Parts of the canopy remain unsaturated, and thus, there will be no TF in such areas (Levia et al., 2011). Herwitz and Slye (1995) found that the spatial variability of TF is also influenced by wind speed, as wind can change the behaviour of precipitation in the canopy cover. Higher wind speeds increase the wind speed variability within the tree crown and preferential deposition patterns of precipitation are the result.

From the canopy, the water either evaporates or, when storage capacity is exceeded or other factors, e.g. wind, disturb the equilibrium state and decrease the water storage, drains to the ground (Levia et al., 2011). Throughfall can reach a 100% of the GR in open areas without canopy cover, depending on event intensity and wind condition (Carlyle-Moses and Price, 2007). Herwitz and Slye (1995) found out, that variations in TF volume are also driven by rain angle.

Interception losses, TF and SF amounts for forests and ground cover like shrubs, grass and crops are extremely variable. However, this was not addressed by many studies in the past. Llorens and Domingo (2007) stated, that trees generally have higher TF rates and a lower SF rate than shrubs. Heather (*Calluna vulgaris*) is the dominant vegetation in large areas in Great Britain and therefore plays an important role. In a study of Miranda et al. (1983), evaporation loss of intercepted water for heather was high and comparable to those rates of much taller vegetation. From a hydrological perspective, shrubs and their morphological characteristics play an important role in controlling and modifying evaporation and precipitation redistribution in many catchments (Domingo et al., 1998; Zhang et al., 2015). However, studies investigating TF and SF patterns of shrubs are very rare (Zhang et al., 2015). Zhang et al. (2015) investigated TF and SF for different shrubs during the growing season in a revegetated desert in the northwest of China and found that air temperature, humidity and wind speed didn't show significant correlations with precipitation partitioning in the shrubs.

As the canopy interception loss (C) cannot be measured directly, it can be calculated subtracting TF and SF from the gross precipitation (Helvey and Patric, 1965). An accurate assessment of interception losses on event basis is difficult. It is easier to measure the factors affecting interception losses on seasonal or periodic basis (Crockford and Richardson, 2000). In a study by Crockford and Richardson (2000) it was found that similar rainfall values and event size distributions had different interception losses. They suggested that additional variables and not only location of the forest, slope, aspect, exposure to wind and climatic variables might have major influences.

Stemflow

In Many studies SF is not often taken into account due to its minor relative contribution (Ikawa et al., 2011). However, studies like Levia and Frost (2003) and Ikawa et al. (2011) pointed out that SF is potentially an important factor for groundwater recharge and nutrient supply. SF generation is very variable, even within the same species, and has the potential to influence multiple abiotic and biotic factors (Levia et al., 2011). Several studies state that increasing precipitation leads to an increasing amount of SF (e.g. Clements, 1972; André et al. 2008). However, SF is mainly affected by precipitation type, wind speed, wind direction, and storm characteristics such as magnitude, duration and intensity (Herwitz and Slye, 1995; Xiao et al., 2000; Levia et al., 2011). Wind speed (U) and wind direction (WINDR) not only influence isolated trees (Xiao et al., 2000) but also trees in forests (Kuraji et al., 2001). Higher wind speeds increase SF by wetting a higher part of the crown. Storms with one dominant wind direction lead to precipitation preferentially wetting one side of the tree, and are able to generate SF before reaching the total interception storage capacity of the canopy, whereas trees in a wind shadow or sheltered from the dominant wind direction may not produce any SF during that event (Levia et al., 2011).

SF yield generally increases with increasing trunk diameter and crown area (Crockford and Richardson, 2000; Park and Hattori, 2002). Among the biotic factors that affect SF production, the tree species is by far the most critical one. Species and age often govern branch geometry, contributing surface area, leaf shape and orientation and bark morphology (Crockford and Richardson, 2000; Levia and Frost, 2003). Tree species with rougher bark need a higher threshold to produce SF as the bark's water storage capacity and resistance to allow water flowing along the stem are higher (Voigt, 1960; Crockford and Richardson, 2000; Carlyle-Moses and Price, 2006; Levia et al., 2011). SF contribution to the soil is also higher when tree branches have a steep inclination angle, as intercepted precipitation is less likely to be lost as TF (Herwitz, 1987). This might be one major reason why SF contribution is very different between deciduous and coniferous trees as branching angles normally vary with species (Levia et al., 2011).

Forest characteristics such as stand density can also influence SF generation. Gaps in the canopy cover of sparse stands can increase SF generation as more of the rainfall reaches the contributing area (Ford and Deans, 1978). The opposite effect can occur in dense forest stands where rain-shadowing effects can lead to less wetting of the contributing area and decrease SF generation (Herwitz and Slye, 1995). Larger trees with a higher projected surface area usually have a greater SF generation (Ford and Deans, 1978). However, despite greater crown size, SF amounts can also decrease with aging of trees as the bark roughness increases (Johnson, 1990). Experiments with simulated vertical rainfall showed that most of the SF (98%) was generated in the upper half of the canopy. Nevertheless, lower and better sheltered branches are still important for rainfall driven by wind and falling at different angles (Hutchinson and Roberts, 1981). Ford and Deans (1978) found that rainfall intensity is an important factor driving SF generation. Whereas low intensity events mainly evaporate off the canopy, high intensities can lead to a point where no additional water can be funnelled down the stem as canopy and stem are saturated and water drips off. They observed, that for trees with rough bark (e.g, Scots Pine) SF remained constant during intense events whereas the TF fraction increased. However, if rain mainly falls from one direction and does not wet the whole stem, SF can be produced even though the storage capacity of the whole tree is not exceeded (Crockford et al., 1996).

Cape et al. (1991) found in an interspecies comparison of TF and SF that 15% of the non-intercepted precipitation reaching the forest floor was SF which was more enriched in solutes and might be also important concerning transfer of nutrients and pollutants. SF might influence the heterogeneity of the soil wetting pattern in a greater way than TF as water is infiltrating in a narrow area around the tree’s stem (Levia and Frost, 2003).

1.1.2 Isotopic Composition

Stable isotopes, e.g. deuterium (^2H or D) and oxygen 18 (^{18}O) are commonly used as conservative environmental tracers to track the movement of water in catchments all over the world (Kendall, 1998; Makoto et al., 2000). The isotopes ^2H and ^{18}O are expressed as $\delta^{18}O$ and δ^2H, as parts per million in the standard notation and are related to a standard value, the V-standard mean ocean water (Craig, 1961; Tetzlaff et al., 2014).Transit times (Tetzlaff et al., 2011), the sources of stream water (Welker, 2000; Dutton et al, 2005), plant water sources (Goldsmith et al., 2012), groundwater recharge and other parts of the hydrological cycle have been estimated using the isotopic composition ($\delta^{18}O$ and δ^2H) of the different waters and comparing them to the signature in precipitation (Zhang et al., 2010; Allen et al., 2015). The availability of cheaper and more reliable instruments to conduct the isotope analysis enables now a more widespread use of this method and more intense applications (Tetzlaff et al., 2014).

The isotopic composition of water samples can be used to estimate both different water sources and flow paths and transit times of waters (Tetzlaff et al., 2014). Dansgaard (1964) identified several physical and meteorological factors driving the global distribution of stable isotopes, for example altitude, latitude, distance to the coast, air temperature and precipitation amount influence the isotopic composition of precipitation. Further studies stated that variabilities in signatures are caused by isotope fractionation occurring along with the phase changes of water in the hydrological cycle (Yurtsever and Gat, 1981; Rozanski et al., 1993; Ingraham, 1998; Gat et al., 2001). Several effects (Figure 1-2) like the "continental", "latitudinal effect" and "altitude effect" could be identified. Air masses that move along surface temperature gradients lose water when moving from the sea towards inland locations (continental effect), the tropical towards the polar regions (latitudinal effect) or whilst moving from lower to higher altitudes (altitude effect) (Gourcy et al., 2005).

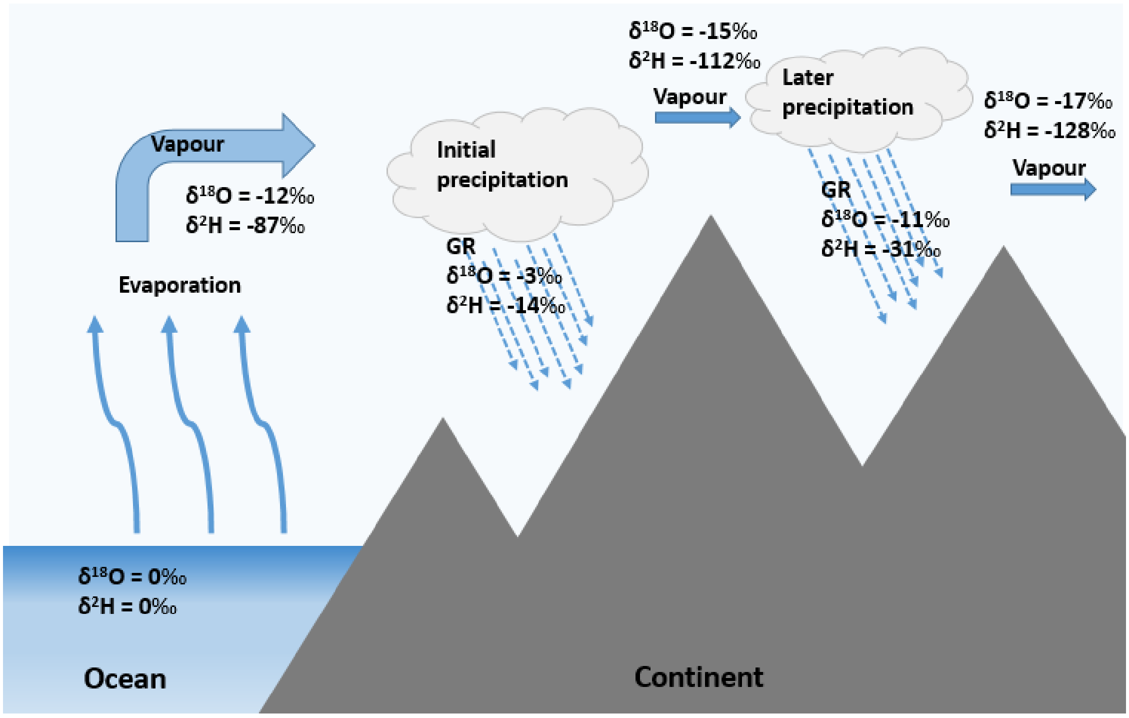

Figure 1-2: GR isotopic composition (δ^2H and $\delta^{18}O$) during evaporation and precipitation events. Based on Hoefs (1997) and Coplen et al. (2000).

Isotopes are a valuable tool to differentiate between event water, water that is delivered by rainfall or snowmelt, and pre-event water, water that has been stored in the catchment before the event (Tetzlaff et al., 2014). Infiltration processes, interaction with the canopy cover, especially interception and evaporation, can change the characteristics isotopic composition of the GR (Gat and Tzur, 1968; Allen et al., 2015). Several studies showed that due to fractionation processes TF is mostly isotopically heavier than GR and is very variable between and even within one event

(Saxena et al., 1986; Ikawa et al., 2011; Kato et al., 2013). The studies of Ikawa et al. (2011) and Saxena (1986) focussed on the differences in the mean isotopic composition between TF and GR.

Several studies showed that the isotopic composition of the GR is altered by its passage through the vegetation canopy (Brodersen et al., 2000; Cappa et al., 2003; Liu et al., 2008). Brodersen et al. (2000) showed that the $\delta^{18}O$ composition of TF was significantly different to the $\delta^{18}O$ composition of GR through isotopic fractionation of the GR in the canopy proceeding isotopically enriched drip or TF (Saxena, 1986; Dewalle and Swistock, 1994). Drip, mixing and exchanging with ambient air vapour in the canopy can also alter the isotopic composition of TF (Saxena 1986; Brodersen et al., 2000). Liu et al., (2008) agreed with these findings and additionally concluded that the isotopic composition of TF is highly altered by canopy structure and ongoing evaporation processes in the canopy and showed an even higher correlation of canopy structure and evaporation during light intensity events. However, experiments based on weekly water sampling of TF in several forest stands failed to find any correlation between the enrichment of ^{18}O in TF and interception rate (Allen et al., 2014), though this could have been related to sampling strategy.

Characteristics for the SF isotope composition are still poorly understood (Ikawa et al., 2011). Gersper and Holowaychuck (1971) investigated chemical differences between SF and TF and discovered that SF is more enriched in ^{18}O and ^{2}H. Kubota and Tsuboyama (2003) compared the $\delta^{18}O$ composition of SF and TF. Water samples were collected during rainfall events and reported more enriched values for the SF samples. As SF is often a mix of rainwater of different events, the isotopic composition is also a result of this mix (Levia and Herwitz, 2005; Staelens et al., 2008).

Despite the efforts that have been made over the last years, it is apparent that some of the basic mechanisms and driving factors of vegetation influenced rainwater fractionation have not yet been completely understood (Ikawa et al., 2011). However, knowing the isotopic composition of TF instead of GR could improve tracing water origins, transient time modelling and could help to understand these systems in a more detailed way (Allen et al., 2014).

1.2 Importance of the Study and Research Gap

Northern high-latitude catchments such as the Bruntland Burn catchment in Scotland are likely to be affected by changing precipitation and temperatures regimes due to climate change in the next decades. According to the low emission scenario for Scotland (UKCP09), the total annual mean precipitation will remain steady, but there will be a shift towards less precipitation in summer (-12%) and more in winter (+11%). The mean temperature will increase by around 2.1°C in winter and 2.7°C in summer (UKCP09; Capell et al., 2013). A changing precipitation pattern in both magnitude and timing plus a change in temperature will have consequences for pedogenic processes, vegetation and hydrology (e.g. water balance and flow path partitioning) (Kundzewicz et al., 2007; Capell et al., 2013; Tetzlaff et al., 2013).

It is not yet well understood how hydrological processes are affected by climate induced changes in vegetation distribution and communities in northern, low energy regions (Tetzlaff et al., 2014; Tetzlaff et al., 2015). As vegetation communities will change with as a consequence of shifts in precipitation and a changing climate, hydrological processes, e.g. release, storage and mixing of water in a basin will be affected (Wookey et al., 2009). Interception of rainfall is an important factor in water resource management (Arnell, 2002), especially in forested areas where interception loss can reach a quarter of the gross precipitation (Dingman, 2002). It is therefore crucial to gain knowledge about the influence of different vegetation types on water partitioning. Further findings will help to assess possible vegetation feedbacks on water availability in high latitude catchments under a changing climate. A more detailed understanding of rainfall interception will also improve the understanding on atmospheric deposition of contaminants, solute leaching and tracing gas fluxes (Hansen, 1995; Whelan and Anderson, 1996). Understanding the processes that drive precipitation redistribution will help to better predict quantities of canopy interception loss, water yield and storage in forested areas as well as the infiltration pattern into the soil and soil storage characteristics (Kato et al., 2013).

In addition to climate induced changes in Scotland, The Scottish Forestry Strategy (2006) stated, that it is planned to increase Scotland’s woodlands from 17.1% in 2006 to about 25% by the second half of this century and establish forestry as a major role in helping to adapt for climate change scenarios. It is therefore important to understand how these planned land use changes in certain areas in Scotland might influence the water availability and partitioning.

Recent studies have shown that the isotopic composition of GR can be affected by processes such as fractionation in the forest canopy. TF is the most important water input for forested areas, and understanding the processes influencing its isotopic composition is important for isotope hydrology studies (Kato et al., 2013). It is also important to understand the spatiotemporal variability of the isotopic composition of TF, especially when it is used as an input variable in isotope tracer studies (Allen et al., 2015).

TF and SF studies have not been undertaken in the Bruntland Burn catchment so far and not many studies have quantified amounts of TF, SF and interception loss for heather (*Calluna vulgaris*), even though it is a dominant vegetation type in many northern upland catchments. The Bruntland Burn catchment experiences a maritime climate (precipitation ~1100 mm per annum). Rain events in the Scottish Highlands are mostly frontal, low intensity events (Tetzlaff et al., 2014), there is little seasonality in the climate, and evapotranspiration is low (~400 mm). To predict consequences of climate change and land use changes in northern upland catchments it is crucial to understand the role of vegetation on water partitioning and the underlying processes.

Studies that quantify the differences in isotopic composition of precipitation on its way through the canopy are limited, and further investigations have to be carried out to understand the influencing factors. Quantifying interception, TF and SF and its variability also helps to improve model calibration and therefore helps to better represent and predict key processes in these environments (Muzylo et al., 2009).

2 RESEARCH OBJECTIVES

The overarching goal of this study was to estimate interception losses in a northern, high latitude, low energy catchment. The study focussed on spatial variabilities of both amount and isotopic composition of TF and SF to investigate which of possible influencing factors such as climate variables, branch geometry, canopy coverage, vegetation type and topography are the major controls on variabilities. Altogether four sites were compared, two on a north and two on a south facing slope, respectively. The study aimed to answer the following research questions:

- To investigate the influence of canopy cover of different vegetation types on spatio-temporal dynamics of interception and precipitation partitioning.
- To investigate the influence of vegetation cover on spatio-temporal differences in isotopic composition of TF and SF and to identify the major controls of isotopic composition.

3 STUDY SITE

This study was conducted in the Bruntland Burn catchment (Figure 3-1), a 3.2 km² tributary of the Girnock Burn catchment located in the Cairngorm National Park in the north-western part of Scotland, about 75 km west of the city of Aberdeen. The Bruntland Burn is a typical moorland stream, draining into the river Dee. The climate is oceanic with mean annual temperatures of around 6.8 °C, with a winter average of 1.2 °C and a summer average of 12.4 °C. The mean annual precipitation is about 1100 mm mostly falling as frontal events with low intensities (Tetzlaff et al., 2014). The mean annual evapotranspiration is about 400 mm and the mean annual runoff is around 700 mm. In general, the catchment is little influenced by snow (usually <10% of annual precipitation), and peak runoffs are most likely to occur in between November and February, but can happen throughout the year. These high flow periods are mainly derived from large rainfall events. Nevertheless, rain on snow events can produce some of the largest runoff responses in the Bruntland Burn (Tetzlaff et al., 2015).

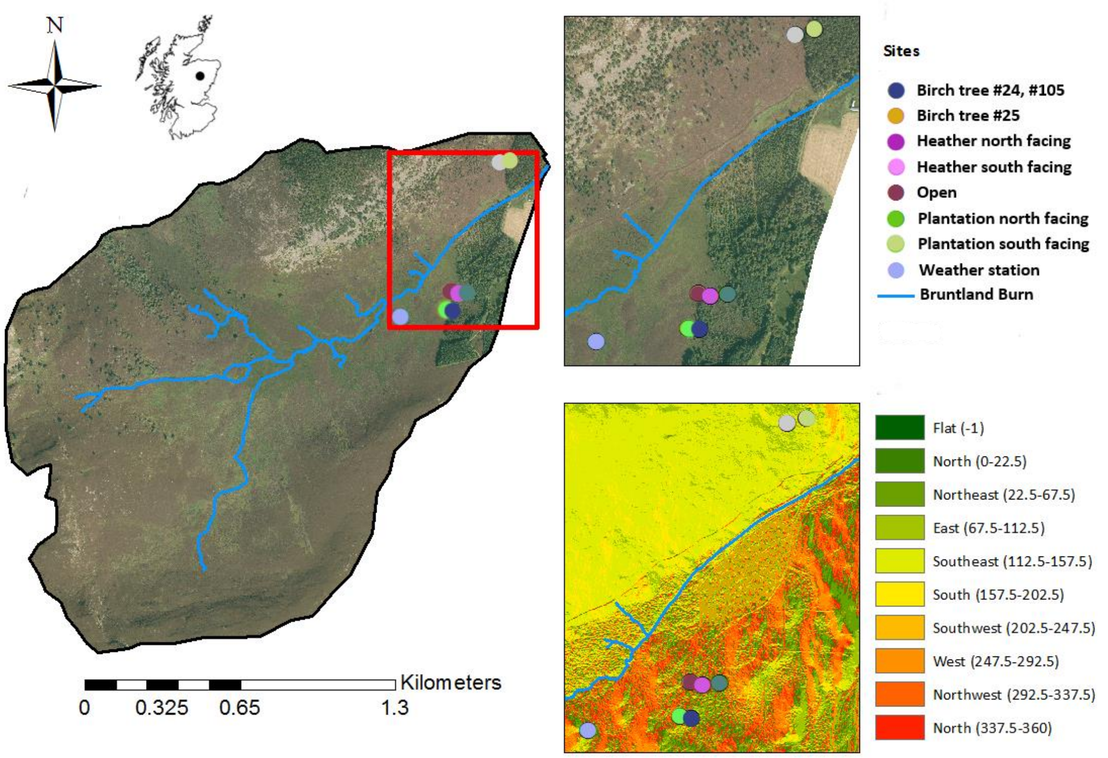

Figure 3-1: Bruntland Burn catchment with all the site locations and the Bruntland Burn stream. Locations of collectors are pictured in differently coloured dots. The lower right picture shows the different aspects of the sample sites.

The catchments elevation ranges between 248 and 539 m with an average of 350 m. Mean slopes are 13° (Birkel et al., 2011; Tetzlaff et al., 2014). The area was glaciated during the last glacial maximum, and altitudes below 400 m consist of drift draped topography, with poorly sorted glacial till deposits, which reach a depth of 40 m in the valley bottoms (Soulsby et al., 2015).

Histosols such as deep peats are the dominant soil type in the valley bottom, and can reach a thickness up to 4 m in the valley bottom riparian zones. There are mainly shallow peats up to 0.5 m depth on the lower hillslopes, with podzols and rankers to be found on the steeper slopes where overlying freely draining mineral soils abound (Birkel et al., 2011; Tetzlaff et al., 2014; Dick et al., 2015)

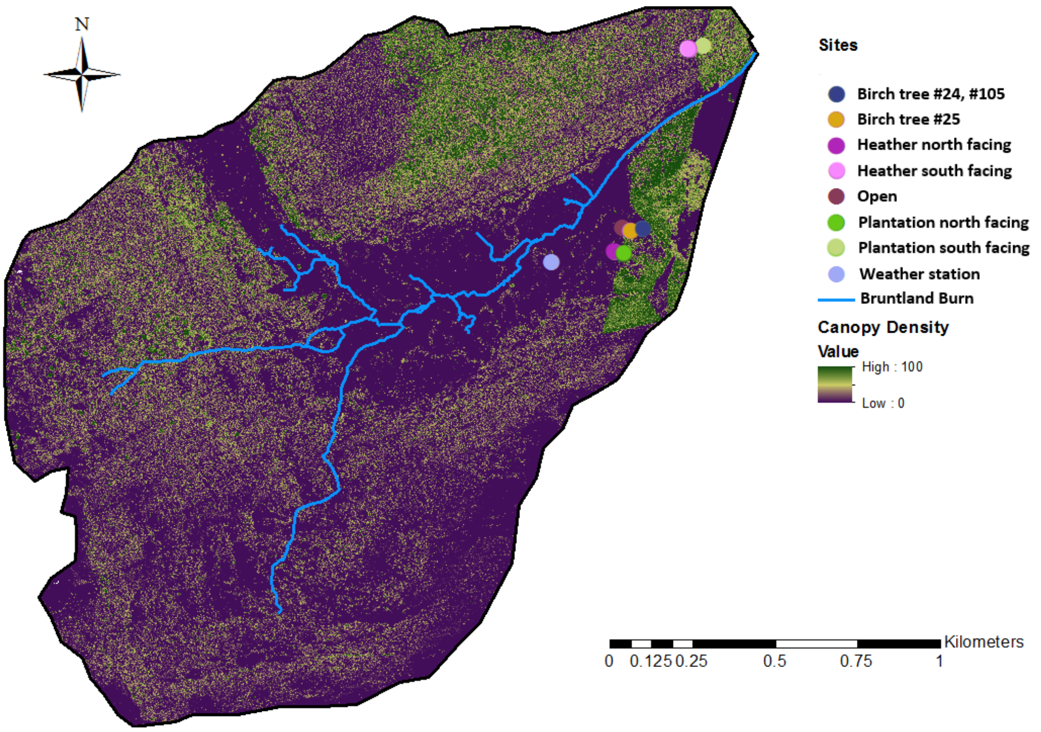

Figure 3-2: Canopy coverage in the Bruntland Burn catchment. Green indicates a high canopy coverage, purple indicates low canopy coverage. Canopy Coverage derived from LiDAR data (1 m resolution). The sample locations are indicated by coloured points.

Linked to the dominant soil types, the vegetation consists of mainly heather (*Calluna vulgaris*) and Erica species in the moorland areas, Sphagnum and purple moor-grass (*Molinia caerulea*) in the peaty, riparian zones and Scots pine (*Pinus sylvestris*) and birch (*Betula pendula*) trees in the plantations that, due to historic land management only represent small areas of the catchment (mainly located in the higher altitudes and those areas which exclude deer). Sporadically, trees can also be found on the steeper hillslopes of the catchment (Birkel et al., 2011, Tetzlaff et al., 2014). Historical land management resulting in tree clearance in many headwater catchments in the UK was carried out to create more attractive environments for sheep (*Ovis aries*), red deer (*Cervus elaphus*) or shooting game, e.g. the red grouse (*Lagopus lagopus scotica*) (Dick et al., 2015). The canopy coverage for the entire catchment site is quite low. Higher percentages of canopy coverage can only be found in the plantation sites in the eastern part and in the northern part of the catchment (Figure 3-2).

4 DATA AND METHODS

4.1 Field Work

4.1.1 Equipment Installations

Data sampling was conducted between 1st of June until 24th of September, 2015. Four sites were installed on a south and north facing slope with two sub sites, one in the heather and one in the plantation, respectively. The sites have been equipped with a total of 75 TF and 10 SF collectors. Collectors were randomly located in 20 x 20 m grids for each site, respectively. For further comparison, one TF collector (#38) was located next to the weather station on the hilltop, to allow to capture potential differences in the amount of gross precipitation. There was no significant difference between the GR sampled by the TF collector #38 and the rain gauge station (Wilcoxon signed rank test, significance level = 0.05). To investigate the effects of adding paraffin to the TF samplers (to protect against evaporation), two additional collectors were placed next to each other in the open, one with paraffin (#36), and one without (#37). The comparison between the two collectors showed no significant difference in the isotopic composition of δ^2H and $\delta^{18}O$ (Wilcoxon signed rank test, significance level = 0.05) (Figure 4-1), however, all consequent TF samples were taken with paraffin.

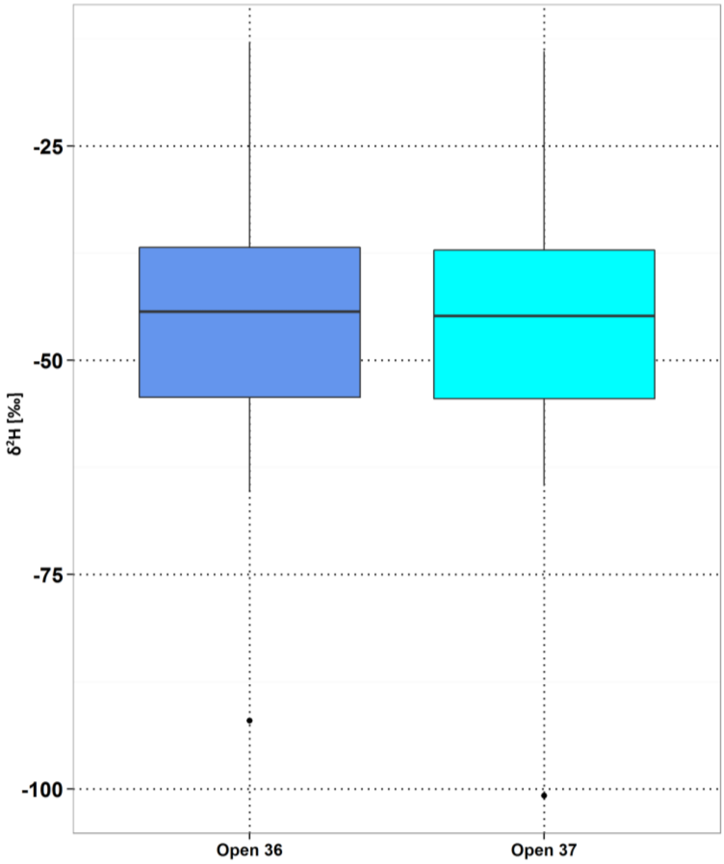

Figure 4-1: Comparison of δ^2H between the two collectors with paraffin (#36) and without paraffin (#37).

Position of collectors and trees within the grid

A grid was established for each sample site to map all collectors and trees in the plantations. Coordinates of the four corner points were taken using a Garmin e-trex 10 GPS. The 20 x 20 m grid was fragmented into 25 4 x 4 m sub-grids and the locations of collectors and trees in each sub-grid (X and Y value) were listed. Collectors were located at random locations at all sites to capture most of the site variability in canopy coverage. More TF collectors in the plantation were needed to better cover their greater spatial variability compared to the heather sites.

Sampling design

Collectors on the north facing site were labelled with numbers 1-38 for the TF and 101-105 for the SF collectors (Table 4-1). Twenty-three TF collectors and five SF collectors were installed in the grid of the north facing younger plantation. As there was no birch tree in the 20 of 20 m grid chosen, two of the TF collectors and one SF collector were located about 50 m north of the grid in a birch grove. Ten collectors were placed in the north facing heather grid. Twenty-five TF collectors (#51 – 75) and five SF collectors (#106- 110) (Table 4-1) have been placed in the south facing plantation and 13 TF collectors in the south facing heather grid (#76 – 87).

Table 4-1: Overview of the sites with throughfall (TF) and stemflow (SF) collectors and characteristics of collector locations.

Site	*Type*	*Collector #*	*Collector Characteristics and #*	
Plantation north facing				
	TF	1-25	Clear	# 3, 7, 8, 23
			Dense	# 4, 5, 9, 14, 17, 18
			Birch	# 24, 25
	SF	101-105	Scots pine	# 101-104
			Birch	# 105
Plantation south facing				
	TF	51-75	Clear	# 51, 67, 68, 75
			Birch	# 62
	SF	106-110	Scots pine	# 106, 108 - 110
			Birch	# 107
Heather north facing	TF	26-35	Open	#32
Heather south facing	TF	76 - 87	Open	#78
Open, test collectors	TF			#36, 37, 38

Structure of the throughfall collectors

The designed TF collectors consisted of three parts: a bottom part that was put on the ground, an inner part that was the actual collector with a measuring scale on it and a top part that collected the TF and funnelled it into the inner part. To prevent leafs and litter plugging the entry of the collector, a fine mesh was fixed to the top of the funnel (Figure 4-2). The collectors were attached to shortened bamboo sticks using cable ties to make sure they were not moved by wind or deer. Collectors in the heather site had to be buried in the ground for approximately 10 cm due to the low canopy of the heather shrubs.

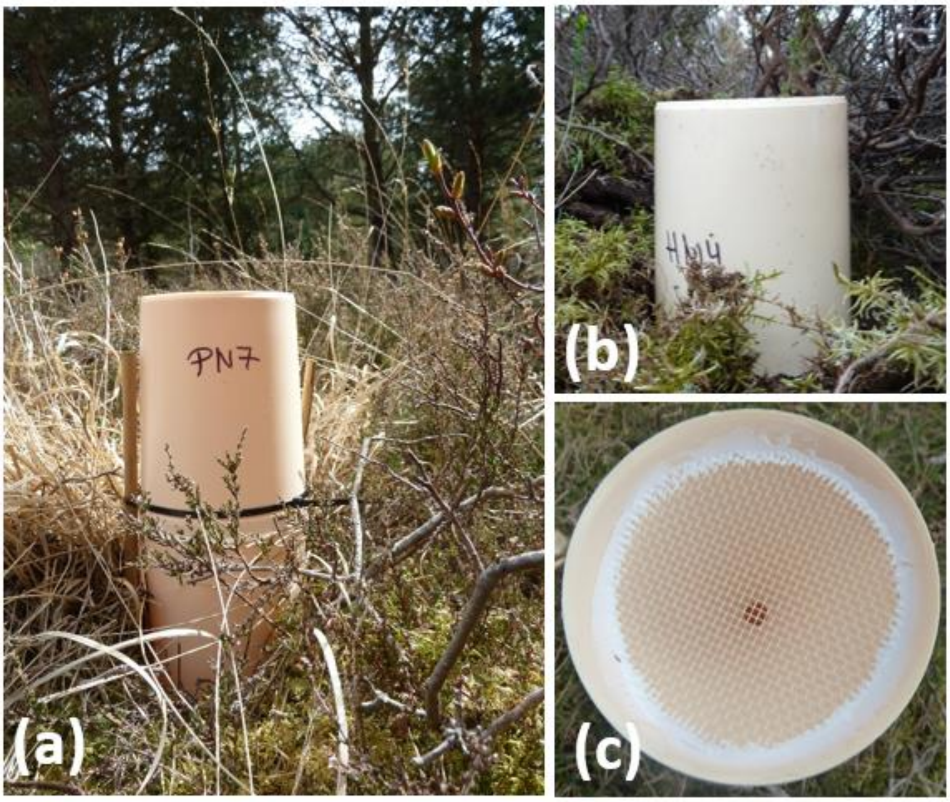

Figure 4-2: Throughfall collectors designed for the study. (a) Shows a collector in the north facing plantation. (b) Shows a collector in the south facing heather site. (c) Shows the mesh that was applied to each collector.

Structure of the Stemflow Collectors

For the SF collectors (Figure 4-3) 10 trees of different height, breast height diameter (BHD) and species were selected (Table 4-2). Following the instructions of Reynolds and Stevens (1987) a 30-40 cm section in approximately 1.50 m height above the ground and free of whorls and branches was chosen and cleaned of loose bark and moss, avoiding damage to the tree's bark. A PVC flexible tube with a diameter of 15 mm was wrapped around this area in a single spiral to cover the circumference of the tree. The tube was adjusted using four to five plastic pipe clips. The gap between the tree's bark and the tubing was sealed with silicon and a silicon border to the tube was applied (Figure 4-3). Small holes where cut into the plastic tube every 10-20 cm allowing the SF to enter the tube that lead into a canister with a capacity of 15 l.

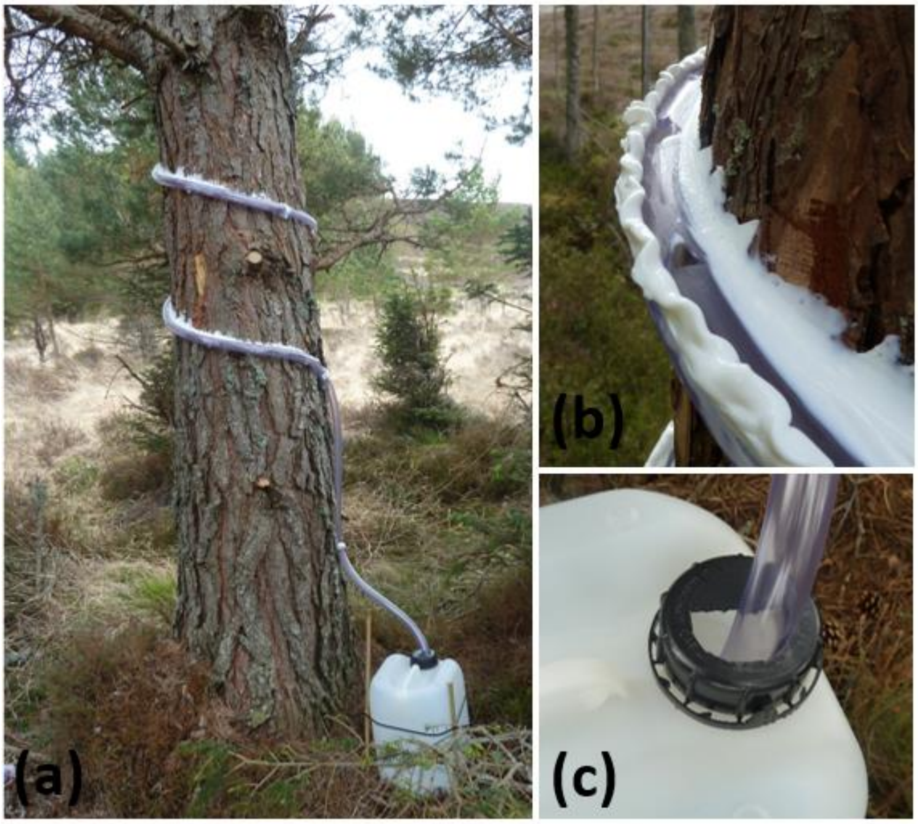

Figure 4-3: Stemflow Installations at one tree for the north facing site. (a) The whole setting on the tree can be seen, (b) shows the funnelling system and (c) entrance point to the collector.

Table 4-2: Stemflow collectors, tree type and breast height diameter (BHD) in cm.

Site	*Tree Type*	*Collector #*	*BHD [cm]*
Plantation North Facing			
	Scots pine	101	10.66
	Scots pine	102	19.74
	Scots pine	103	28.33
	Scots pine	104	39.79
	Birch	105	14.01
Plantation South Facing			
	Scots pine	106	29.29
	Birch	107	15.28
	Scots pine	108	26.58
	Scots pine	109	23.24
	Scots pine	110	25.15

4.1.2 Sampling

Quantity and Isotope Sampling

Samples were taken over a 4 months period, from 1st of July till 24th of September. Days in between the sampling dates ranged from 4 to 14 days (depending on whether there have been precipitation events), generating a data set over 16 sampling dates. For each of the 75 TF collectors, the amount of TF was determined and an isotope sample was taken. Isotope samples were sampled into 8 ml glass vials. Vials were filled completely forming a meniscus to make sure that there was no air or headspace in the sample. The glass vials had a lid containing a silicone seal, which when closed tightly, formed an air tight seal to prevent evaporation. To prevent evaporation in the collectors, 1 ml of paraffin was added to each TF collector and 5 ml to each SF collector using a graduated syringe. This amount was later subtracted from the actual TF amounts.

Stemflow Sampling

The SF in the 10 SF collectors was measured on the same dates as the TF. To determine the amount, the collector was emptied into a graduated measuring cylinder. An isotope sample was taken using the same 8 ml glass vials as for the TF. BHD of all the trees in a grid was measured to conduct the tree basal area (BA) in the grid.

Canopy Cover

To estimate the canopy cover for each collector, digital photographs above each TF collector were taken with a resolution of 4000 x 3000 pixels. The camera used was a GoPro Hero 3+ digital camera with an ultra-wide angle lens of 127 degrees in the diagonal angle. Due to its non-full fisheye lens, two pictures were taken for each collector, one facing north and one south to cover the whole area. The camera was held in a horizontal position, automatic exposure and automatic release function were used. The photos were taken in upwards direction with the camera positioned on the collector.

4.2 Laboratory Work

4.2.1 Isotope Analysis

The isotope samples were stored in a fridge until analysed for their isotopic composition. To prepare the samples for the analysis they were filtered and 1 ml was injected into 1.5 ml glass vials (Figure 4-4) in accordance with the procedures detailed in (Los Gatos Research Inc, 2010).

The samples were analysed for the stable isotopes of water δ^2H and $\delta^{18}O$ using an off-axis integrated cavity laser spectrometer, an LGR Los Gatos DLT-100 Liquid Water Isotope Analyser.

Each analysis comprised 46 samples (Figure 4-4) and eight vials of distilled water (seven at the beginning and one at the end), and took approximately 15 hours with seven injections per sample.

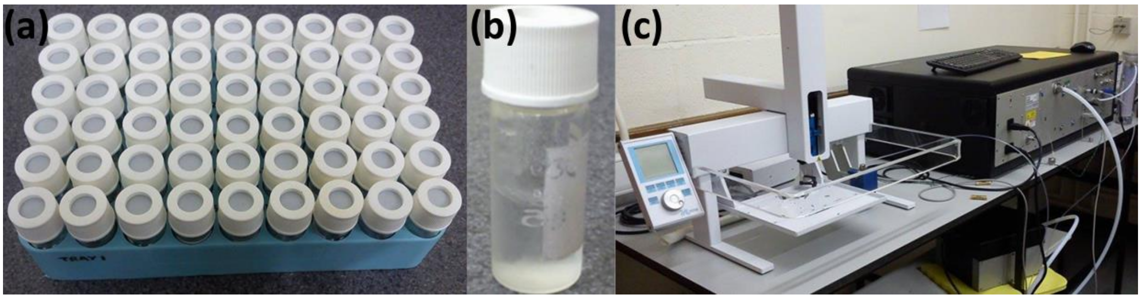

Figure 4-4: (a) Shows the tray with the samples, (b) shows the 1.5 ml glass vials used and (c) shows the Los Gatos isotope analyser.

Samples were taken out of the 1.5 ml glass vials by a robotic arm and then injected into a heated injector block where the sample was vaporised. To apply the absorption technique, the sample was then transferred into the pressure vessel. Using an off axis absorption cell the laser photons were trapped between two mirrors that were very reflective and give a several kilometre long effective laser path length. Beer's law was then applied to identify isotope ratios from the measured absorption. The analyser measured the optical path switching off the laser and measuring the time the light needed to leave the cavity (Los Gatos Research Inc, 2010). After that the sample was evacuated from the vessel, the whole process started again. The analyser ran three samples followed by one standard (**Fehler! Verweisquelle konnte nicht gefunden werden.**), with each sample being run seven times. The first three injections were rejected to avoid any possible influence from the previous samples (Coplen, 2011).

In the post analysis, the sample ratios derived by the Los Gatos analyser were calibrated against the measured standards (Appendix C-2). $\delta^{18}O$ and $\delta^{2}H$ were transformed into a δ notation (ppm) and calibrated against the Vienna Standard Mean Ocean Water (VSMOW) (Green et al., 2015).

Equation 4-1:

$$\delta\ [‰] = \frac{R_{Sample} - R_{VSMOW}}{R_{VSMOW}} * 1000$$

Where:

R $\delta^{18}O / \delta^{16}O$ ratio or $\delta^{2}H / \delta H$ ratio of the TF sample or the VSMOW sample.

4.3 Analysis of the Data

For the data preparation and processing, the programs R (R-3.2.2) and Microsoft Excel 2013 were used. Stemflow values were transferred from ml into mm. Canopy interception loss and evapotranspiration was calculated. A general characterization of the catchment using ArcGIS 10 was conducted. The mean isotopic composition of GR as well as mean isotope TF values per site and per collector were volume weighted.

4.3.1 Quantifying TF and SF

Canopy interception loss

Canopy loss/ Interception (I) and net precipitation (NP) have been calculated for the field season for all sites. The canopy loss was calculated using the following equation (Helvey and Patric, 1965; Crockford and Richardson, 2000):

Equation 4-2:

$$I = GR - (TF + SF)$$

Where:

I	Interception loss [mm].
GR	Gross rainfall [mm].
TF	Throughfall [mm].
SF	Stemflow [mm].

Net precipitation is the sum of TF and SF, therefore Interception = gross rainfall – net precipitation (Crockford and Richardson, 2000).

Equation 4-3:

$$NP = 100 - CL$$

Where:

NP Net precipitation [mm].

CL Canopy loss [mm].

Stemflow amounts in mm

Basal area (BA, in m^2) for each tree was calculated with:

Equation 4-4:

$$BA = \left(\frac{C}{200}\right)^2 \pi$$

Where:

C Circumference of the tree in cm.

To calculate the equivalent of SF in mm for each plantation, SF per BA was determined and related to BA for the whole grid and the canopy coverage for the whole grid. The values were then weighted according to the representativeness of each tree (BA) to get a total SF volume for the plot. This amount was then scaled by the canopy coverage for the plot to get the amount of mm per area.

Evapotranspiration Calculation

The evapotranspiration was calculated using the FAO Penman-Monteith approach. The Penman-Monteith method requires variables such as air temperature, radiation, air humidity and wind speed that were derived from a nearby meteorological station in the catchment. The approach has been recommended as a standard method for computing reference evapotranspiration (Allen et al., 1998).

Equation 4-5:

$$ET_0 = \frac{0.408\,\Delta_s(R_n - G) + \gamma \dfrac{900}{T + 273}\, u_2(e_s - e_a)}{d + \gamma(l + 0.34\, u_2)}$$

Where:

ET_0 Reference evapotranspiration [mm day^{-1}].

R_n Net radiation at the crop surface [MJ m^{-2} day^{-1}].

G Soil heat flux density [MJ m^{-1} day^{-1}].

T Mean daily air temperature at 2 m height [°C].

u_2 Wind speed at 2 m height [ms^{-1}].

e_s Saturation vapour pressure [kPa].

e_a Actual vapour pressure [kPa].

$e_s - e_a$ Saturation vapour pressure deficit [kPa].

Δ_s Slope vapour pressure curve [kPa °C^{-1}].

γ Psychrometric constant [kPa °C^{-1}].

4.3.2 GIS Analysis

A general characterization of the study site was undertaken using the program ArcGIS version 10.3.1. A slope map of the catchment was produced using a high resolution DEM and canopy coverage [%] was calculated and displayed in a map for the whole catchment as well as for the two plantation grids using LiDAR data with a 1 m resolution.

4.3.3 CAN-EYE

The canopy cover or cover fraction was calculated using the free software CAN-EYE V6.1 developed at the EMMAH laboratory (Mediterranean Environment and Agro-Hydro System Modelisation) (CAN-EYE user manual). The cover fraction is defined as the fraction of soil that is covered by the vegetation's canopy as viewed in nadir direction (CAN-EYE user manual). When using hemispherical images, it is necessary to integrate the cover fraction over a range of zenith angles as it is impossible to maintain exact nadir direction. This range as well as the lens properties can be changed prior to analysing the photos (CAN-EYE user manual). The calculations are based on RGB images, the colours are automatically reduced from originally

16,777,216 to 327 (Spath, 1985). Several classification options can be chosen to classify the classes, e.g. vegetation is considered as non-selected pixels or non-selected pixels are considered as gaps (Demarez, 2008). Light contamination due to direct sunlight can be corrected in the program.

In general, the trees were taller and larger at the south facing forest site, and the plantation was less dense compared to the north facing site (Table 4-3). Mean canopy coverage for the collectors ranged between 53% for the south facing heather site and 68% for the south facing plantation. The median and maximum canopy coverage values were quite similar for all sites whereas minimum and mean values differed a lot.

Table 4-3: Canopy Coverage for each site. The values derived using digital photography show values representing only the collector's canopy coverage whereas the values calculated using the LiDAR data show a mean value for the whole site.

	Trees			*Digital photography (CAN-EYE)*				*LiDAR Data (ArcGIS)*
Site	***# of trees***	***mean BHD [cm]***	***median distance collector closest tree [m]***	***Min [%]***	***Max [%]***	***Median [%]***	***Mean [%]***	***Mean [%]***
Plantation north facing	36	13.8	1	28	81	67	63	43
Heather north facing	0	-	-	0	79	65	60	-
Plantation south facing	46	21.8	1.5	50	74	69	68	68
Heather south facing	0	-	-	0	78	62	53	-

4.3.4 Isotopes

Weighting the Values

To derive mean values of the isotopic composition of the GR per sample period, δ^2H and $\delta^{18}O$ values were weighted by the amount of GR using following equation:

Equation 4-6:

$$\delta X = \frac{(P_1 * \ \delta X_1) + \ (P_2 * \ \delta X_2) + \cdots + (P_n * \ \delta X_n)}{((P_1 + \ P_2 + \cdots + P_n)}$$

Where:

δX δ^2H or d^{18}O of GR, TF or SF.

P_1 Amount [mm] of first sample to be weighted.

P_2 Amount [mm] of second sample to be weighted.

P_n Amount [mm] of last sample to be weighted.

δX_1 Isotopic composition (δ^2H or δ^{18}O) of the first sample to be weighted [‰].

δX_2 Isotopic composition (δ^2H or δ^{18}O) of the second sample to be weighted [‰].

δX_n Isotopic composition (δ^2H or δ^{18}O) of the last sample to be weighted [‰].

For mean values in TF per collector or for a sample period per site, the isotope values were weighted by the amount of TF per sample period or per collector respectively.

Local Meteoric Water Line

The local meteoric water line (LMWL) was determined using a least-squared regression on all the GR isotope values for the field season (Landwehr and Coplen, 2006). The equation for the field season was:

Equation 4-7:

$$y = 7.6275 * \delta^{18}O + 2.0779$$

Where:

$\delta^{18}O$ δ^{18}O value of the samples [‰].

Line conditioned excess

The line conditioned excess (lc-excess [‰]) is a direct indicator for the offset of a sample from the LMWL, and thus, an indicator of possible fractionation. It is defined as following (Landwehr and Coplen, 2006):

Equation 4-8:

$$lc-excess = \delta D - a * \delta^{18}O - b$$

Where:

δ^2H δ^2H value of the sample [‰].

a, b Coefficients of the LMWL.

$\delta^{18}O$ δ^{18}O value of the sample [‰].

To take the LMWL for lc-excess into account, the following equation was used for the data set:

Equation 4-9:

$$lc-excess = \delta^2H - 7.6275 * \delta^{18}O - 2.0779$$

Where:

δ^2H δ^2H value of the sample [‰].

$\delta^{18}O$ δ^{18}O value of the sample [‰].

4.3.5 Statistical Analysis

For the statistical analysis of the data the programs R (R-3.2.2), Microsoft Excel 2013 and SigmaPlot 13.0 were used. Meteorological data was averaged for the weekly sample periods to get an average value for air temperature, humidity, wind speed, wind direction and evapotranspiration and to be able to relate TF and SF to this climate data. The gross precipitation was summarized for the sample periods to get a total amount of GR for each period. Maximum wind speed, maximum daily wind speed and precipitation intensity were calculated for the sampling periods as well. Coefficient of variation (CV) was calculated using following equation (Dytham, 2011):

Equation 4-10:

$$CV = \frac{100 * s}{mean}$$

Where:

s Standard deviation of the samples.

To compare the four sites, summary statistics such as mean, median, standard deviation, maximum and minimum values were calculated for all the data sets. To visualize differences between the sites and sample dates, boxplot, showing median, upper and lower quartile, inter quartile range, maximum and minimum value as well as outliers were generated. Scatterplots were used to show the spread, variability and pattern of the isotope data of all sites.

Statistical Analysis with R (R-3.2.2)

Different kind of statistical analysis have been used test the statistically relevant relations between the meteorological variables influencing TF and SF. A Pearson correlation in R (R-3.2.2) has been undertaken to plot a scatterplot and potential relations between the variables.

To only detect combinations of variables that can predict the y-values such as TF, SF and the isotopic signatures of both the function stepAIC(), a stepwise regression, was used. Through adding and subtracting the 'causes' it determines the most important variables in order to reach the best mode fit (Dytham, 2011). The therefore determined variables were then to run the multiple linear regression model (MLRM). The MLRM assumes a relation between dependent and independent variables and can be described by the following equation (Montgomery et al., 2012):

Equation 4-11:

$$y = b_0 + b_1x_1 + b_2x_2 + \cdots + b_nx_n$$

Where:

y Dependent variable.

$b_{0,1,n}$ Regression coefficients.

$x_{1,2,n}$ Independent variables.

The MLRM is a parametric test finding the dimensional plane best describing the data when more than one independent variable is involved. The test is made for normally distributed data showing a constant variance. The Kolmogorov-Smirnov test was used to check if the data is normally distributed. A Spearman rank correlation was used to test for constant variance.

A p-value determines the probability of concluding erroneously that the data is not normally distributed. If the calculated p-value is higher than the p-value set (p=0.05), the test passes.

The model gives a regression equation, R, R^2 and adjusted R values as well as the standard error of the estimate, F statistic and the p-values. The correlation coefficient R and the coefficient of determination R^2 indicate how the data is described by the regression model. Values close to one show a good relation, values close to zero there is no relation between independent and dependent variables. The ratio of the regression coefficient t is used in the t-statistic to check whether the independent variable is important in predicting the dependent variable. Large values lead to the assumption that the independent variable can predict the dependent. P-values calculated for t indicate the probability of making a wrong conclusion whether there is a relation between the variables or not. Very small p-values indicate a greater probability of correlation between the variables. Traditionally p-values < 0.05 are accepted to contribute to the prediction of the dependent variable (Dytham, 2011; Montgomery et al., 2012).

Linear Regression

When there was only one independent variable, a linear regression (LR) was used to check if the data correlates. The linear regression assumes a 'straight line' relation between the dependent and independent variable. This parametric test assumes as well that data is normally distributed. The equation for the LR is (Montgomery et al., 2012):

Equation 4-12:

$$y = b_0 + b_{1,x}$$

Where:

b_0 Intercept or constant term.

$b_{1,x}$ Slope, regression coefficient.

The test also gives R, R^2, adjusted R^2, regression equation, t-statistic and P-values (Montgomery et al., 2012). To check whether the data was normally distributed with constant variances, the same tests as for the MLRM (Kolmogorov-Smirnov and Spearman rank correlation) have been used.

5 RESULTS

5.1 Hydroclimatic Conditions

Figure 5-1 shows the air temperature (T.a), humidity (RH), wind speed (U) and maximum intensity of G (GR.M.Int). A total of 275.8 mm of GR was measured for the 4 months sampling period which is about 25% of the annual precipitation.

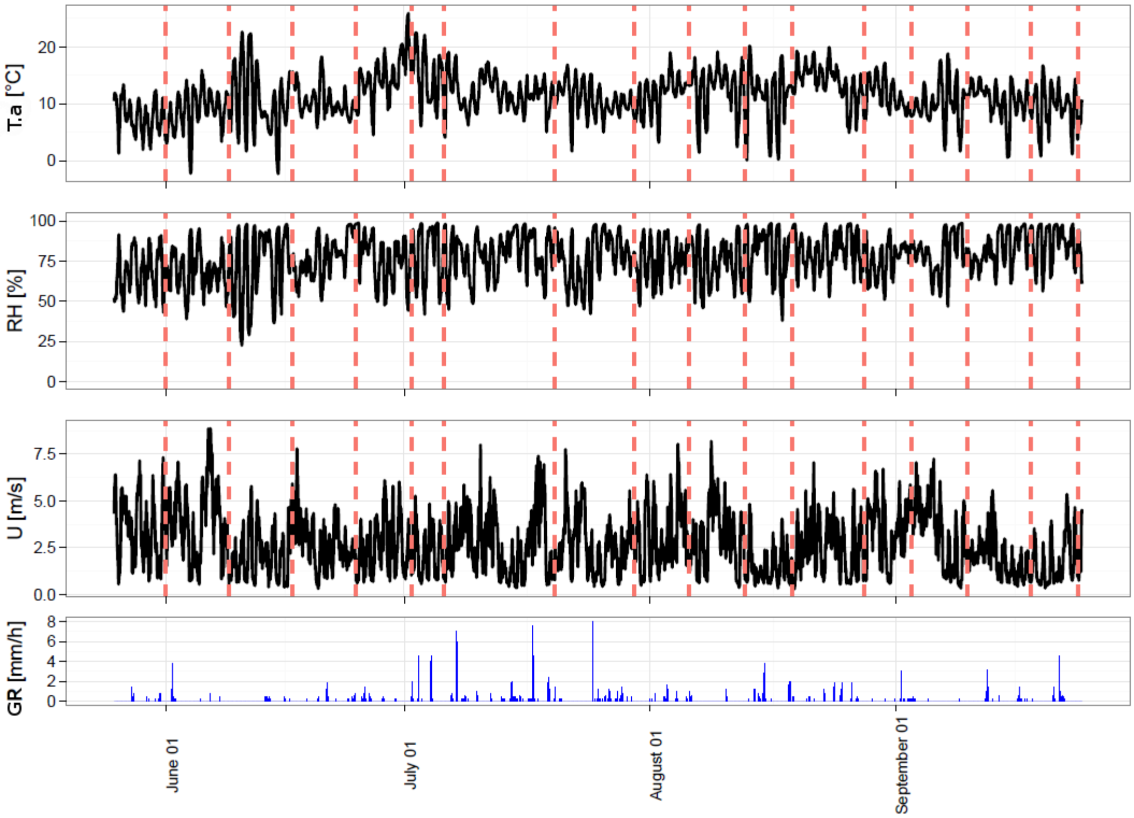

Figure 5-1: Hydroclimatic conditions. Air temperature (T.a [°C], humidity (RH [%]), wind speed (U [m s^{-1}]) and precipitation (GR [mm h^{-1}]) during the field season. The dashed orange lines represent the sample dates.

It is apparent that the variations in the hydroclimatic conditions were high during the entire field season (Figure 5-1). Air temperatures in this period ranged from subfreezing to over 25°C, wind gust reached 8.2 mm s^{-1} and precipitation reached intensities up to 8 mm h^{-1}.

There were only four sample periods where GR.Sum was below 10 mm. Highest measured GR.Sum was 74.8 mm over a 14 days sampling period in July, lowest was 0.8 mm over a 7 day sampling period in September. Most of the precipitation fell in low intensity events below 2 mm h^{-1}. There were a few more intense events in July with intensities above 5 mm h^{-1}. Mean daily air temperatures (T.a.Mean) for the sample periods varied between 7.04 °C and 15.4 °C. Highest T.a.Mean values were registered in July and August, lowest in early June and late September (Table 5-1, Figure 5-1). Mean humidity for the whole period was 77.2% with high values in mid and end of August and September respectively and lower values in early June. Wind speeds were quite low (on average 2.67 m s^{-1}) with some peaks of 7.5 to 8.0 m s^{-1} in some sampling periods (2nd, 4th, 7th, 9th and 10th). Average evapotranspiration was 4.5 mm for the whole period with higher values in the beginning of July and mid of August. Mean daily evapotranspiration reached its lowest value over the sampling period in the week from 18th till 24th of September (Table 5-1). An overview about the meteorological data averaged for the 16 sample periods can be found in Table 5-1. An overview for mean TF values can be found in the Appendix A (Table Appendix A-1).

Table 5-1: Sample dates, summarized GR (GR.Sum), maximum intensity of GR (GR.M.Int), Hours of Rainfall (GR.Hours), air temperature (T.a.Mean), humidity (RH.Mean), Wind speed (U.Mean), (WINDR.Mean) and mean evapotranspiration (ET.Mean) for all sites for the time period in between sample dates.

Sample Date	*GR.Sum [mm]*	*GR.M.Int [mm h^{-1}]*	*GR.Hours [h]*	*T.a.Mean [°C]*	*RH.Mean [%]*	*U.Mean [m s^{-1}]*	*WINDR. Mean [°]*	*ET.Mean [mm]*
01/06/2015	7.6	3.8	14.0	7.04	69.55	3.42	234.25	4.1
09/06/2015	12.2	0.8	13.0	9.05	69.02	3.74	219.53	5.2
17/06/2015	3.6	0.4	13.0	10.89	72.24	2.28	162.36	4.6
25/06/2015	10.4	1.8	26.0	10.15	78.41	2.57	177.08	4.2
02/07/2015	10.4	4.6	23.0	15.40	75.20	2.68	196.24	5.5
06/07/2015	20.8	4.6	12.0	13.75	78.71	2.11	171.45	5.4
20/07/2015	74.8	7.6	79.0	11.89	79.65	2.71	175.76	4.5
30/07/2015	23.6	8.0	31.0	10.53	76.09	2.67	176.47	4.3
06/08/2015	12.8	1.6	28.0	12.17	76.60	3.05	199.66	5.0
13/08/2015	2.2	1.2	4.0	12.16	74.24	3.03	222.44	5.3
19/08/2015	36.2	3.8	37.0	11.69	81.74	1.47	174.85	3.2
28/08/2015	18.8	1.8	27.0	13.56	80.61	2.61	179.63	4.5
03/09/2015	8.8	3.0	19.0	11.40	76.23	3.58	219.05	4.9
10/09/2015	0.8	0.2	3.0	10.31	78.70	3.17	195.69	4.6
18/09/2015	16.8	3.2	21.0	10.50	82.80	1.89	154.96	3.0
24/09/2015	16.0	4.6	19.0	9.37	85.10	1.79	193.74	2.7

5.2 Quantity Differences

5.2.1 Throughfall

In Figure 5-2, TF amount [mm] is plotted against GR [mm] and it shows, that higher GR amounts lead to higher TF. Most of the sampling periods recorded GR.Sum total amounts between 5 mm and 20 mm. For periods where GR.Sum was greater than 15 mm, TF could be measured in all collectors. During smaller events some collectors stayed empty when GR.Sum was below approximately 15 mm. The range for the measured TF in the plantations and the north facing heather was higher for periods with low GR.Sum (Table Appendix A-1). This pattern couldn't be seen for the south facing heather site.

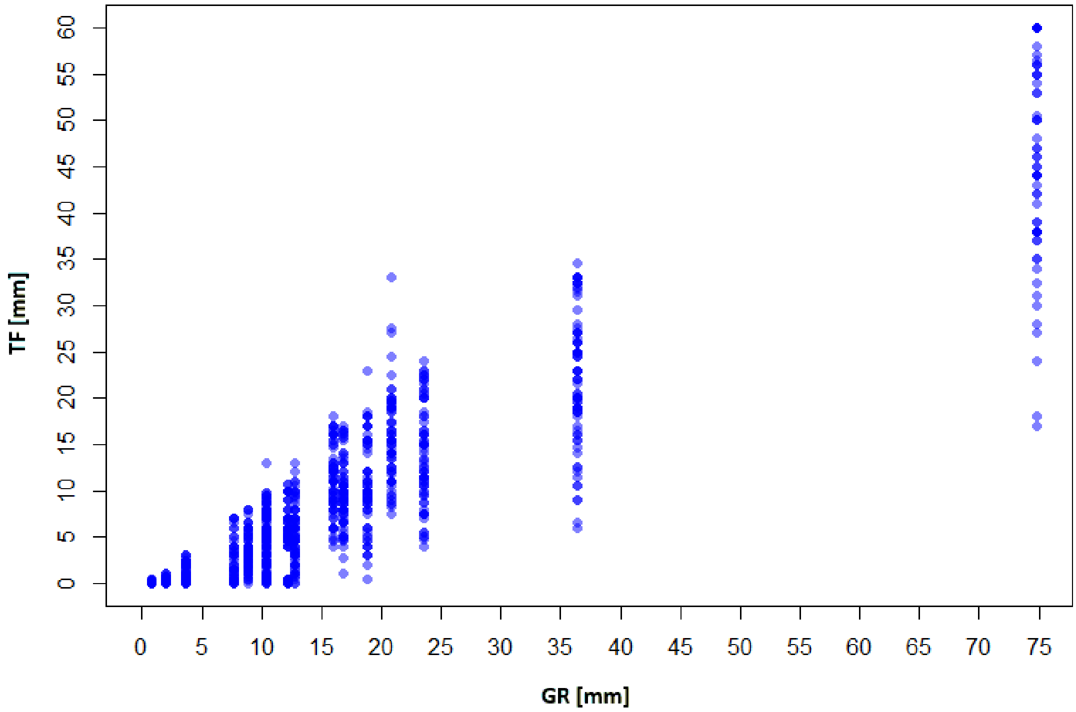

Figure 5-2: TF [mm] of all sampling sites over the sampling period plotted against GR [mm].

Inter-Site Variability

Table 5-2 shows mean TF fractions and TF amount for each site over the whole field season. Mean TF and TF fractions for the sample sites were lower for the plantations compared to the heather sites. The lowest TF values were found for the plantation on the north facing slope and highest for the south facing heather site. A comparison between the different aspects showed that TF and TF fraction were higher for the south facing sites than the north facing ones. The three collectors (#36 - 38) placed in the open collected an average of 94% of the GR measured by the rain gauge.

The interception loss calculated over the whole field period was with up to 47% for the plantations and 41% for the heather quite high. SF as a fraction of the GR.Sum is with 1.6% for the north and 1.0% for the south facing plantation very small (see 5.2.2). The interception loss was found to be higher in the plantations compared to the heather sites.

Table 5-2: Mean amount of TF/SF (q.TF.Mean/q.SF.Mean) and as a fraction of GR (f.TF.Mean/f.SF.Mean) as well as interception loss and net precipitation (NP) for the four sites and the collectors in the open. Values are calculated for the entire field season.

Site	*f.TF. Mean [%]*	*q.TF. Mean [mm]*	*f.SF. Mean [%]*	*q.SF. Mean [mm]*	*Interception. Loss [%]*	*NP [%]*
Plantation north facing	51.8	8.9	1.6	0.4	46.6	53.4
Heather north facing	59.8	10.9	-	-	40.2	59.8
Plantation south facing	58.2	10.1	1.0	0.3	40.8	59.2
Heather south facing	66.6	11.9	-	-	33.4	66.6
Open	94.3	17.0	-	-	5.7	94.3

The two forest sites vary in number of trees, tree size (as indexed by BHD of the trees), distance of the tree to the collector and canopy coverage (Table 4-4). The canopy coverage values derived using digital photography and the software CAN-EYE show min, max, median and mean canopy coverage for the collectors at each site whereas the mean canopy coverage calculated using ArcGIS 10.3.1 show average values for the two 20 x 20 m plantation plots.

Figure 5-3 shows the distribution of TF for each sample date as a fraction of the total GR measured by the rain gauge. In general it can be seen that there is a high temporal variability in the TF fraction for each site as well as variability between the sites. Even though there are high variabilities between the TF fractions amounts at each site, all the sites show a similar temporal pattern. Medians of the TF fractions are high or low at the same dates for all sites for example at the 6th and 20th of July, 19th of August and 24th of September where GR.Sum and GR.M.Int where comparatively high. No data was available for the heather sites on the 1st of June as collectors haven't been installed at that date. There was very little towards no TF at all at sample day 3rd of September.

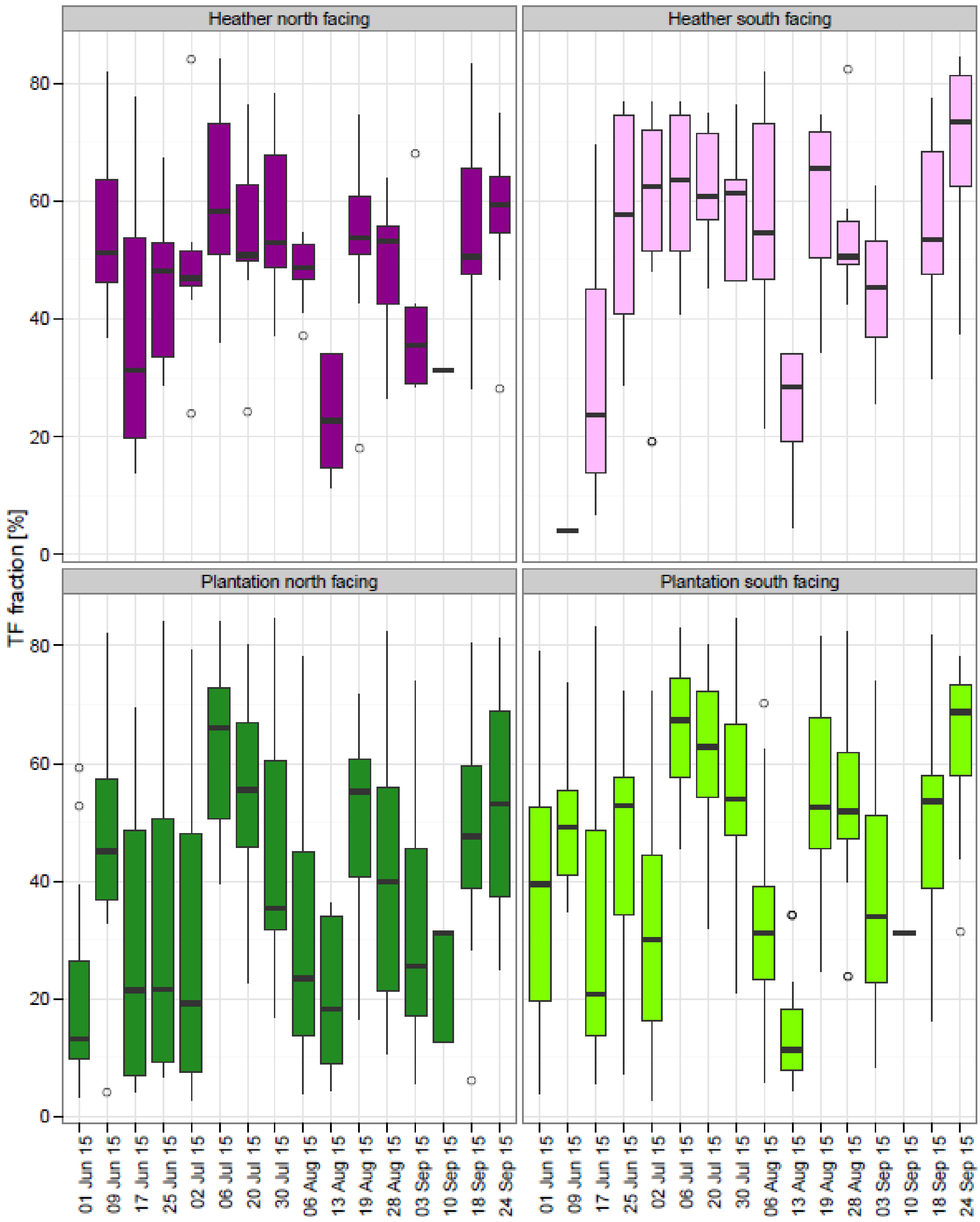

Figure 5-3: Boxplots showing TF fraction in % (TF as fraction of GR collected by the weather station) for all sites. Outliers are marked as points.

The boxplots in Figure 5-4 show the TF fraction [%] for the 4 sites over the entire study period. Consistent with findings in Table 5-2 it can be seen that the TF fractions varied per site. The heather sites had higher median TF fractions. The lowest median TF fraction could be found for the north facing plantation. The south facing sites had higher median values compared to their correspondent north facing sites. The smallest range of values could be found at the north facing heather site. A Wilcoxon singed rank test showed that the two vegetation types are, on a significance level of 0.05, significantly different to each other. Moreover, the TF fractions for the south facing plantation were found to be significantly higher as for the north facing plantation. However, in Figure 5-3, it can be seen that this isn't the case for all sampling periods. For the heather sites, the Wilcoxon signed rank test showed no significant differences of TF fraction between the aspects.

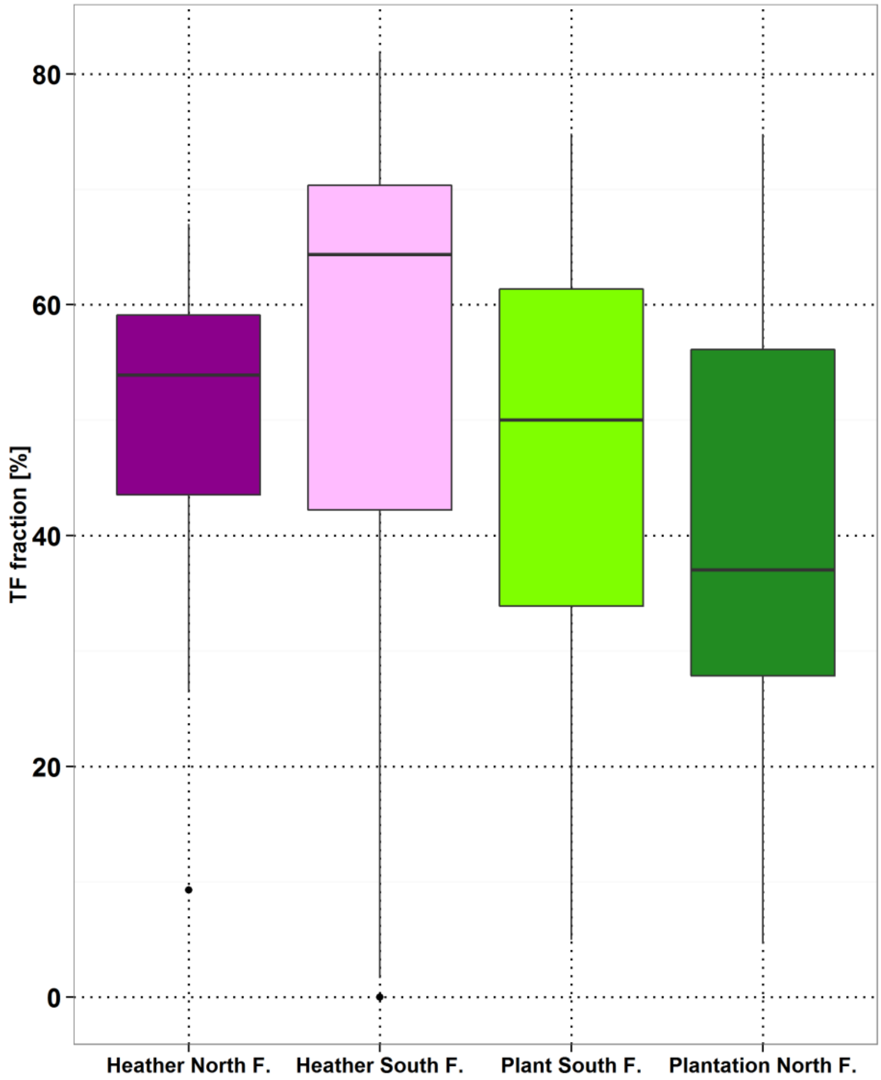

Figure 5-4: TF fraction [%] for the four sample sites summarised for all sampling dates: Heather north facing, heather south facing, plantation north facing and plantation south facing. The boxplots show median, inter quartile range, minimum and maximum values and the black dots represent the outliers.

Figure 5-5 shows the Pearson correlation between the TF fraction and quantity values and some of the meteorological parameters for the north facing site. The correlations for the other sites can be found in Appendix A (Figure Appendix A-3, Figure Appendix A-4, Figure Appendix A-5). The goodness of fit is quantified using the Pearson coefficient. Mean (q.TF.mean) and median (q.TF.median) TF values of both plantations and heather sites strongly correlated with the sum of GR and showed strong correlations with the maximum intensity of the GR. The TF variability, here expressed as the coefficient of variation (CV), however, shows the strongest correlation with mean wind speed, maximum daily wind speed and evapotranspiration. The latter one showed a stronger correlation with the TF of the south facing plantation and the TF quantity CV (0.61) for the south facing heather site (Appendix A).

The mean and median TF fraction values (f.TF.Mean, f.TF.Median) show correlations with wind speed (U.Mean, U.D.Max, U.Max), evapotranspiration (ET.Mean) and wind direction (WINDR.Mean). WINDR.Mean showed higher correlations for the heather sites. The CV (f.TF.CV) of the TF fraction mainly correlated with sum of GR (GR.Sum), maximum intensity of GR (GR.M.Int) and humidity (RH).

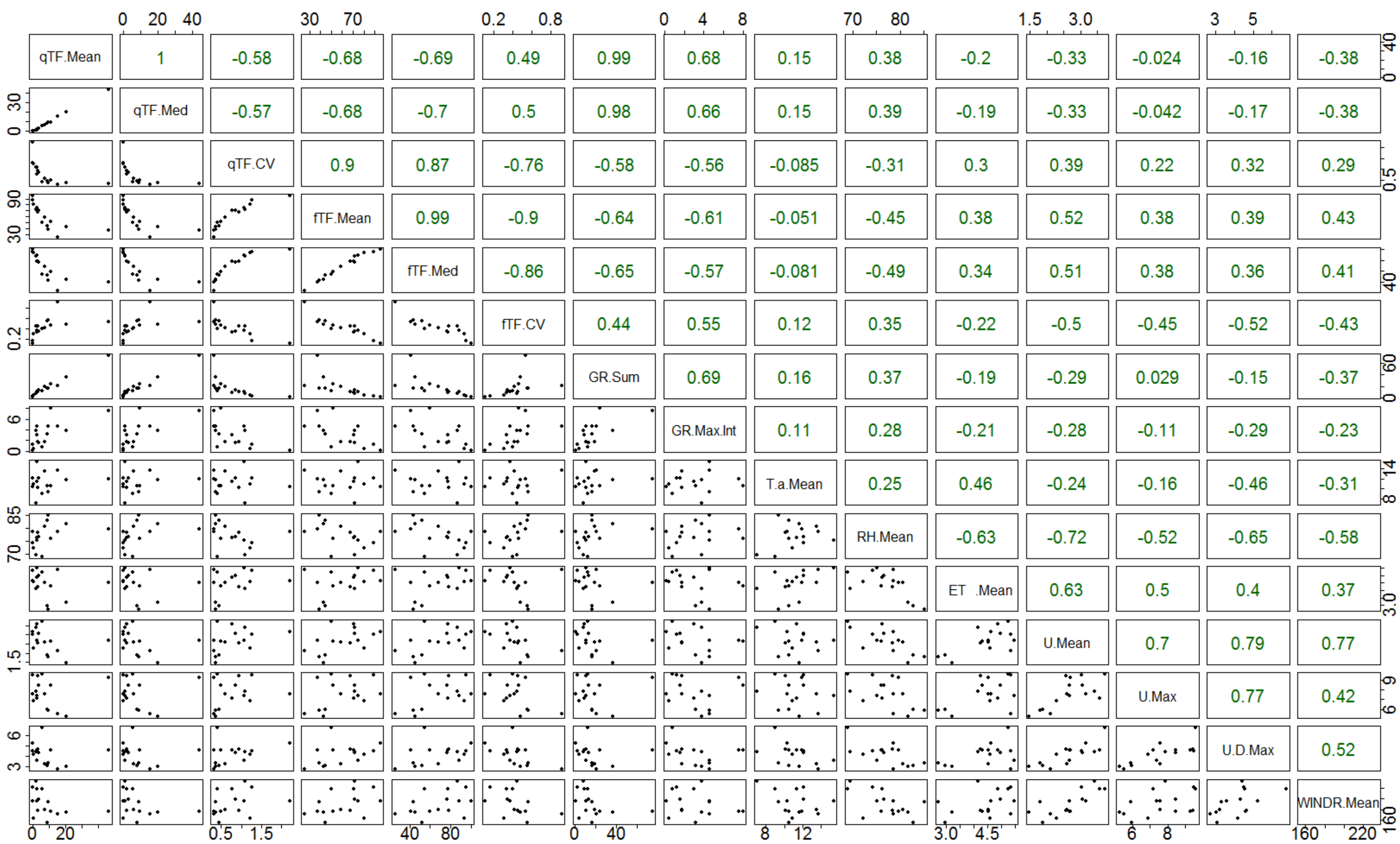

Figure 5-5: Pearson correlation and scatterplot for TF quantity (qTF.Mean, qTF.Median and qTF.CV) and TF fraction (fTF.Mean [mm], fTF.Median [mm] and fTF.CV [mm]) values for the north facing plantation and some hydroclimatic variables like GR.Sum [mm], GR.M.Int. [mmh^{-1}], T.a.Mean [°C], RH.Mean [%], ET.Mean [mm], U.Mean [ms^{-1}], U.Max [ms^{-1}], U.D.Max [ms^{-1}] and WINDR.Mean [°]. The green numbers represent the correlation coefficient r.

Similar findings could be seen analysing the results of the MLRM. To test for inter-site differences on dominant controls on temporal variations in TF, a multiple linear regression model was employed. Dependent input parameters (Y-values) were quantity mean, median and CV as amount of measured TF and fraction mean median and CV as fractions of GR. The parameters were averaged for each sample period and each site. The independent variables (X-variables) were the same meteorological parameters already used for the Pearson correlation (Figure 5-5), also summarized and averaged for the sample periods respectively. A stepwise AIC algorithm was employed in order to identify important parameters (Table 5-4, Table 5-5, Table 5-6, Table 5-7). Other parameters were rejected as they didn't show any significant improvement to the model accuracy. The models passed the normality test of the residuals.

Main influencing parameter for mean and median TF quantities for all sites (plantation and heather) is GR.Sum and U.Mean with very low p-values ($p<0.001$) for GR.Sum. All R^2 values for mean and median TF quantity were very high (≥ 0.97) indicating a good model fit. The quantity TF.CV showed very low R^2 values for the plantation sites, where it was either influenced by maximum wind speed (U.Max, north facing plantation) or maximum intensity of GR (GR.M.Int, south facing plantation). R^2 values were quite high for the quantity and fraction CV of the heather sites. The quantity CV for the north facing heather was dependent on GR intensity and wind speed whereas for the south facing plantation also ET, RH and WINDR played an important role. The fraction CV was mainly dependent on daily maximum wind speed, ET and RH for both heather sites.

The MLRM showed a weaker fit for mean and median TF fraction values (f.TF.Mean and f.TF.Median) compared to the TF quantity values but a better fit for TF fraction CV values. Mean and median values of the plantations were mostly influenced by GR.Sum and either U.Max, U.D.Max or U.Mean for all sites. The CV of the TF fraction for the plantation sites was mainly influenced by GR.M.Int and U.Max and U.D.Max accordingly whereas the fraction TF.CV for the heather sites was influenced by more variables (U.D.Max, ET.Mean, RH.Mean, T.a.Mean and WINDR.Mean).

Table 5-3: Multiple linear regression model (MLRM) of the north facing plantation. Y-variables are quantity TF mean, median and CV as well as mean, median and CV values for the TF fractions. X-variables are GR.Sum, U.Max and GR.M.Int. R^2 values show the model fit.

Y	*R^2*	*GR. Sum [mm] p- value*	*U.Max [m s^{-1}] p-value*	*GR M.Int [mm h^{-1}] p-value*
Plantation north facing				
qTF.Mean	0.98	<0.001	0.19	-
qTF.Median	0.97	<0.001	0.18	-
qTF.CV	0.34	-	0.02	-
fTF.Mean	0.57	0.003	0.05	-
fTF.Median	0.58	0.003	0.04	-
fTF.CV	0.46	-	0.08	0.03

Table 5-4: Multiple linear regression model (MLRM) of the south facing plantation. Y-variables are quantity and fraction TF values (mean, median and CV). X-variables are GR.Sum, U.Mean, GR.M.Int and U.D.Max. R^2 values show the model fit.

Y	*R^2*	*GR. Sum [mm] p- value*	*U.Mean [m s^{-1}] p-value*	*GR.M.Int [mm h^{-1}] p-value*	*U.D.Max [m s^{-1}] p-value*
Plantation south facing					
qTF.Mean	0.98	<0.001	0.68	-	-
qTF.Median	0.99	<0.001	0.61	-	-
qTF.CV	0.17	-	-	0.71	-
fTF.Mean	0.64	0.02	0.06	0.003	-
fTF.Median	0.59	0.03	0.07	0.005	-
fTF.CV	0.56	-	-	0.009	0.02

Table 5-5: Multiple linear regression model (MLRM) of the north facing heather. Y-variables are quantity and fraction TF values (mean, median and CV). X-variables are GR.Sum, U.Mean, GR.M.Int, U.D.Max, T.a., RH.Mean and ET.Mean. R^2 values show the model fit. R^2 values show the model fit.

Y	*R^2*	*GR.Sum [mm] p- value*	*U.Mean [m s^{-1}] p-value*	*GR.M.Int [mm h^{-1}] p-value*	*U.D.Max [m s^{-1}] p-value*	*Ta.Mean [°C] p-value*	*RH.Mean [%] p-value*	*ET.Mean [mm] p-value*
Heather north facing								
q.TF.Mean	0.97	<0.001	0.2	-	-	-	-	-
q.TF.Median	0.98	<0.001	0.03	-	-	-	-	-
q.TF.CV	0.62	-	-	0.04	0.003	-	-	-
f.TF.Mean	0.72	-	-	0.005	0.002	-	-	-
f.TF.Median	0.68	-	-	0.008	0.002	-	-	-
f.TF.CV	0.72	-	-	-	0.003	0.008	0.1	0.003

Table 5-6: Multiple linear regression model (MLRM) of the south facing heather. Y-variables are quantity and fraction TF values (mean, median and CV). X-variables are GR.Sum, U.Mean, U.Max, U.D.Max, GR.M.Int, U.D.Max, ET.Mean, RH.Mean and WINDR.Mean. R^2 values show the model fit. R^2 values show the model fit.

Y	*R^2*	*GR.Sum [mm] p- value*	*U.Mean [m s^{-1}] p-value*	*U.Max [mm s^{-1}] p-value*	*U.D.Max [mm s^{-1}] p-value*	*ET.Mean [mm] p-value*	*RH.Mean [%] p-value*	*WINDR. Mean [m s^{-1}] p-value*
Heather south facing								
q.TF.Mean	0.99	<0.001	0.53	-	-	-	-	-
q.TF.Median	0.99	<0.001	0.11	-	-	-	-	-
q.TF.CV	0.32	-	-	0.14	0.01	0.50	0.30	0.1
f.TF.Mean	0.36	0.03	-	-	0.13	-	-	-
f.TF.Median	0.29	0.07	-	-	0.14	-	-	-
f.TF.CV	0.65	-	-	-	0.04	0.50	0.30	0.12

Intra-Site Variability

There were high intra-site variabilities in TF for each sample period and each collector. Figure 5-6 and Figure 5-7 show the average TF for each collector in the north and south facing plantations respectively, as well as the collector's distance to a tree and its canopy coverage. With increasing mean TF throughout the sample period and greater BHD of the trees, the dots and triangles increase in size. The background colour shows the canopy coverage in %. Purple values indicate no canopy cover and dark green values revere to a high canopy cover. Canopy coverage was quite different for the two sites (Table 4-4).

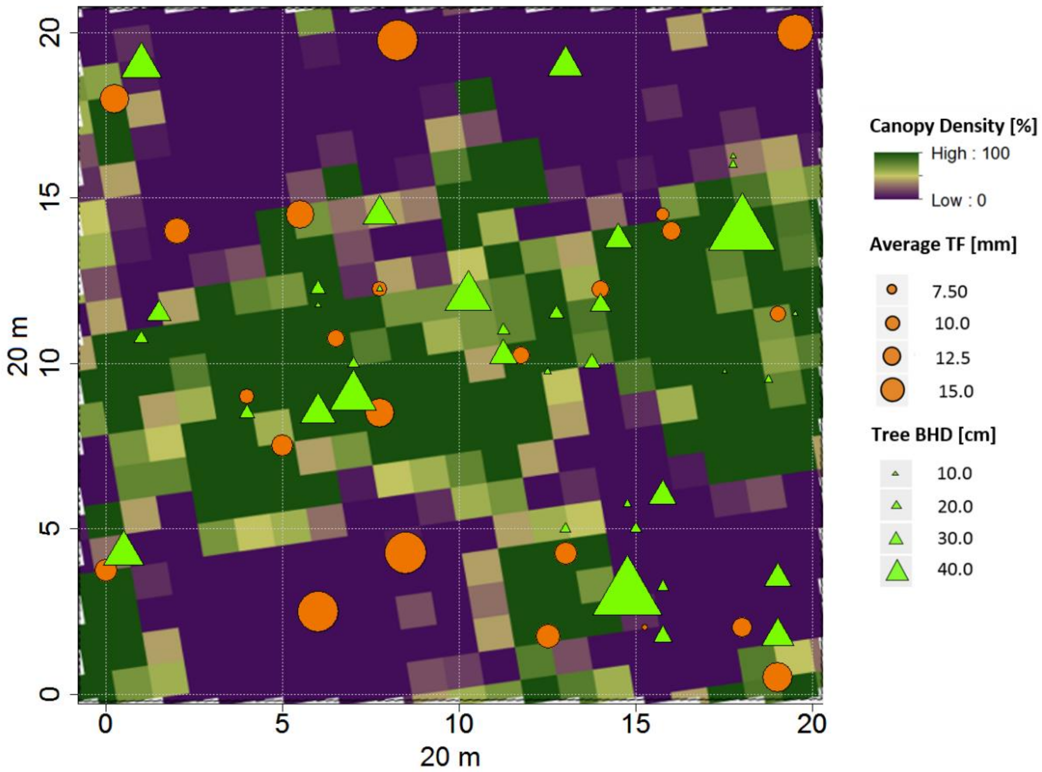

Figure 5-6: 20 x 20 m grid of the north facing plantation with 23 TF collectors (orange dots) and trees (green triangles). Small points indicate small amounts of average TF (over all sample dates) bigger points indicate more TF (up to 15 mm). Bigger triangles represent trees with greater BHD (in cm), smaller triangles represent trees with smaller BHD. Dark green squares indicate high canopy coverage, purple indicates no canopy coverage [%].

Figure 5-6 represents the grid in the north facing plantation. The 23 collectors showed very different mean TF amounts. More TF occurred for collectors placed in the open spots and further away from the trees. There was very little TF for collectors placed in the green areas with very dense canopy coverage and in close proximity to the stem of a tree. Smallest amounts could be found for the collector between two big trees in the lower right square (position: x = 15.5 m, y = 2.25 m). This collector was placed in about 30 cm distance to both of the surrounding trees and its canopy coverage was 81% which was the highest amongst all collectors. The mean TF as a fraction of GR.Sum over all collectors was 39.5%, the minimum was 8.4% and the maximum 79.6%.

Figure 5-7 the 20 x 20 m grid of the south facing plantation with the collectors #51 – 75. There was less variability in TF amounts compared to the north facing site. The canopy coverage in the south facing plantation was less dense with more areas with medium high coverage and less open areas compared to the other plantation. There were more trees with larger BHDs in the south facing plantation (Table 4-4) and they were more evenly spread over the whole plot. TF amounts between the collectors didn't differ as much as for the north facing plantation. There were fewer collectors with very limited amounts of TF and more that collected medium amounts. The mean amount in TF as a fraction of GR per collector over all sample dates was 45.8%. Minimum and maximum amounts were 17.7% and 75.4% respectively.

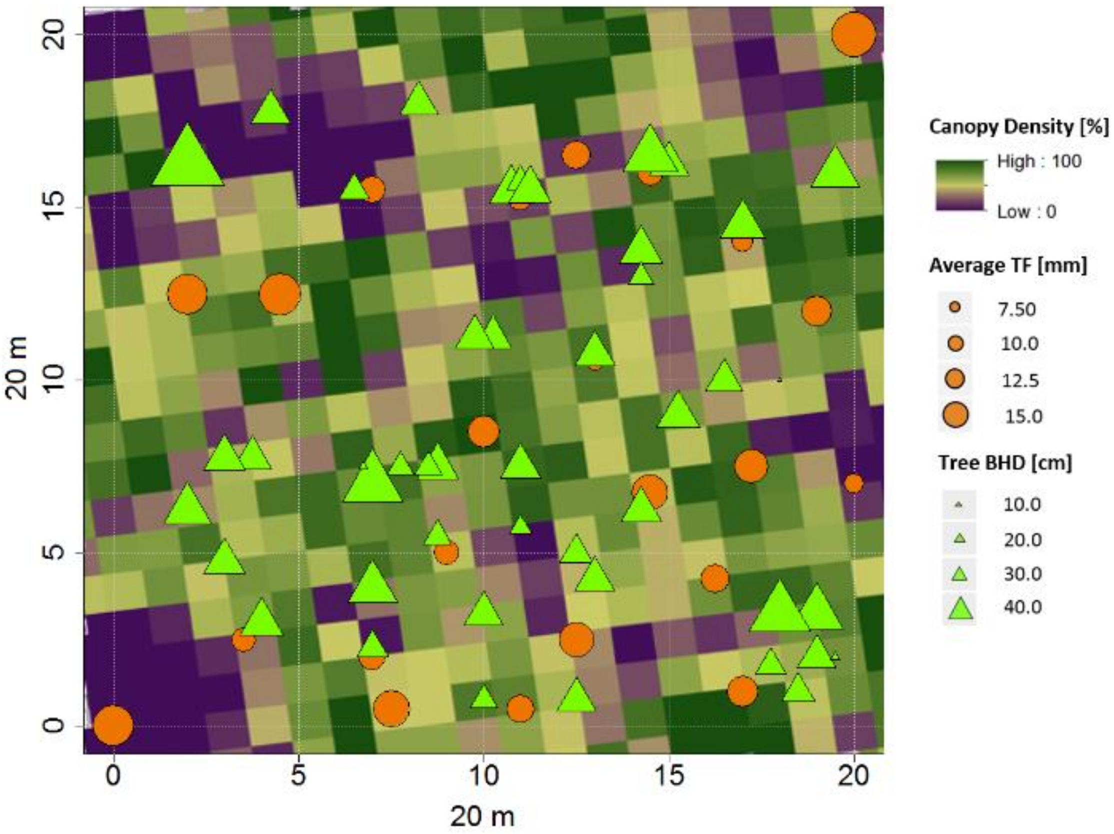

Figure 5-7: 20 x 20 m grid of the south facing plantation with 25 TF collectors (orange dots) and trees (green triangles). Small points indicate small amounts of average TF (over all sample dates) bigger points indicate more TF (up to 15 mm). Bigger triangles represent trees with greater BHD [cm], smaller triangles represent trees with smaller BHD. Dark green squares indicate high canopy coverage, purple indicates low canopy coverage [%].

For an intra-site comparison between the collectors at each site, a MLRM was run for the plantation sites and a linear regression (LR) for the heather sites. Input Y-variables were mean, median and maximum TF averaged for each collector over the entire field season. X-variables that influenced the amount of SF generation were canopy coverage [%] for each collector and distance to the closest tree for the collectors in the plantations [m]. The datasets passed the normality test. The model showed a rather good fit for the median TF at the plantation sites. Also the R^2 value for the mean TF for the north facing plantation were high. P-values for canopy coverage for the plantations were low, especially for the north facing plantation (<0.001) indicating that canopy coverage had a high influence on mean and median TF in the collectors. Distance to the tree improved the model fit slightly. No relationship between canopy cover and the amount of TF for the heather sites could be found ($R^2 < 0.1$). TF mean, median and CV amount cannot be explained by the shrub's canopy coverage.

Table 5-7: Multiple linear regression model (MLRM) to compare intra-site spatial variability of the collectors at the plantations. Y-variables are TF mean, median and max of each site, X-variables are Canopy Coverage (derived from digital photography) and distance to tree. R^2 values show the fit of the MLRM.

Y		*R^2*	*Canopy Cover: p- value*	*Distance Tree: p- value*
Plantation north facing				
	TF.Mean	0.71	<0.001	0.43
	TF.Median	0.76	<0.001	0.98
	TF.CV	0.47	<0.001	0.04
Plantation south facing				
	TF.Mean	0.51	0.014	0.05
	TF.Median	0.79	0.046	0.22
	TF.CV	0.21	-	0.01

5.2.2 Stemflow

Figure 5-8 shows all observed SF values versus GR.Sum. There is some variability in the relationship between GR.Sum and SF generation, however, in general the correlation was strong. Highest SF generation occurred during a sample period with a high intensity event from about 25 mm. Even though event intensities were with 7.6 mm h^{-1} only slightly lower for the period from 06[th] till 20[th] of July (total GR.Sum = 74.8 mm) much less SF was generated. Most SF measurements were below 2000 ml and some were very low (0 ml or close to 0 ml) for some trees during the whole sampling period. There was a threshold for SF generation which was > 7 mm for birch trees and > 10 mm for Scots pine.

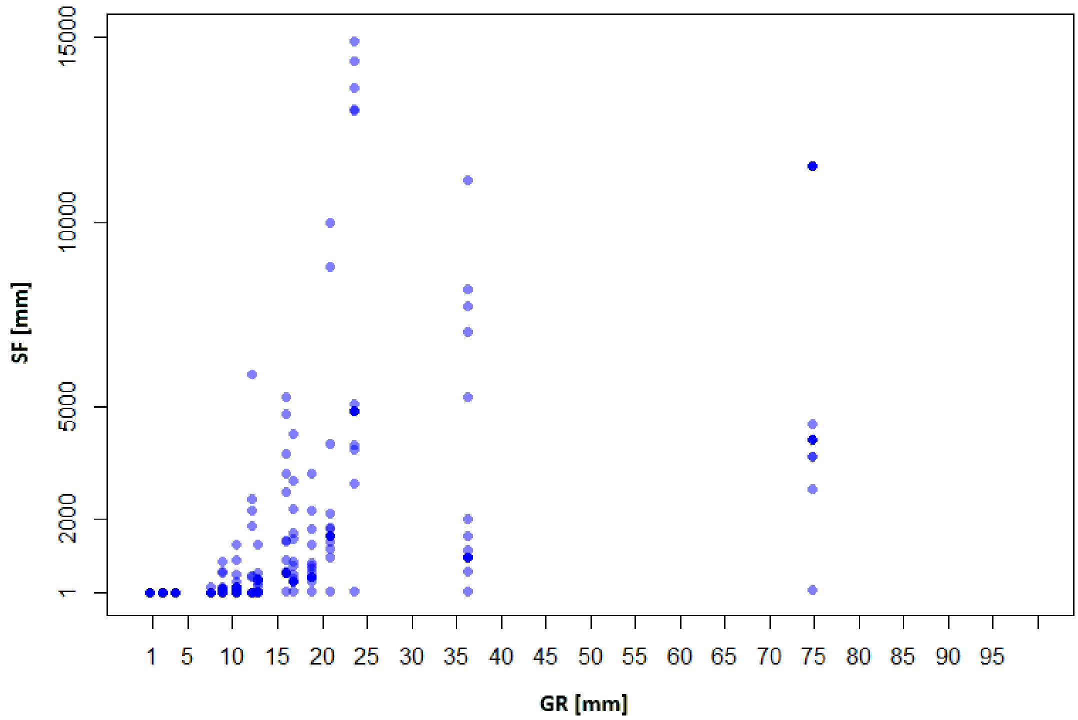

Figure 5-8: Mean SF [mm] of both plantation sites over the 16 sampling periods plotted against mean GR [mm].

Inter-Site Variability

SF amounts were highly variable over the different sample periods. In Figure 5-9 the SF amounts are presented for both plantation sites for the 16 sample periods. Measurements for the younger, north facing plantation were in general higher than values for the south facing plantation. There were three sample periods for the north facing and four for the south facing plantation where GR.Sum values were low and no SF was generated. On the first sample date (1st of June) SF collectors for the south facing plantation had not been installed, yet.

Peaks in SF generation occurred at the same time for both plantations (20th and 30th of July). This pattern could also be seen for very low values for the end of June, beginning of July, beginning of August and beginning of September. In the sample period from 25th of June till 6th of July GR.Sum was 10.4 mm but no SF was generated for the south facing plantation whereas with a GR amount of 8.8 mm in the time period of 28th of August till 3rd of September a mean value of 126.0 mm of SF has been generated. One reason for that could be the maximum event intensity which was higher in the August – September period (3 mm h^{-1}). Highest SF amounts could be measured when maximum event intensity was comparable high, e.g. 20th of July – 30th of July where the event intensity was with 8 mm h^{-1} the highest measured value for the whole sample period.

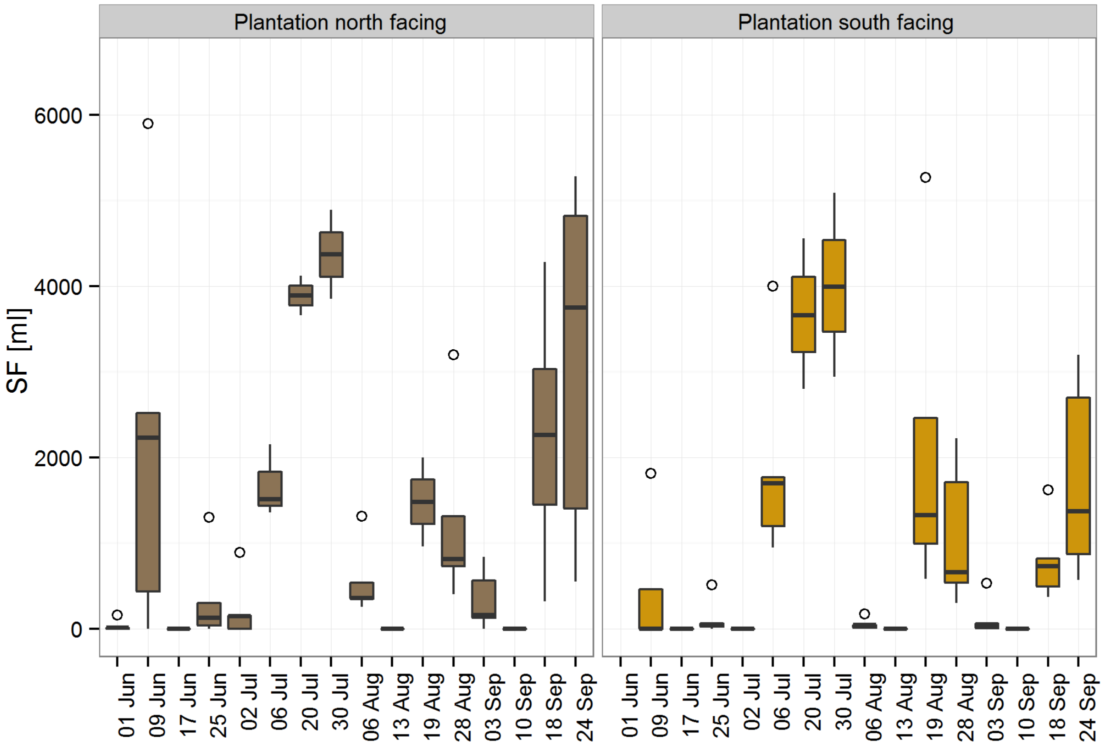

Figure 5-9: SF [ml] for the both plantations. Brown colour represents the north facing, yellow the south facing plantation.

In Figure 5-10 the SF fraction [%] of GR.Sum is shown for each site. SF of both plantation sites only accounts for a very low percentage of the GR.Sum, at maximum of 2.5% of total GR.Sum, not taking the outliers into account. Median and interquartile-range were higher for the younger, north facing plantation. The median for the south facing plantation was below 0.5% and there were more weeks where no SF was generated.

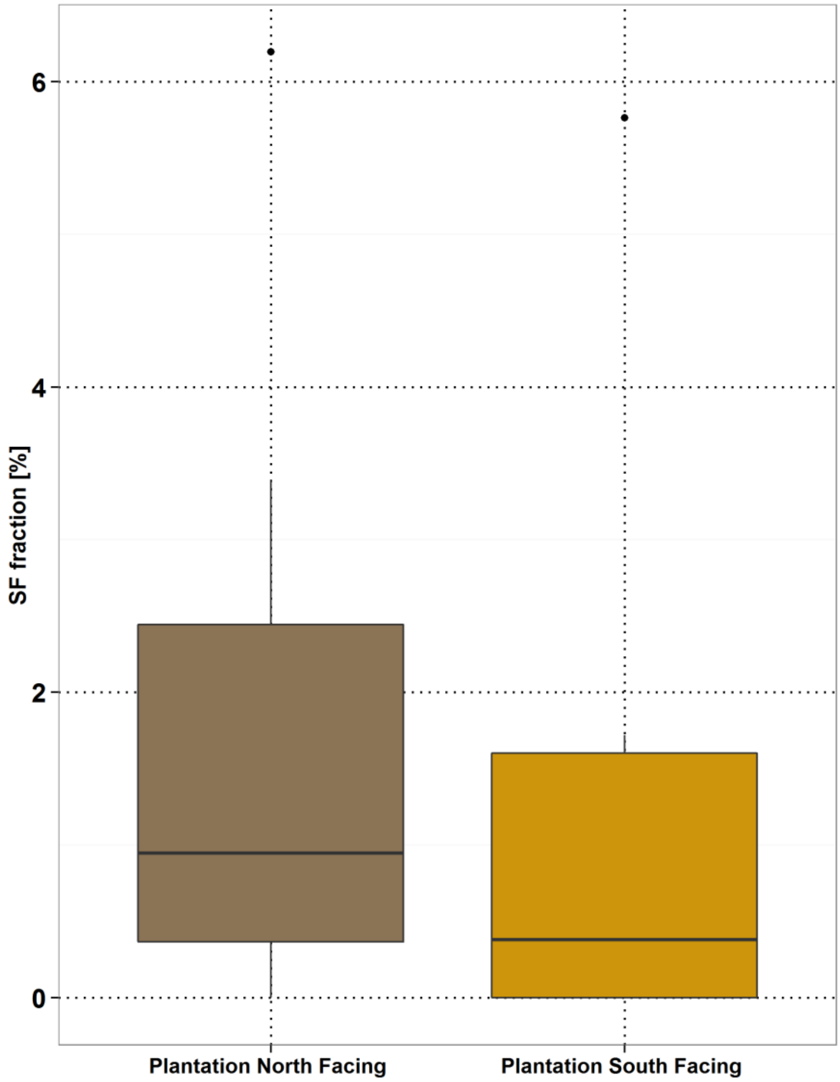

Figure 5-10: SF fraction [%] as fraction of GR for the 2 plantation sites summarised for all sampling dates.

To detect the statistically relevant correlations between the SF amounts and the meteorological parameters, a scatterplot with a correlation using the Pearson approach was generated (Figure 5-11, Figure Appendix B-1). SF shows a strong correlation to GR.M.Int and GR.Sum for both plantations. The CV is mainly dependent on WINDR, U.Mean and ET (north facing site) and is additionally driven by the maximum and daily maximum wind speed at the south facing plantation.

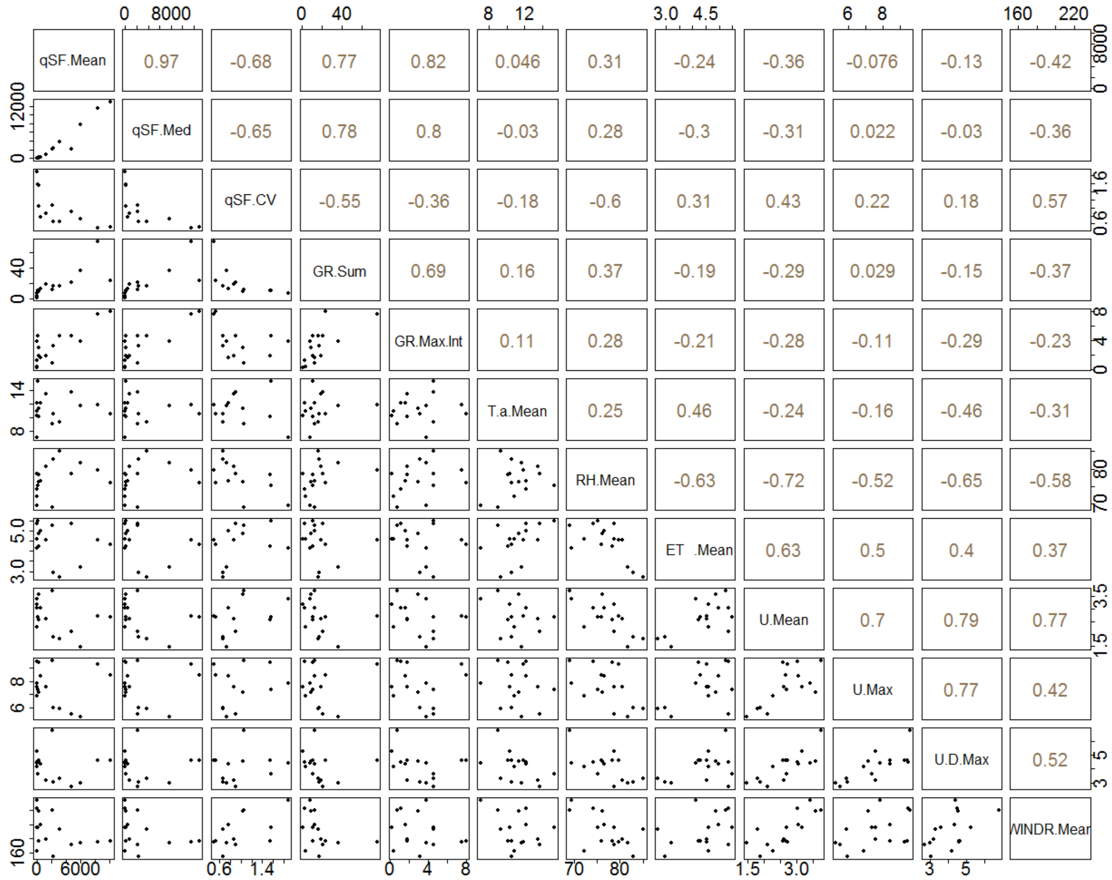

Figure 5-11: Pearson correlation and Scatterplot for SF quantity (qSF.Mean, qSF.Median and qSF.CV) values for the north facing plantation and shydroclimatic variables like GR.Sum [mm], GR.M.Int. [mm h^{-1}], T.a.Mean [°C], RH.Mean [%], ET.Mean [mm], U.Mean [m s^{-1}], U.Max [m s^{-1}], U.D.Max [m s^{-1}] and WINDR.Mean[°]. The brown numbers represent the correlation coefficient r.

To compare the SF sites and get the main parameters influencing SF, a MLRM was developed. Dependent input variables (Y-variables) were mean, median and CV of the SF amount. Independent variables (X-variables) were the same meteorological variables as for the TF analysis. R^2 values for mean and median SF were with values between 0.76 and 0.81 quite high, indicating a high ability of those variables to predict SF. Main driving factors for mean and median SF amount were maximum intensity and total amount of GR. R^2-values for the CV were a bit lower (0.47 and 0.63 respectively). Influencing parameters were maximum intensity of GR, wind speed mean and air temperature for both sides plus maximum and daily maximum wind speed and humidity for the north facing plantation.

Table 5-8: Multiple linear regression model (MLRM) to compare the SF sites. Y-variables are SF mean and median of each site, X-variables are Wind direction and GR.M.Int. R^2 values show the model fit. P-values show the influence of the variables.

Y	R^2	*GR.M.Int [mm] p- value*	*U.Mean [m s^{-1}] p-value*	*U.Max [mm s^{-1}] p-value*	*U.D.Max [mm s^{-1}] p-value*	*RH.Mean [%] p-value*	*WINDR [°] p-value*	*Ta [°C] p-value*
North facing plantation								
qSF.Mean	0.76	<0.001	0.01	-	0.02	-	-	-
qSF.Median	0.80	<0.001	0.005	-	0.002	-	-	-
qSF.CV	0.47	0.19	0.28	0.12	0.11	0.13	0.19	0.19
South facing plantation								
qSF.Mean	0.76	<0.001	-	-	-	-	-	0.11
qSF.Median	0.81	<0.001	-	-	-	-	-	0.11
qSF.CV	0.63	0.06	0.03	-	-	-	-	0.25

Intra-Site Variability

The beach was found to produce in average more SF than the Scots pine trees. However, statistical testing was due to marginal number of representatives per species (four Scots pine trees and one birch tree per plantation) not possible. The different amount of SF produced by trees showed no relevant correlation with the BHD ($R^2 < 0.2$).

5.3 Differences in Isotopic Composition

5.3.1 Throughfall Isotopes

Isotopic composition was temporally very variable. $\delta^{18}O$ for GR ranged from -15.21‰ to -0.92‰ whereas δ^2H ranged from -115.08‰ to -13.86‰. Comparing both $\delta^{18}O$ and δ^2H compositions for TF and GR samples, it could be shown, that values were most negative, hence most depleted in heavy isotopes for the first sample period (1st of June, 2015) where mean T.a (7.0 °C) was the lowest during the whole field season (Table 5-1). GR isotopes were more enriched in heavy isotopes during sample periods with higher mean T.a (15.4 °C) (e.g. 25th of June - 2nd of July, 2015). Insufficient amounts of GR (< 1.0 mm) precluded any collection of isotope samples for 10th of September.

Figure 5-15 shows GR amount, $\delta^{18}O$ values for GR and weighted GR $\delta^{18}O$ values for the sample dates as well as the boxplots for the $\delta^{18}O$ composition of all sample sites. TF $\delta^{18}O$ values from -15.29‰ to -0.56‰ for all periods. $\delta^{18}O$ was very variable over the different sample periods.

Samples were more depleted in ^{18}O the beginning, mid of July and towards the end of the field season and were enriched in ^{18}O for late June, early July and around August. For weeks with greater precipitation events, samples (both GR and TF) were more depleted in ^{18}O. TF $\delta^{18}O$ boxplots for all sites are very similar to the weighted precipitation $\delta^{18}O$ values of GR. The greatest differences between weighted $\delta^{18}O$ values of GR and TF boxplots occurred on the 2nd sample date in June (2nd boxplot) and the first sample period in September.

A similar pattern could be seen for Figure 5-13 that shows the δ^2H signatures of GR and the δ^2H TF boxplots. There were distinctive variations in daily δ^2H values of GR with values ranging between -119.54‰ and -12.89‰. Following the pattern already seen for $\delta^{18}O$, δ^2H values are most depleted in early June, mid of July and in the end of the field season and the weighted δ^2H values for the GR were also out of range with the TF boxplots for the 2nd sample date in June and first sample date in September. For the other sample dates, weighted δ^2H were within the range of the δ^2H values of the TF boxplots.

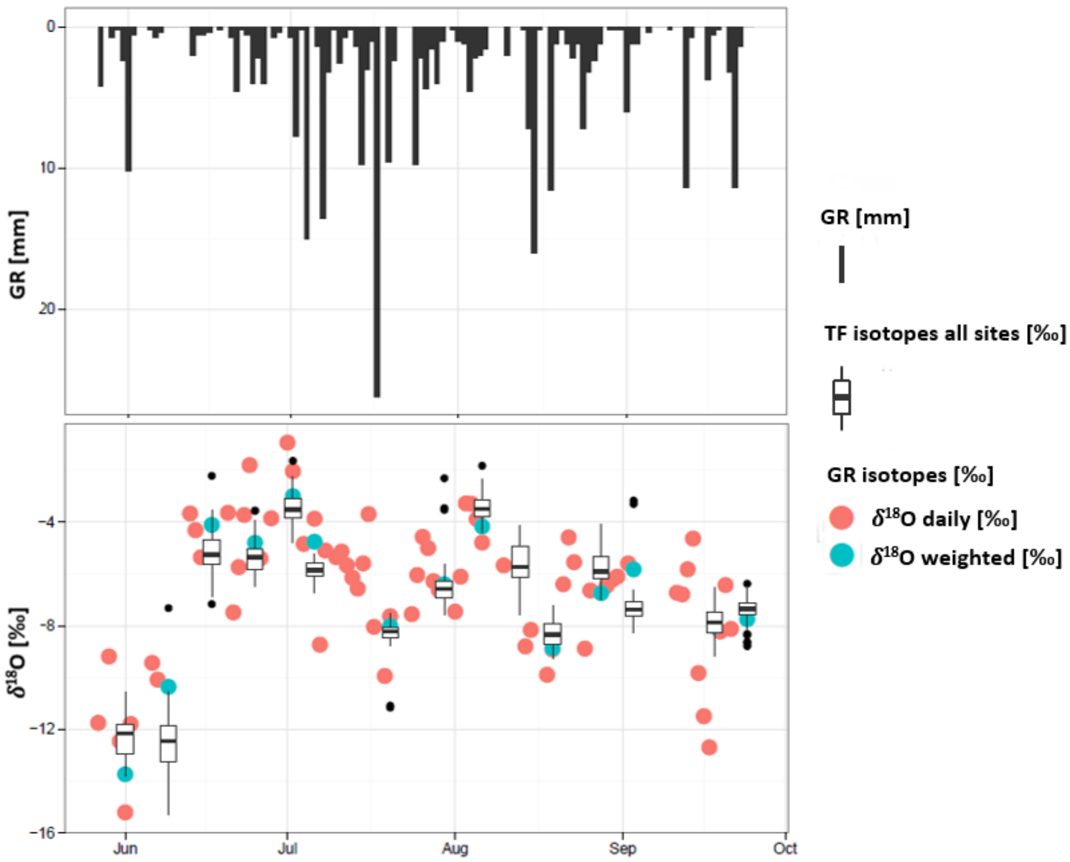

Figure 5-12: $\delta^{18}O$ boxplots [‰] with outliers (black points) of TF and $\delta^{18}O$ [‰] values of GR daily (red) and weighted for the sample periods (blue).

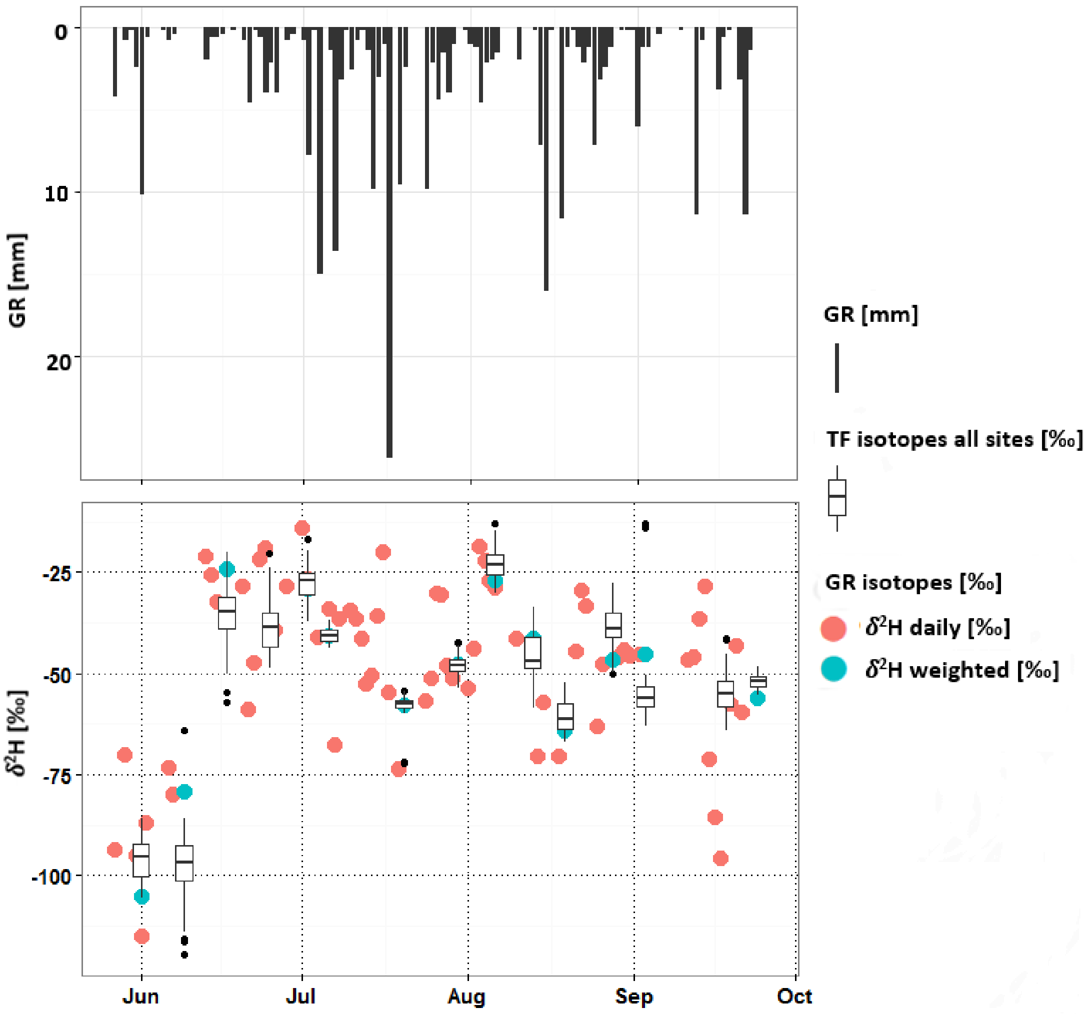

Figure 5-13: δ²H boxplots with outliers (black points) [‰] of TF and δ²H values [‰] of GR daily (red) and weighted for the sample periods (blue).

Inter-Site Variability

To detect the offset of the TF isotope samples from the LMWL, lc-excess was calculated. Figure 5-14 shows lc-excess of GR and TF for all sample dates. There were major differences between TF values for the plantation and the north facing heather sites that occurred from late June till mid of July where daily air temperatures were at their maximum (Table 5-1). For the south facing heather site those major differences were found most of July. In those periods, TF lc-excess values for all sites were around +5‰ to +10‰, whereas GR lc-excess showed values of -5‰ to -10‰. Minor differences occurred in early June where T.a was low. Here, lc-excess values were negative for the plantation, whereas GR and heather lc-excess values were positive. Spatial differences between the sites were small, whereas higher differences were found between the heather sites. For the warmer early July periods, the south facing heather site had lower lc-excess values compared to the north facing site. The peak for the north facing heather site in late August cannot be explained and seems to be an outlier or measuring mistake.

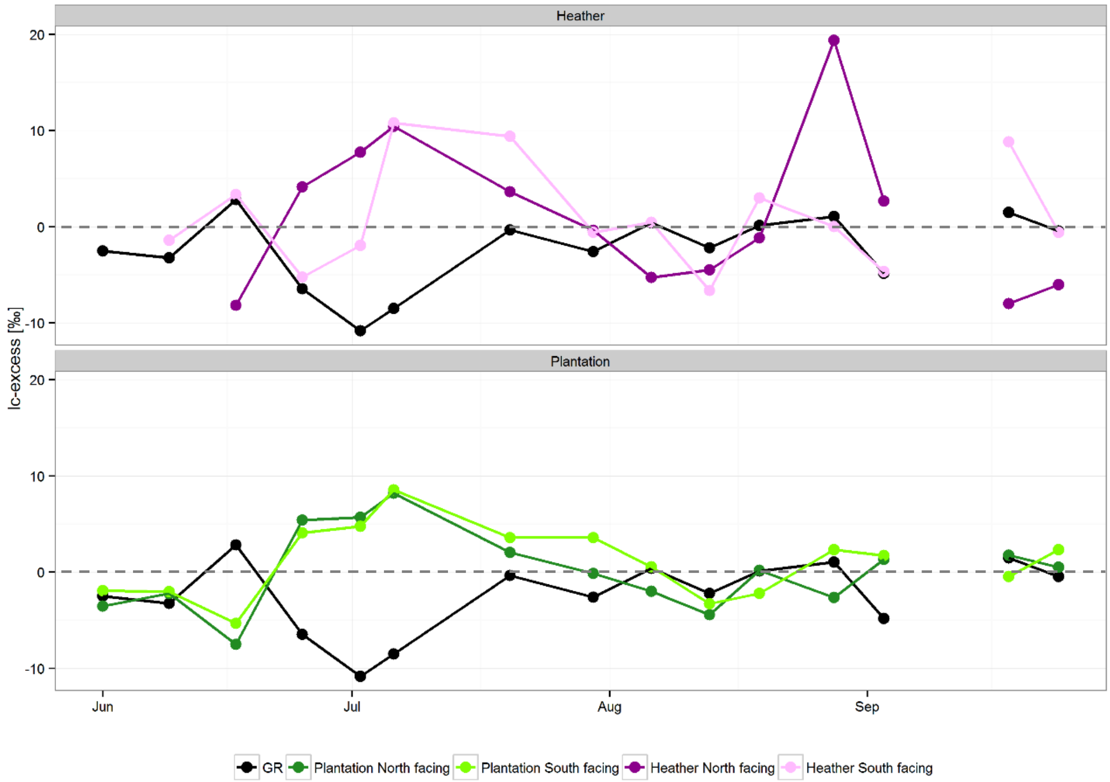

Figure 5-14: TF lc-excess values for the heather and plantation sites. The points represent the values calculated for the sample dates.

Figure 5-15 shows the $\delta^{18}O$ Boxplots of TF over all sample sites and dates. The $\delta^{18}O$ values were highly variable over the field season. Boxplots for the heather sites showed a smaller inter-quartile range compared to the plantations. However, $\delta^{18}O$ values showed the same pattern for all sites, e.g. were most depleted or enriched in ^{18}O for the same sample dates. It is very noticeable, that for the coldest weeks (early June) the $\delta^{18}O$ values were very negative for both plantation sites and the north facing heather site (the south facing heather site hasn't been installed at that time). Intra-site differences were quite strong for some of the sample dates (e.g. early and mid of June and 13th of August), whereas this effect could mostly be seen for the plantation sites. A similar pattern was found for the $\delta^{2}H$ TF boxplots Figure 5-16. The $\delta^{2}H$ values showed a high temporal variability and higher inter-quartile differences for the plantation sites. Lowest values, thus most depleted in ^{2}H also occurred for the first two sample dates in early June, most enriched values were found for the 5th and 9th sample date where T.a was high (Table 5-1).

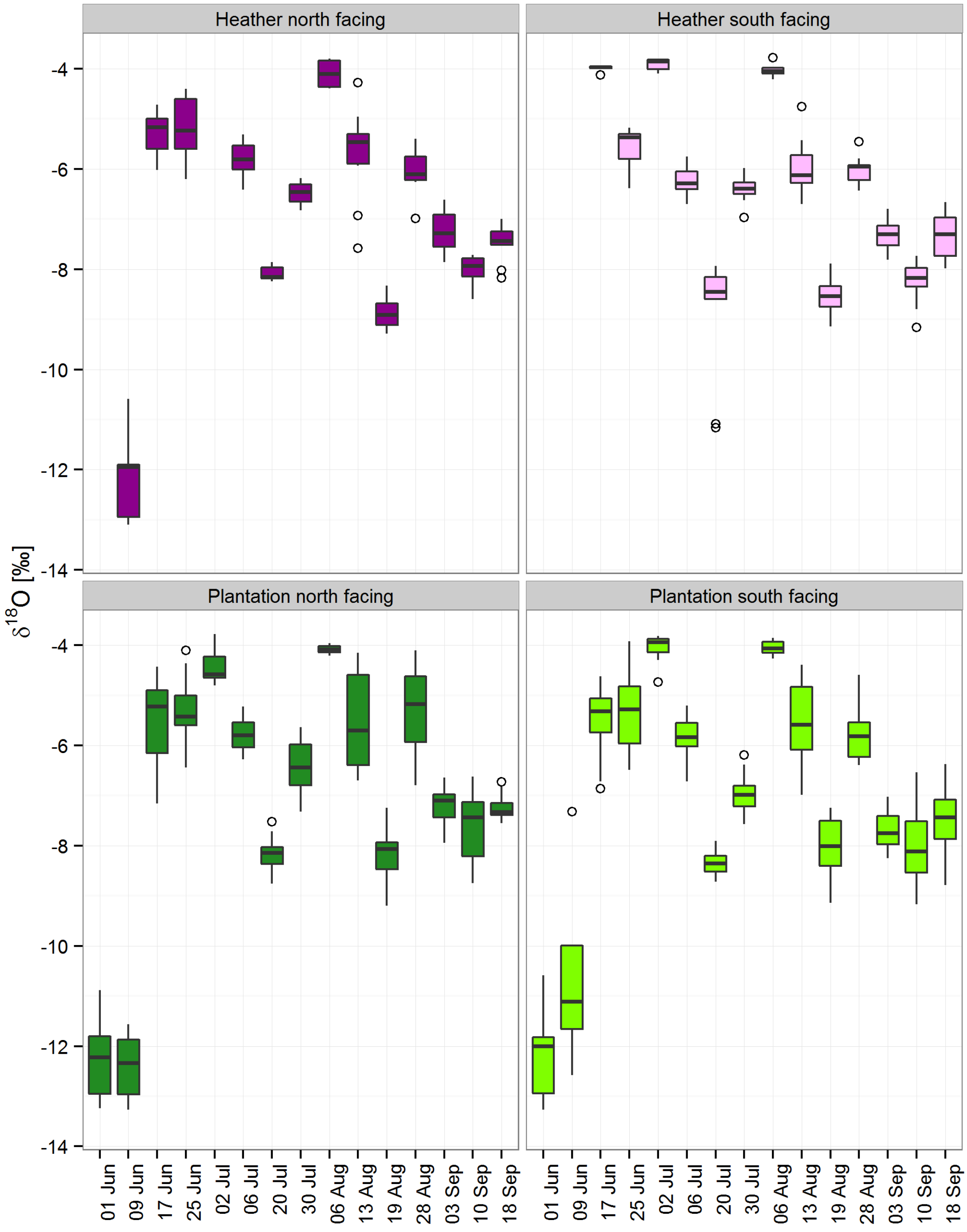

Figure 5-15: δ^{18}O Boxplots of TF over all sample sites and dates. Outliers are marked as points.

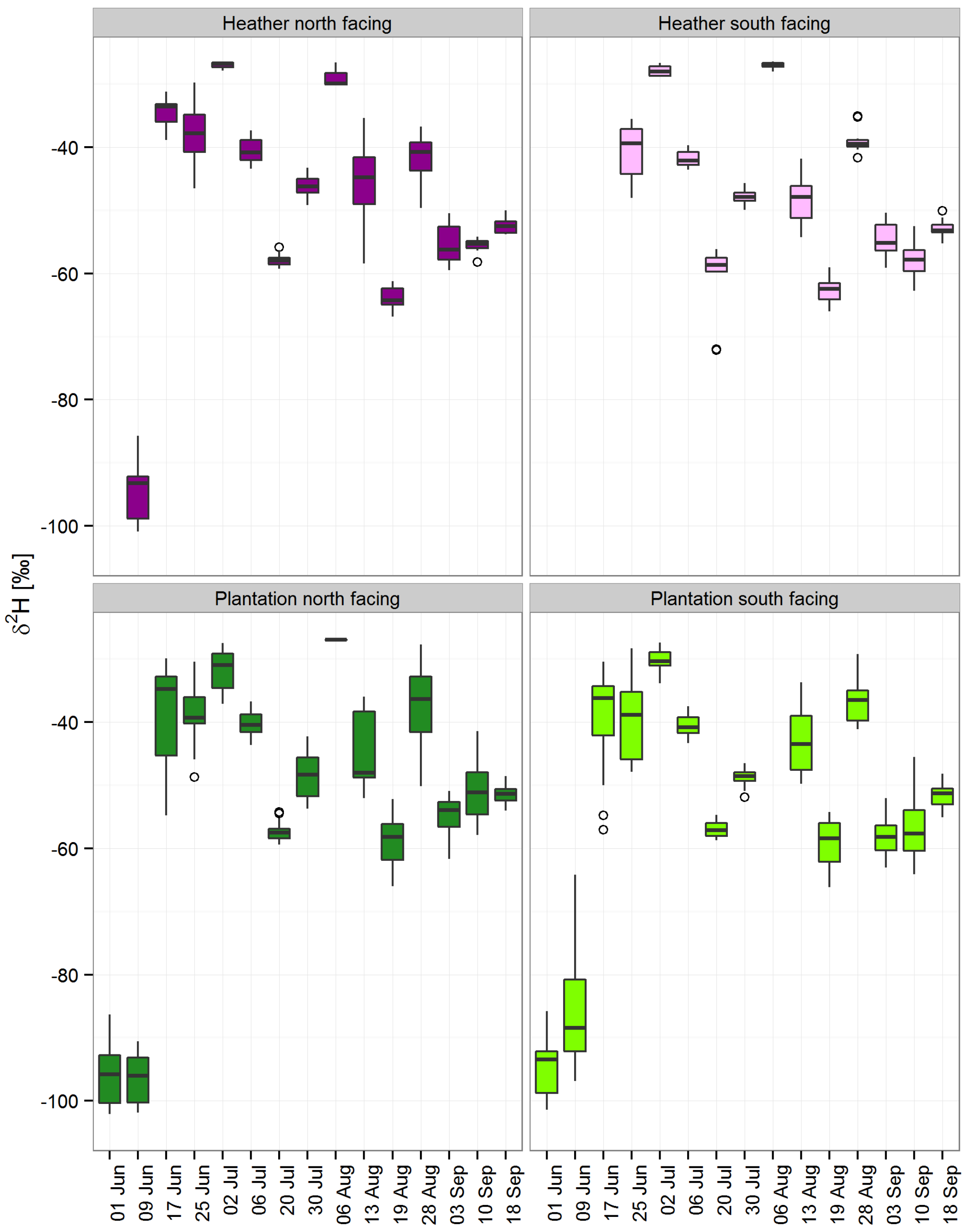

Figure 5-16: δ^2H Boxplots of TF over all sample sites and dates. Outliers are marked as points.

The Person correlation (Figure 5-17) showed high correlations between the volume weighted TF δ^{18}O/δ^2H values, the isotopic composition of the volume weighted GR δ^{18}O/ δ^2H values and T.a for the north facing plantation. Pearson correlations for the other sites can be found in Appendix C (Figure Appendix C-3, Figure Appendix C-4, Figure Appendix C-5). Low to medium high correlations occurred between the isotope values and RH. There was no correlation between isotope values and the amount of GR, maximum event-intensity and wind speed or wind direction.

For the TF CV however, a low correlation with GR.Sum and RH was found. Similar results were found for the south facing plantation and the heather sites (Figure Appendix A-3, Figure Appendix A-4, Figure Appendix A-5). However, the TF CV of the south facing plantation was additionally influenced by maximum intensity of GR.

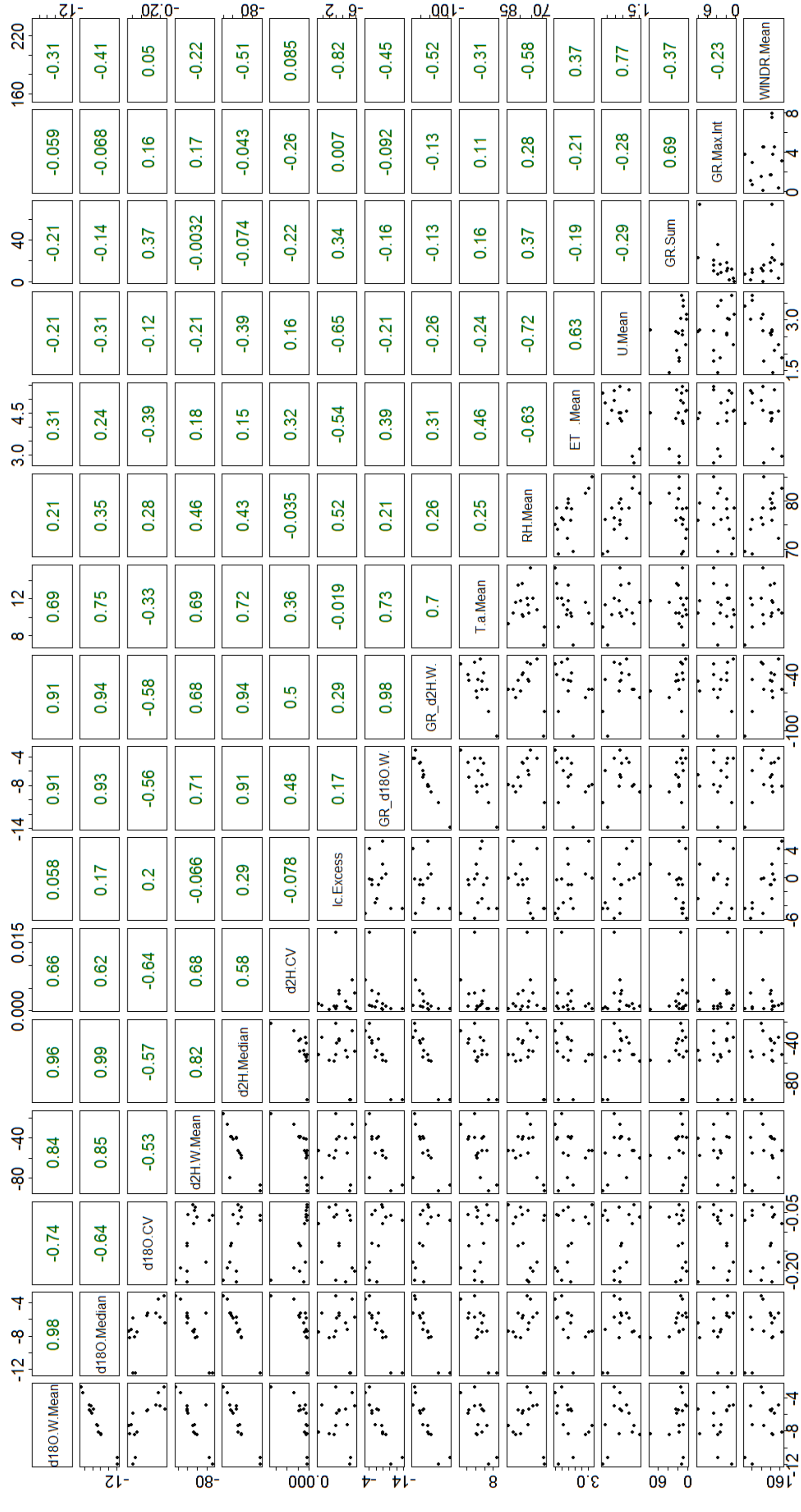

Figure 5-17: Pearson correlation and Scatterplot for TF isotopic compositions (d18O.W.Mean, d18O.W.Median and d18O.W.CV) values for the north facing plantation and isotopic signatures for the GR (GR_d18.W, GR2H.W), lc-excess and hydroclimatic variables like T.a.Mean [°C], RH.Mean [%], ET.Mean [mm], U.Mean [ms^{-1}] and WINDR.Mean [°]. The green numbers represent the correlation coefficient r.

The MLRM for the plantation sites showed similar results compared to the Pearson correlation. Dependent input parameters (Y-values) were volume weighted δ^{18}O and δ^2H values for each site and sample date (δ^{18}O.TF.Mean/ δ^2H.TF.Mean), median δ^{18}O and δ^2H (δ^{18}O.TF.Median/ δ^2H.TF.Median) and δ^{18}O and δ^2H coefficient of variation (δ^2H.TF.CV/δ^{18}O.TF.CV). The independent x-variables were the same parameters already used for the Pearson correlation (Figure 5-24), also summarized and averaged per site for each sample period.

Minimum and median δ^{18}O/ δ^2H of TF were highly influenced by the GR isotopic composition. Additionally, daily maximum wind speeds, temperature and maximum intensity of GR were influencing factors as well. The R^2 values for these regressions were high (R^2 >0.8). The CV for δ^{18}O/ δ^2H was mainly influenced by GR isotopic composition for the north facing plantation (low to median R^2) and was driven by daily maximum wind speed and maximum intensity for the south facing plantation.

The heather TF isotopic composition was mainly dependent on GR isotopes as well. T.a.Mean, ET and daily maximum wind speed played an important role, too. The CV was driven by many different parameters (GR isotopic composition, T.a.Mean, ET.Mean, U.Mean and GR.M.Int) with low R^2 values for the south facing heather sites.

Table 5-9: MLRM for the north facing plantation. Y-variables are mean, median and CV of δ^2H and δ^{18}O, X-variables are the meteorological parameters derived by the weather station and calculated ET [mm]. R^2 values show the fit of the model. P-values show the importance of the parameter.

Y	*R^2*	*GR δ^{18}O/ GR δ^2H [‰] p- value*	*Ta. Mean [°C] p-value*	*U.D.Max [mm s^{-1}] p-value*	*U.Mean [mm s^{-1}] p-value*	*ET.Mean [mm] p-value*
Plantation north facing						
δ^{18}O.TF.Mean	0.82	<0.001	-	0.18	-	-
δ^{18}O.TF.Median	0.9	<0.001	-	0.04	0.21	0.24
δ^{18}O.TF.CV	0.25	0.03	-	-	-	-
δ^2H.TF.Mean	0.46	0.18	0.18	-	-	-
δ^2H.TF.Median	0.93	<0.001	-	0.004	-	-
δ^2H.TF.CV	0.18	0.07	-	-	-	-

Table 5-10: MLRM for the north facing heather. Y-variables are mean, median and CV of δ^2H and $\delta^{18}O$, X-variables are the meteorological parameters derived by the weather station and calculated ET [mm]. R^2 values show the fit of the model. P-values show the importance of the parameter.

Y	R^2	*GR δ18O/ δ2H [‰] p- value*	*Ta. Mean [°C] p-value*	*ET.Mean [mm] p-value*	*U.D.Max [mm s-1] p-value*	*GR M.Int [mm h-1] p-value*	*U.Mean [mm s-1] p-value*
Heather north facing							
δ18O.TF.Mean	0.93	<0.001	0.08	0.05	0.17	-	-
δ18O.TF.Median	0.95	<0.001	0.03	0.02	0.11	-	-
δ18O.TF.CV	0.66	0.02	0.05	0.12	0.05	0.04	-
δ2H.TF.Mean	0.96	<0.001	0.02	0.26	0.29	-	0.19
δ2H.TF.Median	0.96	<0.001	-	-	-	-	0.03
δ2H.TF.CV	0.79	0.01	0.15	-	0.04	0.01	0.12

Intra-Site Variability

The dual isotope plot, pictured in Figure 5-18, shows the isotopic composition of all the TF and SF samples (>1100 samples) for the whole field season and the LMWL and GMWL. There was a high variation in the isotopic composition between collectors and sites and a majority of the values was located below the LMWL as well as the GMWL. Most of the values above both of the lines belonged to the south facing plantation site. There were hardly any isotope TF samples of the heather sites located above both lines. The SF isotopic compositions were very variable and widely spread over the whole plot. Values in the lower left part of the diagram were for the first two sample dates, 7.6 mm and 12.2 mm of GR and average air temperature of around 7.0 and 9.0 °C which were the coldest mean air temperatures during the whole sampling period (Table 5-1).

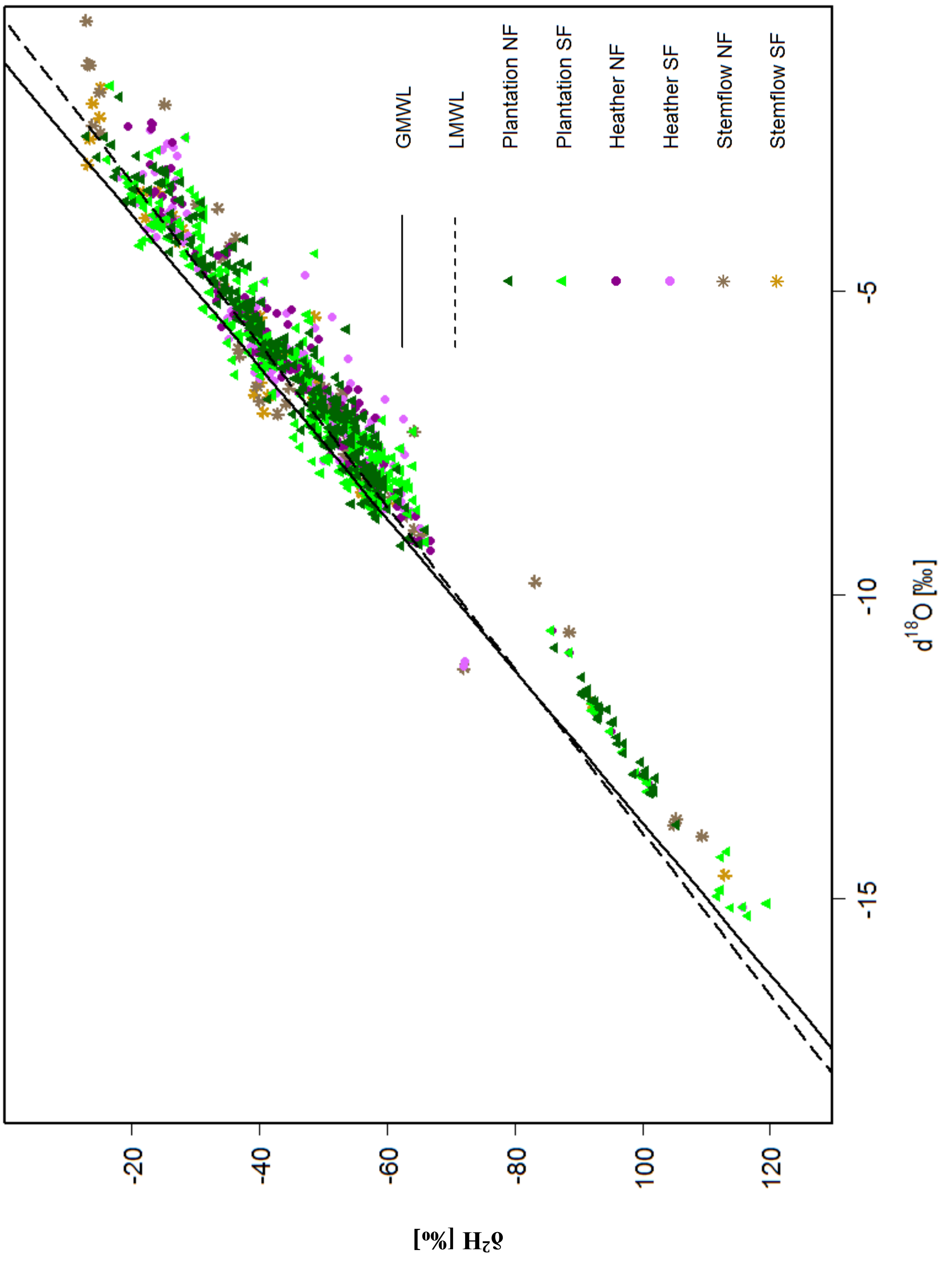

Figure 5-18: Dual isotope plot of δD and $\delta^{18}O$ values in ‰ of all isotope samples over the sample period. Dark and light green triangles represent the plantation sites (NF and SF) and purple and pink dots represent the heather sites (NF and SF). Dark and light brown stars represent the stemflow values (NF and SF). The dashed line shows the LMWL, the continuous line the GMWL.

As already indicated in Figure 5-15 and Figure 5-16, there were distinct differences between δ^2H and δ^{18}O in between the collectors of each site. To better visualize those differences and link the findings to the collector's location within the grid, Figure 5-19 and Figure 5-20 were constructed. To derive average values for each collector over the field season, δ^{18}O values were volume weighted for each collector. There were greater differences in between the collectors for the north facing plantation. It seems that more depleted, hence more negative values (larger circles) occurred in collectors with higher canopy coverage and placed close to trees. The collector in the bottom right that was placed closely to two tree stems and sampled the lowest TF amounts showed the most negative δ^{18}O values over the sampling period (Figure 5-19). Most enriched values could be found for collectors placed in areas with little or hardly any canopy coverage. A similar pattern, even though it is less distinct, could be seen for the south facing plantation (Figure 5-20) and for the δ^2H isotope values (Figure Appendix C-1, Figure Appendix C-2).

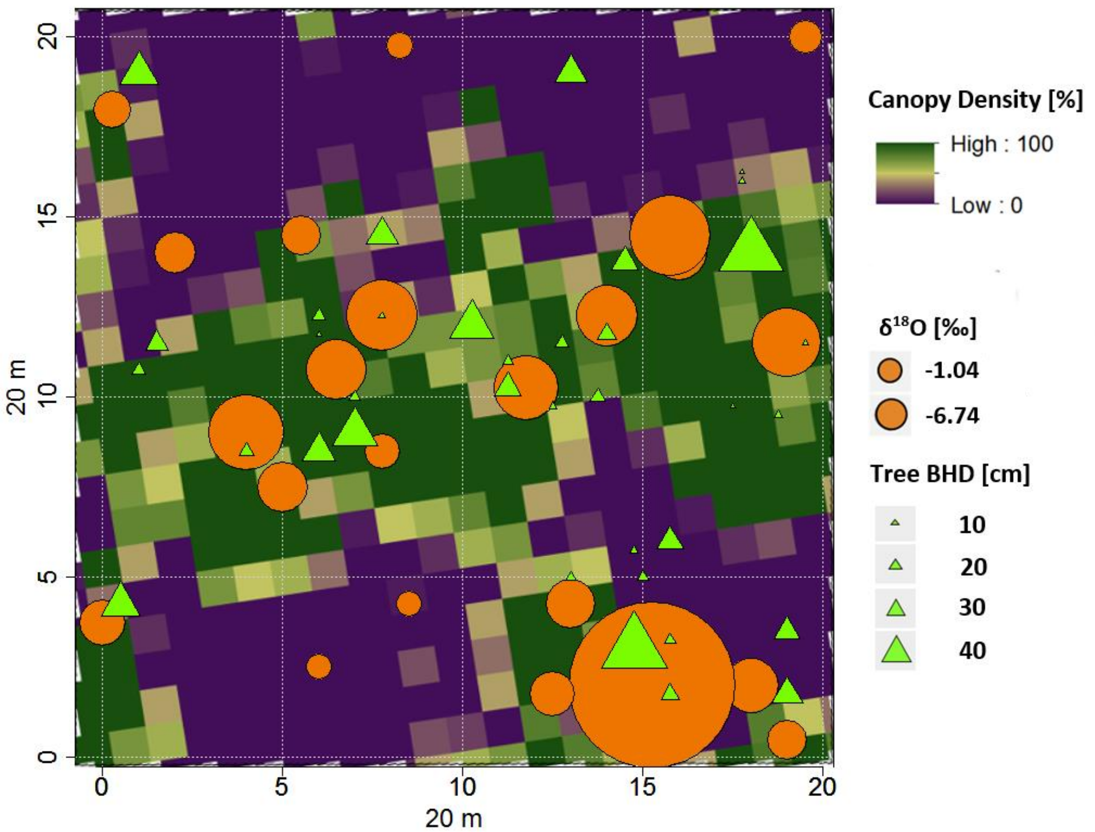

Figure 5-19: 20 x 20m grid of the north facing plantation with 23 TF collectors (orange dots) and trees (green triangles). Orange points represent the δ^{18}O values. Bigger triangles represent trees with greater BHD [cm], smaller triangles represent trees with smaller BHD. Dark green squares indicate high canopy coverage [%], purple indicates no canopy coverage.

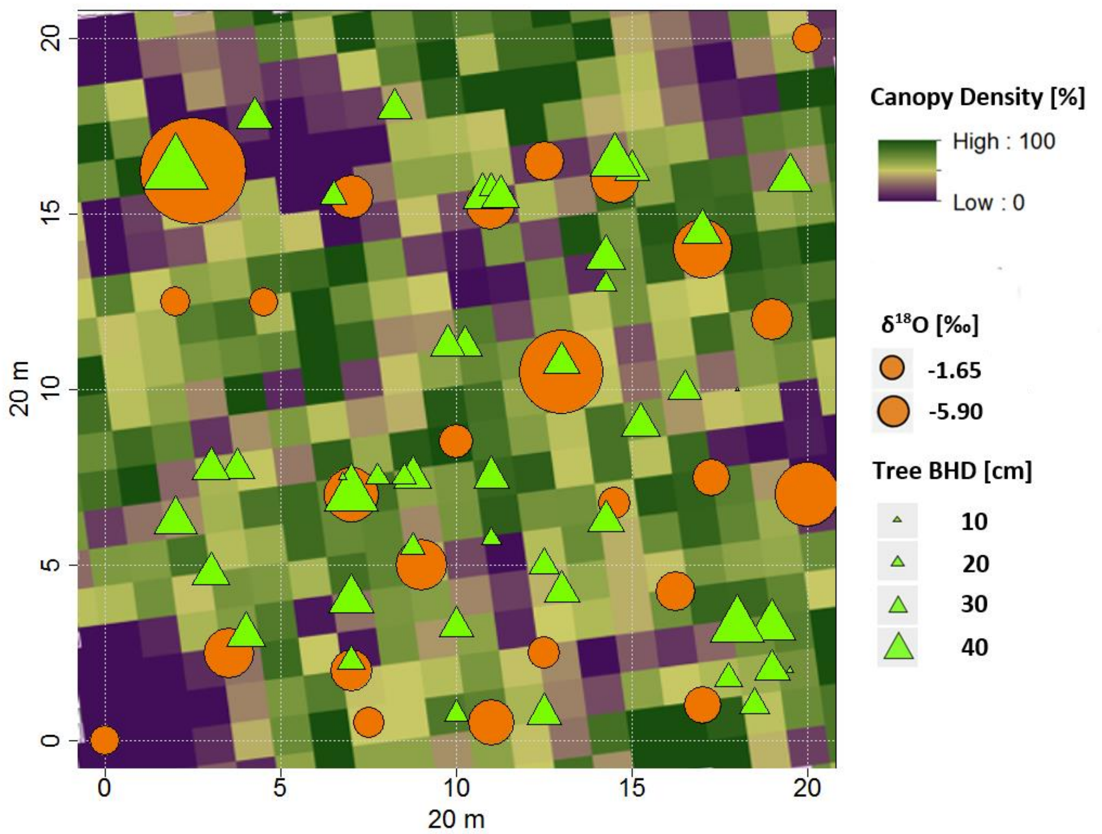

Figure 5-20: 20 x 20m grid of the south facing plantation with 25 TF collectors (orange dots) and trees (green triangles). Orange points represent the $\delta^{18}O$ values. Bigger triangles represent trees with greater BHD [cm], smaller triangles represent trees with smaller BHD. Dark green squares indicate high canopy coverage [%], purple indicates no canopy coverage.

To identify influences on differences in between the collectors in each grid, a MLRM with the input variables mean, median and CV of the volume weighted TF isotopes, TF amount for each collector, canopy coverage (per collector) and distance to the closest tree was run. There are great variations in R^2-values in between mean, median and CV and between TF $\delta^{18}O$ and δ^2H. The distance to the closest tree didn't alter the isotopic composition, whereas an influence by mean TF and canopy coverage could be detected for mean and CV $\delta^{18}O$ for both plantation sites. Mean, median and CV δ^2H showed either showed really low R^2 values or no relationship between TF amount in the collector and canopy coverage at all. For the heather sites, the R^2 values were very low, except for mean and median $\delta^{18}O$ input.

Table 5-11: MLRM for the north facing plantation. Y-variables are mean, median and CV of $\delta^2H/\delta^{18}O$, X-variables are the meteorological parameters derived by the weather station and calculated ET [mm]. R^2 values show the fit of the model. P-values show the importance of the parameter.

Y	*R^2*	*TF [mm] p- value*	*Canopy [%] p-value*
Plantation north facing			
δ^{18}O.TF.Mean	0.99	<0.001	0.08
δ^{18}O.TF.Median	0.27	0.15	0.08
δ^{18}O.TF.CV	0.58	<0.001	0.02
δ^2H.TF.Mean	0.26	0.006	0.06
δ^2H.TF.Median	-	-	-
δ^2H.TF.CV	0.2	-	0.03

Table 5-12: MLRM for the south facing plantation. Y-variables are mean, median and CV of δ^2H and $\delta^{18}O$, X-variables are the meteorological parameters derived by the weather station and calculated ET [mm]. R^2 values show the fit of the model. P-values show the importance of the parameter.

Y	*R^2*	*GR δ18O/ δ2H [‰] p- value*	*Canopy [%] p-value*
Plantation south facing			
δ^{18}O.TF.Mean	0.95	<0.001	-
δ^{18}O.TF.Median	-	-	-
δ^{18}O.TF.CV	0.59	<0.001	-
δ^2H.TF.Mean	0.08	0.1	-
δ^2H.TF.Median	-	-	-
δ^2H.TF.CV	-	-	-

5.3.2 Stemflow

The isotopic composition of the SF samples was found to be very variable over the time. There have been major differences to the isotopic composition of TF and GR samples. This can be seen in Figure 5-21. Temporal variabilities in GR and SF are very high and intra-site differences between the plantations are quite distinct as well. As already seen in the dual isotope plot (Figure 5-18) SF isotopes were mostly on the right side below the LMWL. This, and the fact that most

SF lc-excess values are negative are indicators that isotopic fractionation might have taken place. Even though both sites showed very different lc-excess values, negative and positive values mostly occurred for the same sampling dates on both plantations, except for one date in early September, where the north facing site showed values around -4.5‰ and the south facing plantation 0.5‰. In July and late September, all lc-excess values for SF were higher than for GR, whereas in early June and August, SF lc-excess was lower compared to GR.

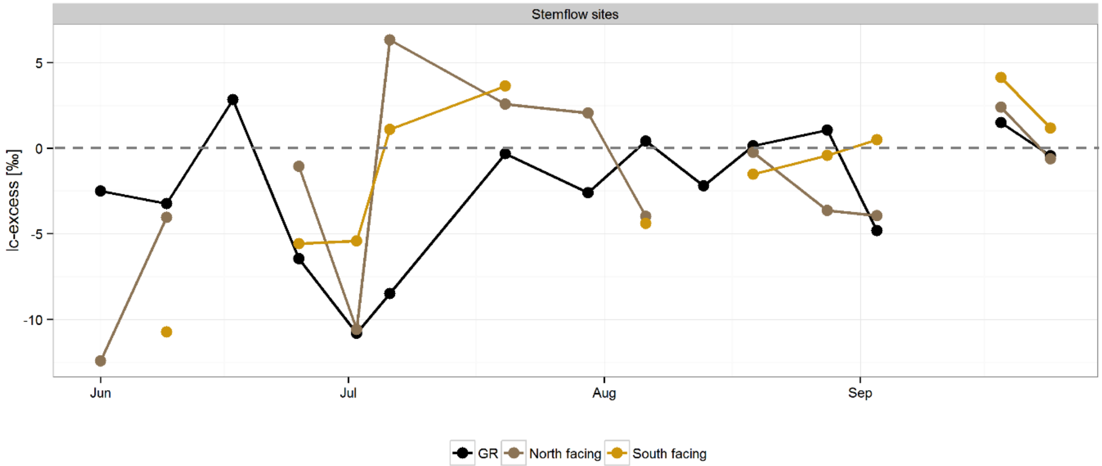

Figure 5-21: Stemflow lc - excess values for both plantations. Points represent the values calculated for the sample dates.

Inter-Site Variability

The SF isotopes have been – as Figure 5-21 shows – different for the two plantation sites even though they followed a similar pattern. This could also be seen in Figure 5-22 and Figure 5-23 which shows δ^{18}O boxplots for both SF sites. Both sites followed the same pattern and were more depleted on the same dates. The values for 30th of July were more enriched for the south facing site. The δ^2H values (Figure 5-23) showed a similar pattern. Isotopic values, enriched in ^{2}H and ^{18}O also occurred mid and end of June as well as mid of August, most depleted values occurred early June. This is similar to the pattern found for the TF isotopic signatures (Figure 5-14).

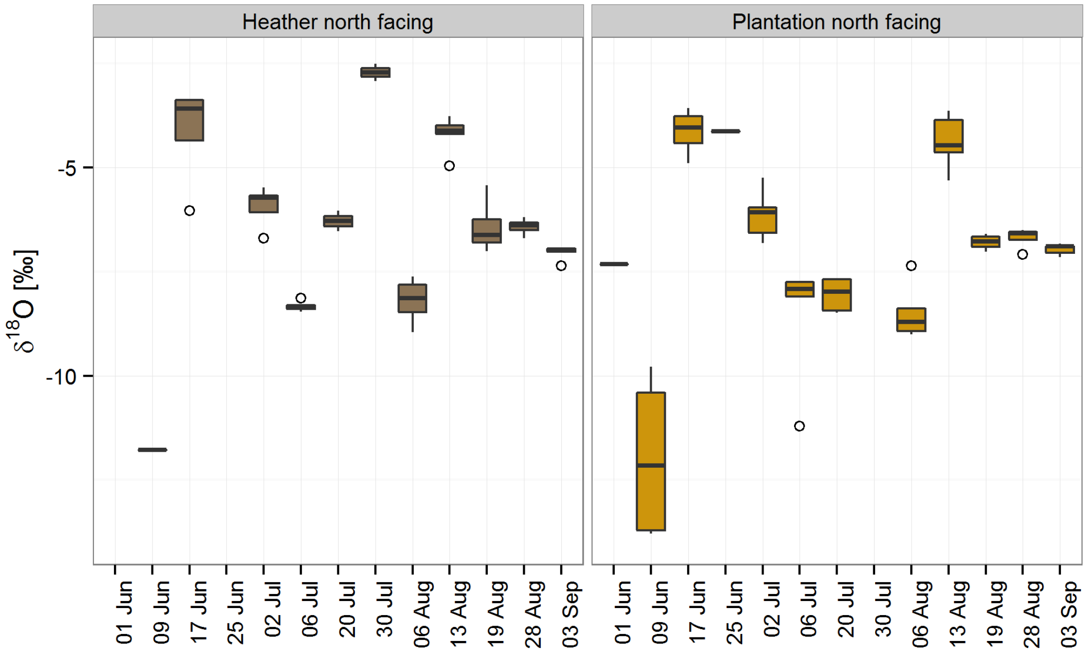

Figure 5-22: $\delta^{18}O$ Boxplots of SF for both plantations over all sample dates. Outliers are marked as points.

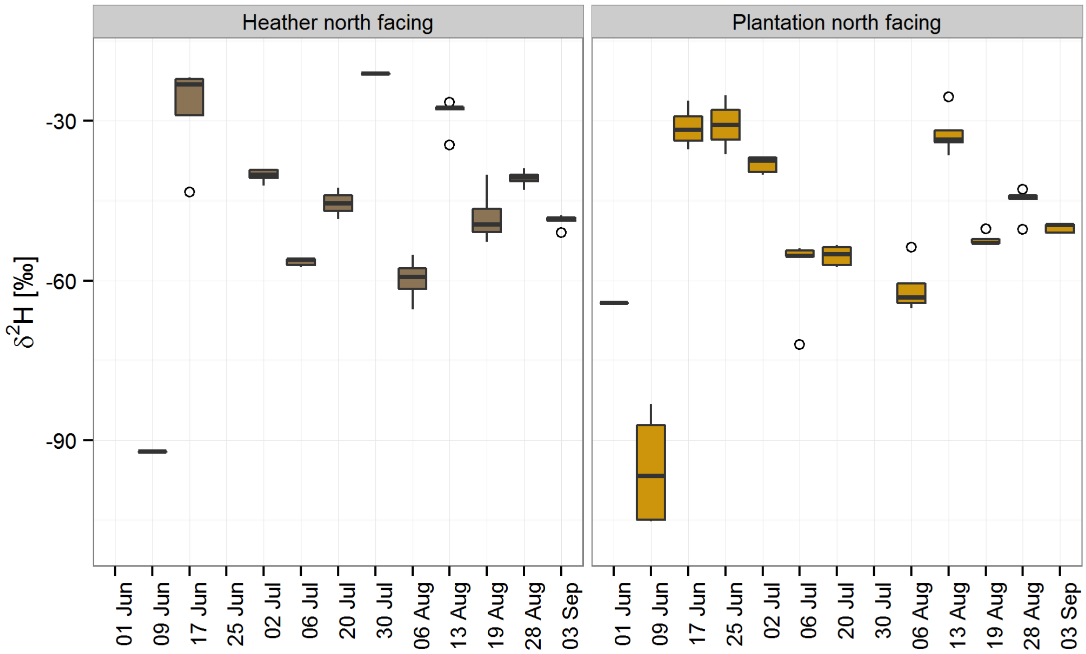

Figure 5-23: $\delta^{2}H$ Boxplots of SF for both plantations over all sample dates. Outliers are marked as points.

The Pearson correlation (Figure 5-24) showed high correlations between the isotopic weighted means and medians for both, $\delta^{18}O$ and $\delta^{2}H$ and the GR isotopic signatures, T.a and lower correlations with RH. The highest correlation coefficients were registered for the GR isotopic signatures, even though r-values were marginally lower for SF compared to TF (Figure 5-17). Higher CVs between SF and GR isotopes could be found for the south facing plantation where r-values were >0.8 (Figure Appendix D-1). Correlations with T.a were found to be similarly important (compared to the north facing site) whereas r-values for RH where slightly higher.

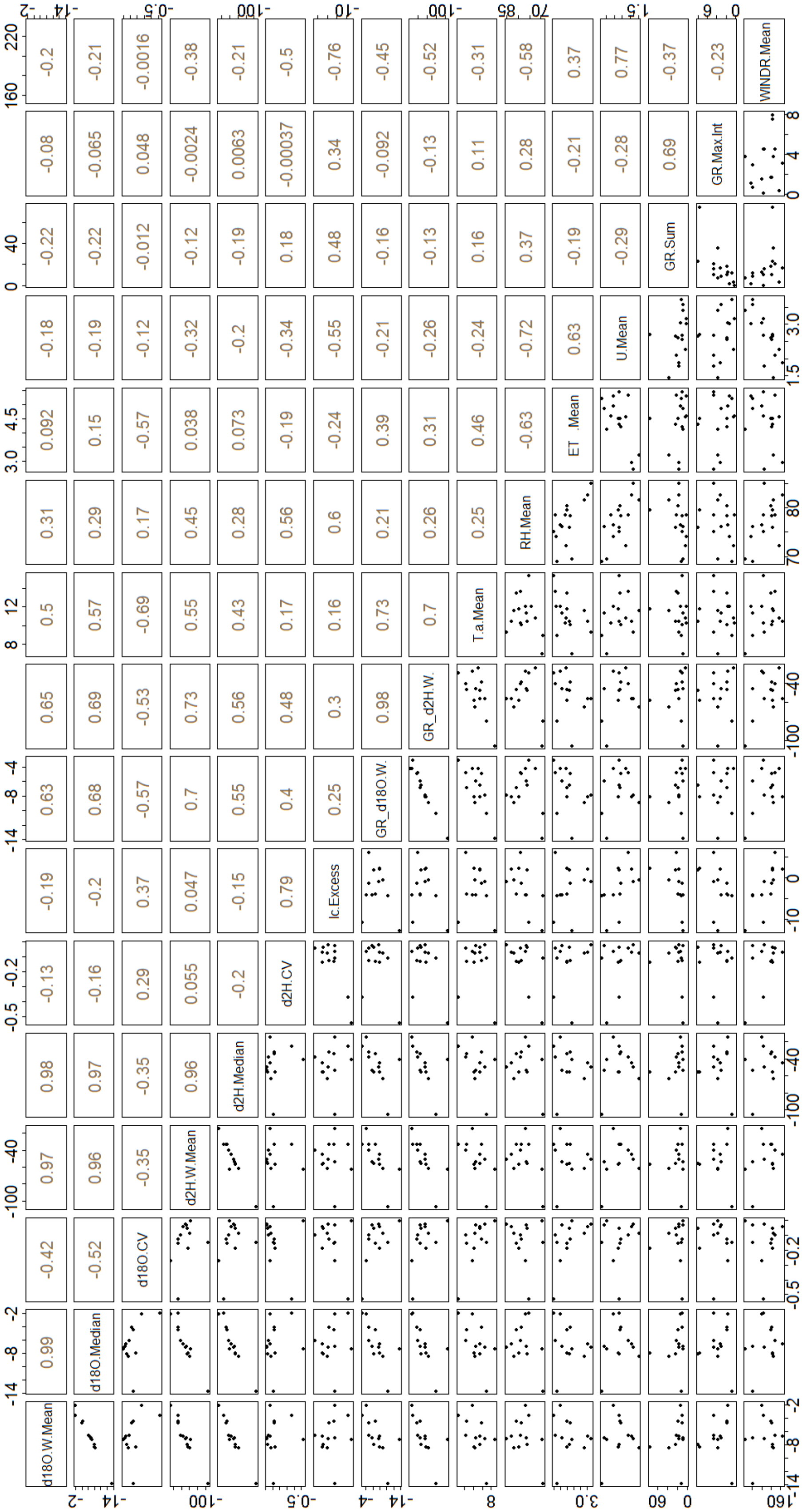

Figure 5-24: Pearson correlation and Scatterplot for SF isotopic compositions (d18O.W.Mean, d18O.W.Median and d18O.W.CV) values for the north facing plantation and isotopic signatures for the GR (GR_d18.W, GR2H.W), lc-excess and hydroclimatic variables like T.a.Mean [°C], RH.Mean [%], ET.Mean [mm], U.Mean [ms^{-1}] and WINDR.Mean[°]. The brown numbers represent the correlation coefficient r.

Input variables for the MLRM were δ^{18}O and δ^{2}H volume weighted mean, median and of SF samples of each site. X-variables the meteorological variables from the Pearson correlation (Figure 5-24) plus daily maximum wind speed (U.D.Max) and maximum wind speed (U.Max). R^2-values are higher for the south facing plantation. For both sites, mean and median are mostly influenced by the isotopic composition of GR. Further influencing variables are mean T.a, ET, U.D.Max, GR.M.Int and U.Mean, where GR.M.Int only influences δ^{2}H median and CV of the south facing plantation. The δ^{18}O CV is only influenced by mean T.a and U.D.Max for both sites. As only five SF collectors were installed per plantation, a statistical intra-site comparison wasn't conducted.

Table 5-13: MLRM to identify influences on the isotopic composition of the SF sites. Y-variables are δ^{18}O and δ^{2}H means (weighted), median and CV for each site. X-variables are the meteorological variables. R^2 values show the model fit.

Y	*R^2*	*GR δ18O/ δ2H [‰] p- value*	*Ta. Mean [°C] p-value*	*ET.Mean [mm] p-value*	*U.D.Max [mm s^{-1}] p-value*	*GR M.Int [mm h^{-1}] p-value*	*U.Mean [mm s^{-1}] p-value*
SF plantation north facing							
δ^{18}O.SF.Mean	0.59	0.02	-	0.20	0.02	-	0.04
δ^{18}O.SF.Median	0.60	0.02	-	-	0.03	-	0.10
δ^{18}O.SF.CV	0.55	-	0.002	-	0.07	-	-
δ^{2}H.SF.Mean	0.75	0.004	0.11	-	0.01	-	0.06
δ^{2}H.SF.Median	0.60	0.03	0.16	-	0.01	-	0.03
δ^{2}H.SF.CV	0.25	0.25	0.09	-	0.15	-	0.10
SF plantation south facing							
δ^{18}O.SF.Mean	0.72	0.003	0.21	0.10	0.2	-	-
δ^{18}O.SF.Median	0.93	<0.001	0.02	0.01	0.04	-	-
δ^{18}O.SF.CV	0.28	-	0.02	-	0.05	-	0.16
δ^{2}H.SF.Mean	0.83	<0.001	-	0.06	-	-	-
δ^{2}H.SF.Median	0.94	<0.001	0.10	0.03	0.25	0.02	-
δ^{2}H.SF.CV	0.56	0.02	-	0.06	0.02	0.02	0.06

6 DISCUSSION

6.1 Influences on Quantity

6.1.1 Throughfall

Great temporal and spatial variabilities in TF due to changing precipitation patterns and site-specific influences could be found. Differences between the vegetation types (heather vs. plantations) were higher than between the slopes. Interception losses for all sites were found to be quite high but still within reported values for pine trees. Both net precipitation and TF fractions were higher for the heather sites compared to the plantations. Lowest TF fractions could be found at the younger north facing plantation. Canopy coverages for the collectors, derived from digital photography, however, differences in TF fractions could be due to different canopy cover distribution in the younger north facing plantation. The north facing plantation was, untypical for Scots Pine very dense in the middle part of the plot and showed, unlike the south facing plantation, shrub-sized trees and understorey vegetation. Scots pine usually is characterized by a low and open canopy, with denser stands occurring in the east of Scotland (Hall et al., 2001). Tree sizes, age, crown density and canopy coverage of the collectors varied a lot at this site, whereas all of those attributes are fairly uniform for the south facing plantation.

As expected and shown by several studies in the past (e.g. Marin et al., 2000; Peng et al. 2014; Stockinger et al., 2015), a strong positive correlation between TF volume and the total amount of GR could be found at all sample sites. It was shown that the TF amount and fraction can be predicted well using GR amount and intensity with high correlation coefficients of > 0.97 for all sites. A strong linear relation between TF and GR was also found by Stockinger et al. (2015) and Peng et al. (2014). The slopes for the linear relation between GR and TF for the south facing sites were very similar with their findings (~ 0.71 and 0.78) and smaller for the north facing sites (~0.62 and 0.65). Peng et al. (2015) stated that any deviation of a slope of one in the TF-GR relationship is an indicator for evaporative processes in the canopy.

Interception losses during the field period were with values ranging from 33.4% for the south facing heather sites to 46.6% for the north facing plantation quite high (Table 5-2) and according to Llorens and Domingo (2007) in the upper range of reported values. However, the values were comparable to other studies and according to Kittredge (1948) interception loss in a hardwood forest can range between 6 to 43%. Ranges for a Scots pine forest were found to lie between 13% and 49% (Llorens et al., 1997) and studies with comparable trees concerning bark texture and branch architecture from Brodersen et al. (2000) and Stockinger et al. (2015) found values between 40 to 41% as well. The studies were conducted in a 130 to 170 year old spruce stand in the Black Forest in Germany and in a mixed spruce forest in the Eifel national park in Germany, respectively.

One reason for the high interception losses could be that most of Scotland's precipitation falls in low intensity events. A decreasing interception loss was found in weeks with increasing GR intensities (Figure Appendix A-2). For weeks with low intensity events, interception losses were as high as 95% - 100% whereas for high intensity weeks with intensities > 7 mm h^{-1}, losses ranged between 22% - 45% of GR. Scatena (1990) also observed in his studies, that high interception amounts and canopy loss were attributed to rain events with very low intensities (≤ 2mm h^{-1}). As small raindrops are greater affected by wind speed and wind direction, they are more likely to be blown away from the collector (Crockford and Richardson, 2000). This might be one reason for low net precipitation/high interception loss even though wind speeds, ranging from 2 - 8 m s^{-1}, classified as moderate to fresh winds (Smyth et al., 2013) were quite low for the field season.

The MLRM showed, that TF amounts for all sites were statistically dependent on wind speed and wind direction. Especially the intra-site variability was mainly driven by wind speed and evaporation as wind speed can lead to a preferential deposition pattern of precipitation and change the GR behaviour in the canopy cover and was found to be a factor influencing spatial variability of TF (Herwitz and Slye, 1995). The higher correlation between TF fraction and maximum intensity for the heather sites (Table 5-5, Table 5-6) compared to the plantation sites showed, together with the results derived from the MLRM, that especially in the plantations other factors such as wind speed, wind direction and canopy coverage played an important role. Crockford and Richardson (1990), who compared a pine plantation with a nearby eucalypt forest came to the same conclusion. They found highly different TF for their plantations, even though basal area (per ha) and rainfall were similar. They suggested that not only climatic variables and location characteristics such as slope, aspect and exposure to wind, have a distinct influence on TF. Although no correlation of wind speed and TF was found for the heather sites, wind speed and wind direction could potentially influence the amount of TF for the heather sites if the rain event comes from east as the plantations might cause a rain shadow effect or through luv and lee effects from the hillslopes. As the heather shrubs have a marginally smaller contact surface for wind, compared to trees, it could also be that wind driven influences play a minor role in the redistribution of TF in those areas. This was also shown by Zhang et al. (2015) who investigated TF and SF for different shrubs but could not find significant correlations with temperature, humidity and wind speed either.

A statistically relevant negative correlation could be found between TF values for the plantations (both TF amounts and TF fraction), canopy coverage and distance to the closest tree (Table 4-4). This was also shown by early studies from Stout and MacMahon (1961) and Helvey and Patric

(1965), Aussenac (1970, different canopies) and Johnson (1990, spruce stand). Especially for small precipitation events, where the canopy coverage remains unsaturated, it can have a great influence on TF amount and variability as all or a major amount of TF will be caught in the canopy and only reaches the ground through gaps. As GR amount increases and the canopy storage gets more saturated, each additional raindrop generates TF (Loustau et al., 1992). Influences of the canopy coverage and distance to the nearest tree stem on TF were more distinct for the north facing plantation (Table 4-4). This again could be due to the fact that the vegetation cover is more heterogeneous at this site. Due to a wider range of values the leverage of regression points is higher and the correlation becomes stronger. No such statistical relevant relation could be found for the two heather sites. However, TF amounts for the south facing heather site - which has less canopy coverage - were higher than for the north facing heather site.

A great spatial and temporal variability in TF amount, TF fraction and therefore as well interception loss was monitored. Especially for weeks with low and medium intensity events and small GR sums the spatial variability was high. Main factor certainly was the temporal variability of GR events in both amount and intensity as well as other meteorological factors. Even though, the MLRM showed that the intra-site variability (expressed as the coefficient of variation) of TF and TF is not perfectly predictable ($R^2 = 0.17$ -0.56), it still shows the linkages to maximum wind speed and rainfall intensity in the plantation sites. Correlations also showed that wind (mean, and daily maximum values) had a higher effect in south facing plantations (Figure Appendix A-3), this could be due to the fact that this plantation was more accessible for wind as no shrub or understory vegetation was present here. Great variability for TF could also be found by studies undertaken by Staelens et al. (2006) and Levia et al. (2011) that stated correlations with branch cover and canopy leaves.

It could be observed, that spatial variability decreases with increasing GR amounts and for events with higher intensity (Figure Appendix A-1). The dataset also showed a threshold of approximately 15 mm above which all of the TF collectors, even the ones with a high canopy coverage and close to a tree bole, were collecting TF. This again can be explained by the canopy saturation effect mentioned above as well as the raindrop size and effects on both by wind speed and direction. Marin et al. (2000) also found high variabilities in their study and mentioned that many Y-variables are necessary to predict TF variability.

6.1.2 Stemflow

SF values were found to be quite low and are with 2.5% for the north facing and 1.0% for the south facing site of limited importance. Values found by studies of Llorens and Domingo (2007) and Molina and del Campo (2012) showed with 1.74% and 1.5% similar ranges. During the field season, certain GR amounts (> 7mm for beech and >10 mm for Scots pine) and GR intensities were needed to produce SF. The relation between SF and sum of GR showed a threshold above which SF generation did not increase with higher amount of GR but stayed approximately constant (~25 mm; Figure 5-2). The same effect was mentioned by Ford and Deans (1978) who discovered that high intensity precipitation events in a Scots pine forest lead to a point where SF remained constant even though TF increased. To generate SF, canopy and bark water storage have to be reached first.

Peaks in SF generation and TF amount did not occur on the same sampling dates as SF is higher influenced by event intensities compared to TF. However, the lowest measured SF and TF amounts occurred on the same dates, when both, GR sum and maximum intensity were low. SF was found to be highly variable between the sites. Lower SF values were found for the older south facing plantation. Trees for both plantations varied in BHD, age, heights and crown area. Whereas the tree characteristics for the south facing plantation were very similar, the north facing plantation was very variable in all characteristics. Crown area of some of the older trees on the north facing plantation was denser and larger than for the south facing plantation where more trees were spread in the 20 x 20 m grid allowing less space for the trees to develop a major crown. Younger bark is also meant to allow a higher SF production as bark roughness might increase with age (Johnson, 1990).

Mean and median SF were mainly dependent on maximum intensity and wind speed and additionally air temperature for the south facing plantation. The CV was mainly influenced by wind direction, wind speed, humidity and air temperature. Xiao et al. (2000) and André et al. (2008) found that higher wind speeds increased the SF production as they reduced the initiation threshold.

The intra-site comparison showed, that main differences were due to species diversities, however, there is no statistical evidence as the basic population was too low to apply statistical tests. Higher SF amounts were measured for the birch trees for all events. This might be mainly the result of smoother bark composition of the birch trees which allows more SF generation due to less resistance and lower and accompanied bark storage capacity (Crockford and Richardson, 2000; Levia and Frost, 2003).

No connection between BHD and SF amount could be found. Probably a more detailed investigation of the vegetation cover (like crown area, branch architecture, bark composition) could help to improve the prediction of SF generation. More trees in general, as well as subsets of different species would have been necessary to test further correlations, however, studies from Ford and Deans (1978) and Loustau et al. (1992) also could not adequately explain SF amounts and variations between trees.

6.2 Influence on Isotopic Composition

6.2.1 Throughfall

TF isotope values in this study have shown temporal and spatial variability which was also found by Ikawa et al. (2011) and (Kato et al., 2013). The dataset showed three different variabilities concerning the isotopic composition of the TF samples: the major temporal variability between the events (inter-event) (Figure 5-12, Figure 5-13) the differences between the sites (inter-site) and the variability within one site (intra-site) (e.g. Figure 5-14).

The temporal inter-event variability in the isotopic TF signature was found to be mostly driven by the variability in GR isotopic composition. δ^{18}O TF values range from -15.29‰ to -0.56‰ for all periods and $\delta\,^{18}$O GR values from -15.21‰ to -0.92‰, which is in the range within values found by Stockinger et al., (2015) in a spruce dominated, humid temperate catchment in western Germany (- 14.27‰ to -3.04‰ in TF and -16.40‰ to -2.77‰ in GR ^{18}O values). GR δ^{18}O can range from -20.93‰ to -2.50‰ in the Cairngorm Mountains whereas values less depleted in heavy isotopes occur in summer (-2.5) (Soulsby et al., 2000). There was no statistical relation between GR amount, GR maximum intensity and isotopic composition of TF. This lack of correlation was also observed by Allen et al. (2015, Douglas-fir dominated catchment in northern Oregon) and Kato et al. (2013; cypress plantation in eastern Japan).

TF lc-excess showed high variabilities (negative and positive values) for GR and TF samples of all sites, however, differences between the sites were quite small. In the summer months of June and July the effect of evaporative processes on GR isotopic composition could be identified by the observed negative lc-excess values in this period. This pattern could not be seen in the isotopic TF signatures. Positive lc-excess values showed an enrichment in lighter isotopes compared to the GR signature, which is an indicator that GR isotopic composition was altered by its passage through the canopy. Alterations could be due to mixing processes of old and new event water in the canopy and isotopic exchange with atmospheric water vapour (Saxena, 1986; Tsujimura and Tanaka, 1998). These exchange processes can potentially lead to both, depletion and enrichment in ^{18}O dependent on adjacent conditions.

Compared to the temporal variability in TF isotopic composition, variability between the sites was found to be small but still considerable. Ranges in δ^{18}O were around 2.2‰ for the plantations and around 1.3‰ for the heather sites. These results are similar to findings presented in studies by Kato et al. (2013) and Brodersen et al., (2000). δ^{18}O ranges in their studies were between 1‰ (Kato et al., 2013) and up to 3‰ for weekly TF isotope samples (Brodersen et al., 2000). The TF isotopic variability in the plantations was found to be higher compared to the variability in the heather sites. The more complex vegetation cover of the plantation sites influence the isotopic composition in a greater way than the more uniform vegetation cover of the heather sites. More variability in flow paths and interception patterns lead to more variability in isotopic fractionation and mixing.

Ranges within a site are indicators for a high spatial isotopic variability resulting from storage capacity, flow path heterogeneities and selective storage in the canopy (Brodersen et al., 2000; Kato et al., 2013; Allen et al., 2014). There might be differences in collectors placed in the centre of the canopy cover and the ones that are located further to the edge. Kato et al. (2013) found out, that canopies that drain the GR towards the edge might derive isotopically lighter TF in the centre of the canopy cover at the end of the precipitation event. Collectors with less dense canopies might gather more direct TF and might therefore show a different isotopic composition (Kato et al., 2013). However, this might only be an indicator and according to Brodersen et al. (2000) it is it quite difficult to explain differences in these low magnitudes.

6.2.2 Stemflow

SF isotopic compositions were different to the TF and GR isotopes and very variable within the sites. This could be due to SF generating processes, as SF often occurs later in the event and can be a mix of different event waters (Ikawa et al., 2011). SF is also highly affected by mixing processes, canopy cover, bark storage capacity and meteorological conditions (e.g. rainfall intensity, wind speed etc.) (Levia and Herwitz, 2005; Staelens et al., 2008; Ikawa et al., 2011). The event-mixing should play a minor role in this study, as sampling occurred weekly and not event based.

Lc-excess values for SF showed high differences to TF and GR lc-excess and between the sites. Most of the values were negative, indicating evaporation and subsequent fractionation processes. The MLRM revealed the dependency of SF isotopic composition on GR isotopic composition, wind speed and temperature to a certain extent. However, some of the lc-excess values were found to be positive, which leads to the assumption that physical fractionation is probably not the dominant process (Brodersen et al, 2000). This water might have rather undergone a sequence of fractionation and mixing processes in the canopy.

6.3 Wider Implications and Future Work

The results shown in this study provide insights into TF and SF generation processes and help to understand the mechanisms of flow path partitioning in the Bruntland Burn catchment. The field study demonstrated the importance of vegetation characteristics such as canopy coverage, age, height, density, BHD on both, TF amounts and isotopic compositions.

Understanding the canopy rainfall partitioning processes and characteristics are important, especially in regards of future vegetation changes driven by a changing climate (Tetzlaff et al., 2013). Many northern landscapes are already experiencing and responding to those shifts (Tetzlaff et al., 2014), climate projections for Scotland predict longer dry and warm periods and shifting precipitation patterns (Capell et al., 2013). This, combined with large scale afforestation plans by the Scottish government (The Scottish Forestry Strategy, 2006) will be affecting catchment characteristics and therefore water balance and flow path partitioning and leads to an increasing importance in understanding vegetation influences on water partitioning and storage dynamics and water availability in high latitude catchments (Geris et al., 2015).

However, to fully understand the processes of GR partitioning and its influences on both quantity and isotopic composition, further research is required. It would be interesting to extend the study period into the winter months. Different processes in the colder period (e.g. snow interactions and phase changes) could alter both TF variability and isotopic composition in a different way, even though the annual total snow accumulation is not especially high in the catchment. Evaluating TF rates and isotopic composition in winter might especially become more important as climate change predictions extinguish a shift of +11% of precipitation for the winter months in the Scottish highlands (UKCP09; Capell et al., 2013).

Knowing the isotopic composition of TF is also of interest when investigating the changes in isotopic composition along flow paths in the soil. Water pathways in those research questions play a key role and the vegetation and soils in a catchment have an important role regarding isotopic “systematics” and water cycle (McDonnell, 2014; Tetzlaff et al., 2015).

Further insights into the isotopic pattern of TF could be gained by a short term study on event basis. Variabilities within an event can be high as GR isotopic compositions are changing during one event. This could result in differences in isotopic composition between collectors placed under the exterior part of the canopy and one’s close to the tree’s stem, as might tend to collect preferential earlier or later event water. For the in this study randomly located collectors, distance to the closest tree didn’t show a significant correlation, however, this might be different on event-basis.

Interception loss was found to be higher than expected and it is important to take these findings into account for further studies investigated in the Bruntland Burn or similar catchment areas. However, the accurate estimation of TF is difficult as variabilities are very high. To make sure that variabilities were not enhanced by the field setup, Helvey and Patric (1965), Lloyd and de Marques (1988) and Wilm (1943) suggested to randomly relocate measuring collectors when measuring TF on a periodic basis. However, this gives only an estimation of TF for the whole grid monitoring of TF but gives little insight of temporal or spatial variability or the direct influence of canopy coverage.

The number of observations needed to get a distinct degree of reliability of the data was calculated. There were enough collectors ($N = (Std.Dev./Std.Error)^2$) in the heather sites and the south facing plantation site to guaranty a reliability with less than 10% error. However, more samples would have been needed for the north facing plantation (about 27 for the whole field season and up to 49 for really small events below 5 mm of GR). Stuart (1962) found out, that number of gauges is more relevant than the type of gauges. It is also noticeable, that gauges might underestimate TF due to wind and splash effects (Crockford and Richardson, 2000). However, in this study the collectors in the open were found to measure within a mean error of 5.7% compared to the GR amounts collected by the rain gauge and where not statistically significant.

7 CONCLUSION

In the here presented study the processes of throughfall (TF) and stemflow (SF) were analysed in respect to their spatial and temporal variability in quantity and isotopic composition under different vegetation cover and aspects.

The study was able to identify great temporal and spatial differences in TF. The findings show that the measured TF amounts are mainly governed by the size of the rain event and correlate closely with GR amount and event intensity. The temporal variation of TF (as both, amount and fraction of GR) induced by this correlation was found to be higher than intra-site and especially inter-site variations. However, intra-site variability in TF observations was still substantially and showed to be mainly influenced by canopy cover and the distance to the nearest tree. The results also suggest that the intra-site variations in TF are influenced by changes in wind speed and rainfall intensity over time for most sites. The difference in collected TF between the vegetation types was found to be higher than the difference between the aspects. It was shown that the distribution of TF values varies significantly (α=0.05) between the two vegetation classes. A higher fraction of the GR was intercepted in the plantation canopy, whereas in average more TF could be collected under the heather. This shows the influence of geometry and interception capacity of different vegetation types on TF production. Moreover, the study shows that in average the south facing slope produced more TF than the north facing one. However, this finding is only significant (α=0.05) for the plantation sites, but not for the heather plots. Because the effect of topography on precipitation pattern and evaporation rates is assumed to be rather small in this environment, these findings can be linked to differences in canopy cover of the two plantation sites. Both heather sites show a more uniform vegetation cover and no significant differences in vegetation density. The contribution of SF to the overall water balance was found to be of minor importance (in average between 1 and 2.5% of GR). Birch trees generated more SF, but were however little represented in the Scots pine catchment area. SF was found to correlate to maximum precipitation intensity However, the MLRM revealed no simple and consistent correlation of the intra-site variability of SF – expressed as the CV – and meteorological site specific parameters. The subsequent interception losses – as calculated from GR, TF and SF – were in the upper range of reported literature values, which might be mainly due to low intensity rainfall events which are typical for the region.

Much like the TF amounts, high temporal and less spatial variation could be identified for the isotopic signature of collected TF samples. Again, differences between the different topographic expositions were found to be minor, whereas differences between the vegetation classes were comparatively high. $\delta^{18}O$ and $\delta^{2}H$ TF values were mainly influenced by the isotopic composition of GR, which showed a high variation over time. Furthermore, the MLRM indicated additional correlation of the isotopic composition with wind speed and air temperature. Intra-site variability of the isotopic TF signature for the plantations could be explained by TF amount and canopy coverage. The fact that the TF was not consistently found to be isotopically heavier than GR suggests that the rain water undergoes a series of multiple processes during its passage through the canopy. Mixing, exchange and evaporation can be seen as likely processes which result in this complex isotopic signal. Even though, physical fractionation was found to be of minor importance in this study, and selection and mixing processes were found to alter the isotopic composition of GR during its passage through the canopy, it could not be shown which process prevailed. Similarly, the isotopic composition of SF also suggests that mixing and local storage processes take place. SF isotope signature correlated to the GR isotope signal, however, not as strong as the TF. Furthermore, the MLRM identified additional parameters e.g. air temperature and wind speed to influence SF. However, these correlations are weak and have probably no explanatory power for processes, but show that SF is linked to complex mechanisms.

8 REFERENCES

Allen, R.G., Pereira L.S., Raes D., Smith M., 1998. Crop evapotranspiration: guidelines for computing crop water requirements Food and Agriculture Organization of the United Nations, Rome.

Allen, S. T., Brooks, J. R., Keim, R. F., Bond, B. J., McDonnell, J. J., 2014. The role of pre-event canopy storage in throughfall and stem flow by using isotopic tracers. Ecohydrology, 868(July 2013), 858–868. http://doi.org/10.1002/eco.1408.

Allen, S.T., Keim, R. F., McDonnell, J. J., 2015. Spatial patterns of throughfall isotopic composition at the event and seasonal timescales. Journal of Hydrology, 522, 58–66. http://doi.org/10.1016/j.jhydrol.2014.12.029.

André F., Jonard M., Ponette Q., 2008. Influence of species and rain event characteristics on stemflow volume in a temperate mixed oak-beech stand. Hydrol. Process 22:4455–4466.

Arnell, N., 2002. Hydrology and Global Environmental Change. Pearson Education, Harlow. 346 pp.

Aussenac, G., 1970. Action du couvert forestier sur la distribution au sol des prècipitations. Annales des Sciences Forestières 27, 383–399.

Bialkowsky, R., Buttle, J.M., 2015. Stemflow and throughfall contributions to soil water recharge under trees with differing branch architectures. Hydrol. Process. 29, 4068–4082 (2015), DOI: 10.1002/hyp.10463.

Birkel, C., Tetzlaff, D., Dunn, S. M., Soulsby C., 2011. Using lumped conceptual rainfall-runoff models to simulate daily isotope variability with fractionation in a nested mesoscale catchment, Adv. Water Resour., 34(3), 383–394.

Bosch, J. M. and Hewlett, J. D., 1982. A review of catchment experiments to determine the effect of vegetation changes on water yield and evapotranspiration, J. Hydrol., 55, 3–23.

Bouten, W., Heimovaara, T.J., Tiktak, A., 1992. Spatial patterns of throughfall and soil–water dynamics in a Douglas-fir stand. Water Resour. Res. 28, 3227–3233.

Brodersen, C., Pohl, S., Lindenlaub, M., Leibundgut, C., Wilpert, K., 2000. Influence of vegetation structure on isotope content of throughfall and soil water. Hydrol. Processes 14, 1439–1448.

Brown A.E., Zhang L., MacMahon T.A., Western A.W., Vertessy R.A., 2005. A review of paired catchment studies for determining changes in water yield resulting from alterations in vegetation. Journal of Hydrology 310:28–61. DOI:10.1016/j.jhydrol.2004.12.010.

CAN-EYE user manual, Weiss, M., Baret, F., 2014. CAN-EYE V6.313 USER MANUAL. EMMAH, INRA, Science & Impact, 76p.

Cape, J.N., Brown, A.H.F., Robertson, S.M.C., Howson, G., Paterson, I.S., 1991. Interspecies comparisons of throughfall and stemflow at three sites in northern Britain. Forest Ecology and Management 46, 165-177.

Capell, R., Tetzlaff, D., & Soulsby, C., 2013. Will catchment characteristics moderate the projected effects of climate change on flow regimes in the Scottish Highlands? Hydrological Processes, 699(December 2012), 687–699. http://doi.org/10.1002/hyp.9626.

Cappa, C. D., Hendricks, M. B., DePaolo, D. J., Cohen R. C., 2003. Isotopic fractionation of water during evaporation, J. Geophys. Res., 108(D16), 4525, doi: 101029/2003JD003597.

Carlyle-Moses D.E., Price A.G., 2006. Growing-season stemflow production within a deciduous forest of southern Ontario. Hydrol Process 20:3651–3663.

Carlyle-Moses D.E., Price A.G., 2007. Modelling canopy interception loss from a Madrean pine-oak stand, northeastern Mexico. Hydrol Process 21:2572–2580.

Clements, J.R., 1972. Stemflow in a multi-storied aspen community. Can J For Res 2:160–165.

Coplen, T. B., 2011. Guidelines and recommended terms for expression of stable-isotope-ratio and gas-ratio measurement results. Rapid Commun. Mass Spectrom. 25: 2538–2560. doi:10.1002/rcm.5129.

Coplen T.B., Huang R., 2000. Stable hydrogen and oxygen isotope ratios for selected sites of the National Oceanic and Atmospheric Administration's Atmospheric Integrated Research Monitoring Network (AIRMoN). US Geological Survey Open-File Report 00-279: Reston; 54 pp.

Craig H., 1961. Standard for reporting concentrations of deuterium and oxygen-18 in natural waters. Science 133, No. 3467, 1833-1834.

Crockford, R. H., Richardson, D. P., 1990. Partitioning of Rainfall in a Eucalypt Forest and Pine Plantation in southeastern Australia: II Stemflow and Factors Affecting Stemflow in a Dry Scleophyll Eucalypt Forest and a Pinus Radiata Plantation. Hydrological Processes, 4(September 1989), 145–155.

Crockford, R. H., Richardson, D. P., 2000. Partitioning of rainfall into throughfall, stemflow and interception: effect of forest type, ground cover and climate. Hydrological Processes, 2920(April 1999), 2903–2920.

Crockford, R.H., Richardson, D.P., Sageman, R., 1996. Chemistry of rainfall, throughfall and stemflow in a eucalypt forest and a pine plantation in south-eastern Australia: 3. Stemflow and total inputs. Hydrological Processes 10:25-42.

Dansgaard W., 1964. Stable isotopes in precipitation. Tellus 16: 436–468.

David, J.S., Bellot, J., Birot, Y., David, T.S., 2011. Water fluxes in forests. In: Birot, Y., Gracia, C., Palahi, M. (Eds.), Water for Forests and People in the Mediterranean Region – A Challenging Balance. What Science Can Tell Us 1. European Forest Institute, Joensuu.

David J.S., Valente F., Gash J.H.C., 2005. Evaporation of intercepted rainfall. In: Anderson MG (ed) Encyclopedia of hydrological sciences. Wiley, Chichester, pp 627–634.

Demarez V., Duthoit S., Baret F., Weiss M., Dedieu G., 2008. Estimation of leaf area and clumping indexes of crops with hemispherical photographs. Agric. Forest. Meteorol. 148, 644-655.

Dewalle D.R., Swistock B.R., 1994. Differences in Oxygen-18 content of throughfall and rainfall in hardwood and coniferous forests. Hydrological Processes 8:75–82. DOI: 10.1029/94WR00758.

Dick, J.J., Tetzlaff, D., Birkel, C., Soulsby, C., 2015. Modelling landscape controls on dissolved organic carbon sources and fluxes to streams. Biogeochemistry, vol 122, no. 2-3, pp. 361-374.

Dingman, S., 2002. Physical Hydrology. Prentice Hall, Upper Saddle River. 646 p.

Domingo, F., Sanchez, G., Moro, M., Brenner, A., Puigdefabregas, J., 1998. Measurement and modelling of rainfall interception by three semi-arid canopies. Agr. Forest Meteorol. 91, 275–292.

Dutton A., Wilkinson B.H., Welker J.M., Bowen G.J., Lohmann K.C., 2005. Spatial distribution and seasonal variation in 18O/16O of modern precipitation and river water across the conterminous USA. Hydrological Processes 19: 4121–4146.

Dytham, C., 2011. Choosing and Using Statistics: A Biologist's Guide. 3rd edition. ©2010, Wiley-Blackwell, 320 pages, ISBN : 978-1-4051-9839-4.

Ford, E.D., Deans, J.D., 1978. The effect of canopy structure on stemflow, throughfall and interception loss in a young Sitka spruce plantation. J. Appl. Ecol. 15, 905– 917.

Gat, J.R., Mook, W.G., Meijer, A.J., 2001. Atmospheric water. Environmental isotopes in the hydrological cycle - Principles and applications, Vol. 2. W.G. Mook (Ed.) IHP-V, Technical Document N. 39, UNESCO, Paris. 113p.

Gat, J.R., Tzur, Y., 1968. Modification of the isotopic composition of rainwater by processes which occurs before groundwater recharge. In: Isotope Hydrology, Proc. Symp. Vienna 1966, International Atomic Energy Agency, pp. 49–60.

Geris, J., Tetzlaff, D., McDonnnell, J., & Soulsby, C., 2015. The Relative Role of Soil Type and Tree Cover on Water Strorage and Transmission in Northern Headwater Chatchments. Hydrological Processes.

Gersper, P.L. and Holowaychuk, N., 1971. Some effetcs of stemflow from forest canopy trees on chemical properties of soils. Ecology 52(4):691-702.

Goldsmith, G.R., Muñoz-Villers, L.E., Holwerda, F., McDonnell, J.J., Asbjornsen, H., Dawson, T.E., 2012. Stable isotopes reveal linkages among ecohydrological processes in a seasonally dry tropical montane cloud forest. Ecohydrology 5, 779–790. http://dx.doi.org/10.1002/eco.268.

Gourcy, L. L., Groening, M., & Aggarwal, P. K., 2005. Stable Oxygen and Hydrogen Isotopes in Precipitation. In Isotopes in the Water Cycle: Past, Present and Future of a Developing Science (pp. 39–51).

Green M.B., Laursen B.K., Campbell J.L., McGuire K.J., Kelsey E.P., 2015. Stable water isotopes suggest sub-canopy water recycling in a northern forested catchment. Hydrological Processes. DOI: 10.1002/hyp.10706.

Guswa A, Spence C., 2012. Effect of throughfall variability on recharge: application to hemlock and deciduous forests in western Massachusetts. Ecohydrology 5: 563–574.

Hall, J.E., Kirby, K.J., Whitbread, A.M., revised 2004. National vegetation classification field guide to woodland, 117 pages A5 softback, ISBN 1 86107 554 5.

Hansen, K., 1995. In-canopy throughfall measurements in Norway spruce: water flow and consequences for ion fluxes. Water Air Soil Pollut. 85, 2259– 2264.

Helvey, J., & Patric, J. H., 1965. Canopy and Litter Interception of Rainfall by Hardwoods of Eastern United States. Water Resources Research, 1(2), 193–206.

Herwitz, S.R., 1987. Raindrop impact and water flow on the vegetative surfaces of trees and the effects on stemflow and throughfall generation. Earth Surf Proc Landforms 12:425–432.

Herwitz S.R., Slye R.E., 1995. Three-dimensional modeling of canopy tree interception of wind-driven rainfall. J Hydrol. 168:205–226.

Hoefs J., 1997. Stable Isotope Geochemistry, 4th edition. Springer: Berlin; 244 pp.

Hofhansl, F.,Wanek,W., Drage, S., Huber,W.,Weissenhofer, A., & Richter, A., 2011. Topography strongly affects atmospheric deposition and canopy exchange processes in different types of wet lowland rainforest, Southwest Costa Rica. Biogeochemistry, 106(3), 371–396.

Hutchinson, I., and Roberts, M.C., 1981. Vertical variation in stemflow generation. Journal of Applied Ecology 18:521-527.

Ikawa, R., Yamamoto, T., Shimada, J., & Shimizu, T., 2011. Temporal variations of isotopic compositions in gross rainfall, throughfall, and stemflow under a Japanese cedar forest during a typhoon event. Hydrological Research Letters, 5, 32–36. http://doi.org/10.3178/HRL.5.32

Ingraham, N.L., 1998. Isotopic variations in precipitation. Isotope Tracers in Catchment Hydrology (C.Kendall, C., J.F. McDonnel, Eds) Elsevier, Amsterdam, Chapter 3, .87-118.

Jennings, S.B., Brown, N.D., Sheil, D., 1999. Assess- ing forest canopies and understorey illumination: canopy closure, canopy cover and other measures. Forestry 72(1): 59–74.

Johnson, R.C., 1990. The interception, throughfall and stemflow in a forest in highland Scotland and the comparison with other upland forests in the UK. J. Hydrol. 118, 281–287

Kato, H., Onda, Y., Nanko, K., Gomi, T., & Yamanaka, T., 2013. Effect of canopy interception on spatial variability and isotopic composition of throughfall in Japanese cypress plantations. Journal of Hydrology, 504, 1–11. http://doi.org/10.1016/j.jhydrol.2013.09.028

Kendall, C., 1998. Tracing nitrogen sources and cycling in catchments. Isotope Tracers in Catchment Hydrology (C. Kendall, J. J. McDonnell, Eds) Elsevier, 521-576.

Kittredge, J., 1948. Forest influences, Interception and Stemflow, chapter XI, pp. 99-114, McGraw-Hill, New York.

Kundzewicz, Z. W., Mata, L. J., Arnell, N., Döll, P., Kabat, P., Jiménez, B., Miller, K., Oki, T., Şen, Z. & Shiklomanov,I., 2007. Freshwater resources and their management. Climate Change 2007: Impacts, Adaptation and Vulnerability. Contribution of Working Group II to the Fourth Assessment Report of the Intergovernmental Panel on Climate Change (ed. by M. L. Parry, O. F. Canziani, J. P. Palutikof, P. J. van der Linden & C. E. Hanson), 173–210. Cambridge University.

Kuraji K, Tanaka Y, Tanaka N, Karakama I., 2001. Generation of stemflow volume and chemistry in a mature Japanese cypress forest. Hydrol. Process 15: 1967–1978. doi: 10.1002/hyp.250.

Landwehr, J.M. and Coplen, T.B., 2006. Line-conditioned excess: a new method for characterizing stable hydrogen and oxygen isotope ratios in hydrologic systems, in Isotopes in Environmental Studies, Aquatic Forum 2004: International Atomic Energy Agency, Vienna, Austria, IAEA-CSP-26, p. 132-135.

Levia, D.F., Frost, E.E., 2003. A review and evaluation of stemflow literature in the hydrologic and biogeochemical cycles of forested and agricultural ecosystems. Journal of Hydrology 274 (1–4), 1–29.

Levia, D. F., Germer, S., 2015. A review of stemflow generation dynamics and stemflow environment interactions in forests and shrublands. Reviews in Geophysics, 53, 673e714.

Levia DF, Herwitz SR. 2005. Interspecific variation of bark water storage capacity of three deciduous tree species in relation to stemflow yield and solute flux to forest soil. Catena; 64:117–37.

Levia, D. F., Keim, R. F., Carlyle-Moses, D. E., Frost, E. E., 2011b. Throughfall and Stemflow in Wooded Ecosystems (pp. 425–443). http://doi.org/10.1007/978-94-007-1363-5.

Liu, W.J., Liu, W.Y., Li, J.T., Wu, Z.W., Li, H.M., 2008. Isotope variation of throughfall, stemflow and soil water in a tropical rain forest and a rubber plantation in Xishuangbanna, SW China. Hydrol. Res. 39, 5–6.

Llorens P., Domingo F., 2007. Rainfall partitioning under Mediterranean conditions. A review of studies in Europe. J Hydrol 335:37–54.

Llorens P., Poch R., Latron J., 1997. Rainfall interception by a Pinus sylvestris forest patch overgrown in a Mediterranean mountainous abandoned area I. monitoring design and results down to the event scale. J Hydrol 199:331–345.

Los Gatos Research Inc, 2010. Liquid Water Isotope Analyser. User Manual. Los Gatos Research, Inc. 67 East Evelyn Avenue, Suite 3, Mountain View, CA 94041-1529

Lloyd, G. R., & De Marques, O. A., 1988. Spatial Variablility of Throughfall and Stemflow measurements in Amazonian Rainforest. Argircultural and Forest Meteorology, 42, 63–73.

Loustau, D., Berbigier, P., Granier, A., Hadj Moussa, F. E., 1992. Interception loss, throughfall and stemflow in a maritime pine stand. I. Variability of throughfall and stemflow beneath the pine canopy. Journal of Hydrology, 138, 449–467.

Makoto T, Tomoe N, Norio T, Jun S., 2000. Stable isotope studies of precipitation and river water in the Lake Biwa basin, Japan. Hydrological Processes 14: 539–556.

Marin, C.T., Bouten, W., Sevink, J., 2000. Gross rainfall and its partitioning into throughfall, stemflow and evaporation of intercepted water in four forest ecosystems in western Amazonia. J. Hydrol. 237, 40–57. http://dx.doi.org/ 10.1016/S0022-1694(00)00301-2.

McDonnell, J. J., 2014. The two water worlds hypothesis: ecohydrological separation of water between streams and trees. WIREs Water, 1(April 2014), 323–329. http://doi.org/10.1002/wat2.1027.

Miranda, A.C., Jarvis, P.G., Grace, J., 1983. Transpiration and Evaporation from Heather Moorland. Boundary-Layer Meteorology 28.

Mizugaki, S., Nanko, K., Onda, Y., 2010. The effect of slope angle on splash detachment in an unmanaged Japanese cypress plantation forest. Hydrol. Processes 24, 576–587.

Moeser, D., Roubinek, J., Schleppi, P., Morsdorf, F., Jonas, T., 2014. Agricultural and Forest Meteorology Canopy closure, LAI and radiation transfer from airborne LiDAR synthetic images. Agricultural and Forest Meteorology, 197, 158–168. http://doi.org/10.1016/j.agrformet.2014.06.008

Molina, A., Del Campo, A.D., 2011. Leaf area index estimation in a pine plantation with LAI-2000 under direct sunlight conditions: relationship with inventory and hydrologic variables. For. Syst. 20 (1), 108–121.

Molina, A. J., Campo, A. D., 2012. Forest Ecology and Management - The effects of experimental thinning on throughfall and stemflow : A contribution towards hydrology-oriented silviculture in Aleppo pine plantations. Forest Ecology and Management, 269, 206–213. http://doi.org/10.1016/j.foreco.2011.12.037.

Montgomery D.C., Peck, E.A., Vining, G.G., 2012. Introduction to Linear Regression Analysis. John Wiley & Sons. 5th edition. 672p.

Muzylo, A., Llorens, P., Valente, F., Keizer, J. J., Domingo, F., & Gash, J. H. C., 2009. A review of rainfall interception modelling. Journal of Hydrology, 370(1-4), 191–206. http://doi.org/10.1016/j.jhydrol.2009.02.058.

Nanko, K., Mizugaki, S., Onda, Y., 2008. Estimation of soil splash detachment rates on the forest floor of an unmanaged Japanese cypress plantation based on field measurements of throughfall drop sizes and velocities. Catena 72, 348–361.

Park H.T., Hattori S., 2002. Applicability of stand structural characteristics to stemflow modelling. J For Res 7:91–98.

Parker G.G., 1995. Structure and microclimate of forest canopies. In Forest Canopies (eds. M. E. Lowman & N. M. Nadkarni), pp.73–106. Academic Press, San Diego, CA, USA.

Peng, H. H., Zhao, C. Y., Feng, Z. D., Xu, Z. L., Wang, C., Zhao, Y., 2014. Canopy interception by a spruce forest in the upper reach of Heihe River basin, Northwestern China, Hydrol. Processes, 28(4), 1734–1741.

Perry, D.A., 1994. Throughfall and stemflow, litterfall, dry deposition. In: Forest Ecosystems. pp. 403-404, 362.393.

Rennermalm, A.K., Wood, E.F., Troy, T.J., 2010. Observed changes in pen-arctic cold season minimum monthly river discharge. Climate Dynamixy 35(6): 923-939.DOI.10.1088/1748-9326/4/2/024011.

Reynolds, B., Stevens, P. A., 1987. British Geomorphological Research Group Technical Bulletin no. 36, 42-55. Geobooks, Norwich.

Reynolds, E.R.C. and Henderson, C.S., 1967.Rainfall Interception by Beech, Larch and Norway Spruce. Forestry 40:165-184.

Rowe P.B., Hendrix T.M., 1951. Interception of rain and snow by second growth ponderosa pine. Trans Am Geophys Union 32:903–908.

Rozanski, K., Araguás-Araguás, L., Gonfiantini, R., 1993. Isotopic Patterns in Modern Global precipitation. Climate Change in Continental Isotopic Records (P.K. Swart, K.L. Lohmann, J. McKenzie, S. Savin, Eds) Geophysical Monograph 78, American Geophysical Union, Washington, DC, 1-37.

Rutter, A.J., 1963. Studies in the water relations of Pinus sylvestris in plantation conditions. J. Ecol. 51, 191–203.

Rutter A.J., Kershaw K.A., Robins P.C., Morton, A.J., 1971. A predictive model of rainfall interception in forests, 1. Derivation of the model from observations in a plantation of Corsican pine. Agric Meteorol 9:367–384.

Saxena R.K., 1986. Estimation of canopy reservoir capacity and Oxygen-18 fractionation in throughfall in a pine forest.NordicHydrology 17:251–260.

Scatena, F. N., 1990. Watershed scale rainfall interception on two forested watersheds in the Luquillo mountains of Puerto Rico, Journal of Hydrology, 113, pp.89-102.

Smyth T.A.G, Jackson D.W.T., Cooper J.A.G., 2013. Three dimensional airflow patterns within a coastal blowout during fresh breeze to hurricane force winds. Aeolian Research 9: 111–123.

Soulsby, C., Birkel, C., Geris, J., Dick, J., Tunaley, C. & Tetzlaff, D. , 2015. Stream water age distributions controlled by storage dynamics and nonlinear hydrologic connectivity: Modeling with high-resolution isotope data. Water Resources Research, vol 51, no. 9, pp. 7759-7776.

Soulsby, C., Malcolm, R., Helliwell, R., Ferrier, R. C., & Jenkins, A., 2000. Isotope hydrology of the Allt a' Mharcaidh catchment, Cairngorms, Scotland: implications for hydrological pathways and residence times. Hydrological Processes, 14(4), 747–762. http://doi.org/10.1002/(SICI)1099-1085(200003)14:4<747::AID-HYP970>3.0.CO;2-0.

Spath, H., 1985. Cluster Dissection and Analysis: Theory, FORTRAN Programs, Examples. Halsted Press, New York.

Staelens, J., Schrijver, A.D., Verheyen, K., Verhoest, N.E.C., 2006. Spatial variability and temporal stability of throughfall water under a dominant beech (Fagus sylvatica L.) tree in relationship to canopy cover. J. Hydrol. 330, 651–662.

Staelens, J., Schrijver, A.D., Verheyen, K., Verhoest, N.E.C., 2008. Rainfall partitioning into throughfall, stemflow, and interception within a single breech (Fagus sylyatica L.) canopy: influence of foliation, rain event characteristics, and meteorology. Hydrological Processes 22(1): 33–45. doi:10.1002/hyp.6610.

Stockinger, M. P., Lücke, A., McDonnell, J. J., Diekkrüger, B., Vereecken, H., & Bogena, H. R., 2015. Interception effects on stable isotope driven streamwater transit time estimates. Geophysical Research Letters, 42(1), 5299–5308. http://doi.org/10.1002/2015GL064622.

Stout, B. B., McMahon, R. J., 1961. Throughfall variation under tree crowns, J. Geophys. Res., 66, 1839-1843.

Stuart, G. W., 1962. A study of rainfall interception by an oak-hickory forest cover on a watershed in central Pennsylvania, M.S. thesis, Pennsylvania State University.

Tetzlaff D., Soulsby C., Buttle J., Capell R., Carey S.K., Kruitbos L., Laudon H., McDonnell J., McGuire K., Seibert S., Shanley J., 2013. Catchments on the Cusp? Structural and functional change in northern ecohydrological systems. Hydrological Processes 27: 766–774.

Tetzlaff, D., Buttle, J., Carey, S. K., Mcguire, K., Laudon, H., Soulsby, C., 2015. Tracer-based assessment of fl ow paths, storage and runoff generation in northern catchments : a review. Hydrol. Processes, 3490 (December 2014), 3475–3490. http://doi.org/10.1002/hyp.10412

Tetzlaff, D., Birkel, C., Dick, J.J., Geris, J. & Soulsby, C., 2014. Storage dynamics in hydropedological units control hillslope connectivity, runoff generation, and the evolution of catchment transit time distributions. Water Resources Research, vol 50, no. 2, pp. 969-985.

Tetzlaff, D., Soulsby, C., Hrachowitz, M., Speed, M., 2011. Relative influence of upland and lowland headwaters on the isotope hydrology and transit times of larger catchments. J. Hydrol. 400, 438–447. http://dx.doi.org/10.1016/ j.jhydrol.2011.01.053.

The Scottish Forestry Strategy, 2006. Forestry Commission Scotland, Edinburgh.

Kubota, T., Tsuboyama, Y., 2003. Intra-and inter-storm oxygen-18 and deuterium variations of rain, throughfall, and stemflow, and two-component hydrograph separation in a small forested catchment in Japan. Journal of Forest Research 8: 179–190. doi:10.1007/s10310-002-0024-9.

Tsujimura, M., Tanaka, T., 1998. Evaluation of evaporation rate from forested soil surface using stable isotope composition of soil water in a headwater basin. Hydrol. Processes 12, 2093–2103.

UKCP09: Jones P.D., Kilsby C.G., Harpham C., Glenis V., Burton A., 2009. UK Climate Projections science report: Projections of future daily climate for the UK from the Weather Generator. University of Newcastle: UK.

Voigt, G.K., 1960. Distribution of rainfall under forest stands. Forest Science 6, 2–10.

Welker JM. 2000. Isotopic (d18O) characteristics of weekly precipitation collected across the USA: an initial analysis with application to water source studies. Hydrological Processes 14: 1449–1464.

Whelan, M.J., Anderson, J.M., 1996. Modelling spatial patterns of throughfall and interception loss in a Norway spruce (Picea abies) plantation at the plot scale. J. Hydrol. 186, 335–354. http://dx.doi.org/10.1016/S0022-1694(96)03020-X.

Wilm, H.G., 1943. Determining net rainfall under a conifer forest, J. Agr. Res., 67, 501-512.

Wookey, P.A., Aerts, R., Bardgett, R.D., Baptist, F., Brathen, K.A., Cornelissen, J.H.C., Gough, L., Hartley, I.P., Hopkins, D.W., Lavorel, S., Shaver, G.R., 2009. Ecosystem feedbacks and cascade processes: understanding their role in the responses of arctic and alpine ecosystems to environmental change. Global Change Biology 15: 1153-1172.

Xiao, Q., McPherson, E.G., Ustin, S.L., Grismer, M.E., 2000. A new approach to modeling tree rainfall interception, J. Geophys. Res., 105(D23), 29173–29188, doi:10.1029/2000JD900343 .

Yurtsever, Y., Gat, J.R., 1981. Atmospheric waters. Stable Isotope Hydrology: Deuterium and Oxygen- 18 in the Water Cycle. (J.R. Gat, R. Gonfiantini, Eds) Technical Reports Series 210, IAEA, Vienna, 103-142.

Zhang, W., Cheng, B., Hu, Z., An, S., Xu, Z., Zhao, Y., & Cui, J., 2010. Using stable isotopes to determine the water sources in alpine ecosystems on the east Qinghai-Tibet plateau, China. Hydrological Processes, 24, 3270–3280. http://doi.org/10.1002/hyp.7754

Zhang, Y.F., Wang, X.P., Hu, R., Pan, Y.X., Paradeloc, M., 2015. Rainfall partitioning into throughfall, stemflow and interception loss by two xerophytic shrubs within a rain-fed re-vegetated desert ecosystem, northwestern China, J. Hydrol., 527 (2015), pp. 1084–1095

APPENDIX A

Table Appendix A-1: Sample dates, days until next sampling date and summarized GR (GR.Sum), maximum Intensity of GR (GR.Max.Int) and mean TF for north- and south facing plantations and heather sites ± standard deviation.

Sample Date	*Days*	*GR.Sum [mm]*	*GR.M.Int [mm h^{-1}]*	*TF plantation north facing ± Std.Dev. [mm]*	*TF plantation south facing ± Std.Dev. [ml]*	*TF heather north facing ± Std.Dev. [mm]*	*TF heather south facing ± Std.Dev. [ml]*
01.06.2015	11	7.6	3.8	2.18 ± 0	2.92 ± 2	-	-
09.06.2015	8	12.2	0.8	6.07 ± 0.5	6.08 ± 1.3	6.8 ± 1.7	0.21 ± 0
17.06.2015	8	3.6	0.4	0.71 ± 0	0.88 ± 0.8	1.33 ± 0.8	1.17 ± 0
25.06.2015	8	10.4	1.8	3.4 ± 0	5.27 ± 2.3	5.2 ± 2	7.29 ± 0
02.07.2015	7	10.4	4.6	2.64 ± 0	3.29 ± 2.2	5.1 ± 1.5	5.96 ± 0
06.07.2015	4	20.8	4.6	15.56 ± 8.3	15.56 ± 3.5	13.95 ± 4.1	17.02 ± 0
20.07.2015	14	74.8	7.6	46.66 ± 17	51.16 ± 12.5	45.9 ± 15.8	57.75 ± 0
30.07.2015	10	23.6	8	11.43 ± 4	14.92 ± 5.3	13.88 ± 3.8	15.92 ± 0
06.08.2015	7	12.8	1.6	3.69 ± 0	4.46 ± 2.3	6.65 ± 1.7	7.54 ± 0
13.08.2015	7	2.2	1.2	0.23 ± 0	0.25 ± 0.2	0.53 ± 0.2	0.53 ± 0
19.08.2015	6	36.2	3.8	20.71 ± 6	21.79 ± 7.1	20.5 ± 6.9	23.5 ± 0
28.08.2015	9	18.8	1.8	7.76 ± 0.5	11.42 ± 3.9	10.1 ± 2.9	13.21 ± 0
03.09.2015	6	8.8	3	2.66 ± 0	3.32 ± 1.6	3.35 ± 1.1	4.58 ± 0
10.09.2015	7	0.8	0.2	0.04 ± 0	0.04 ± 0.1	0.08 ± 0.1	0 ± 0
18.09.2015	8	16.8	3.2	9.36 ± 1	8.42 ± 2.6	9.98 ± 3.5	10.94 ± 0
24.09.2015	6	16	4.6	9.72 ± 4	11.64 ± 3.1	9.9 ± 3	12.98 ± 0

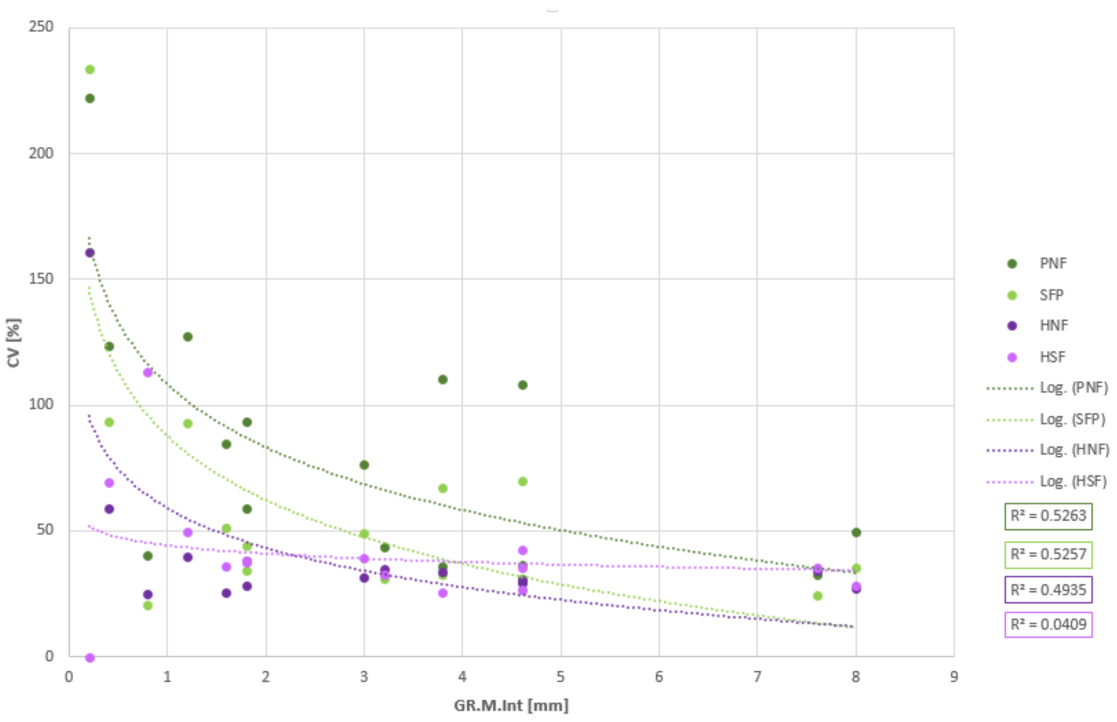

Figure Appendix A-1: Coefficient of variation (CV [%]) against GR.M.Int [mm] for all the sample sites. PNF is plantation north facing, SFP is plantation south facing, HNF is heather north facing, HSF is heather south facing. Log. describes the logarithmic regression between CV and GR.

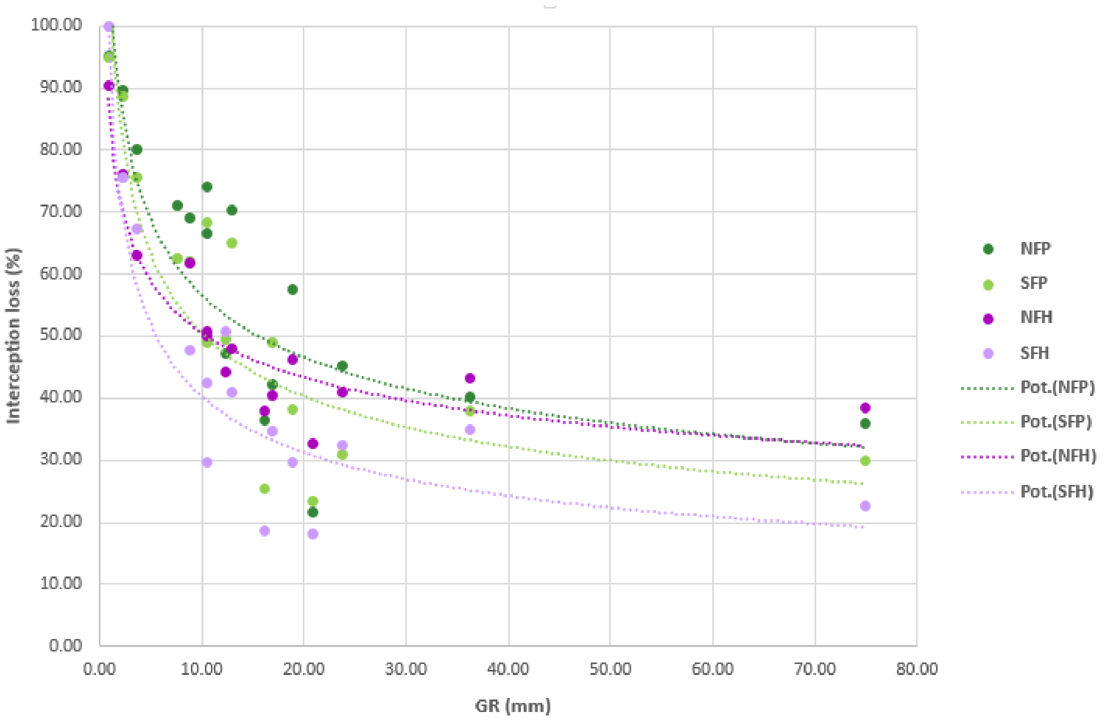

Figure Appendix A-2: Interception loss [%] against GR [mm] for all the sample sites. PNF is plantation north facing, SFP is plantation south facing, HNF is heather north facing, HSF is heather south facing. Pot. describes the polynomic regression between interception loss and GR.

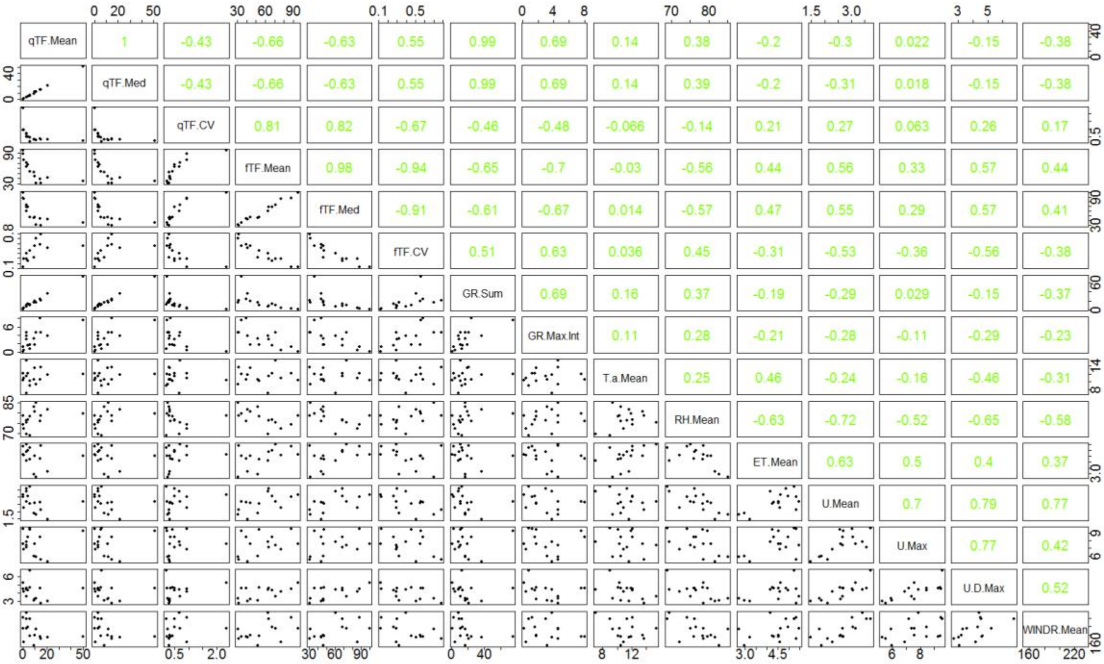

Figure Appendix A-3: Pearson correlation and Scatterplot for TF quantity (qTF.Mean, qTF.Median and qTF.CV) and TF fraction (fTF.Mean [mm], fTF.Median [mm] and fTF.CV [mm]) values for the south facing plantation and some hydroclimatic variables like GR.Sum [mm], GR.M.Int. [mmh^{-1}], T.a.Mean [°C], RH.Mean [%], PETP.Mean [mm], U.Mean [ms^{-1}], U.Max [ms^{-1}], U.D.Max [ms^{-1}] and WINDR.Mean [°]. The green numbers represent the correlation coefficient r.

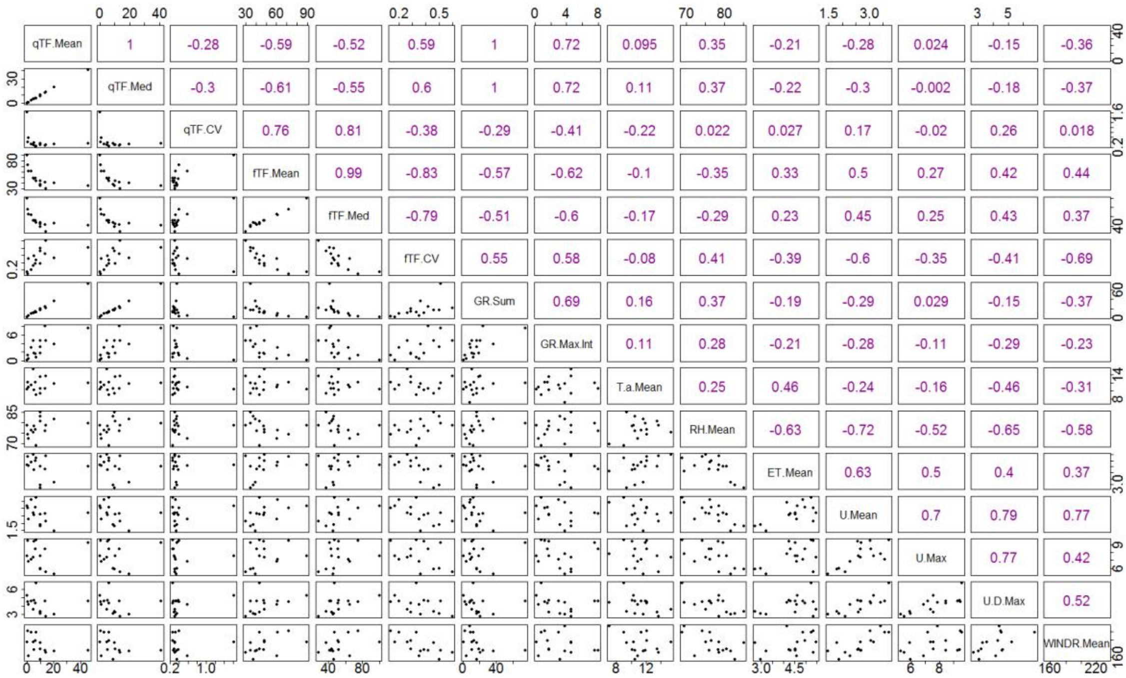

Figure Appendix A-4: Pearson correlation and Scatterplot for TF quantity (qTF.Mean, qTF.Median and qTF.CV) and TF fraction (fTF.Mean [mm], fTF.Median [mm] and fTF.CV [mm]) values for the north facing heather and some hydroclimatic variables like GR.Sum [mm], GR.M.Int. [mmh^{-1}], T.a.Mean [°C], RH.Mean [%], PETP.Mean [mm], U.Mean [ms^{-1}], U.Max [ms^{-1}], U.D.Max [ms^{-1}] and WINDR.Mean [°]. The purple numbers represent the correlation coefficient r.

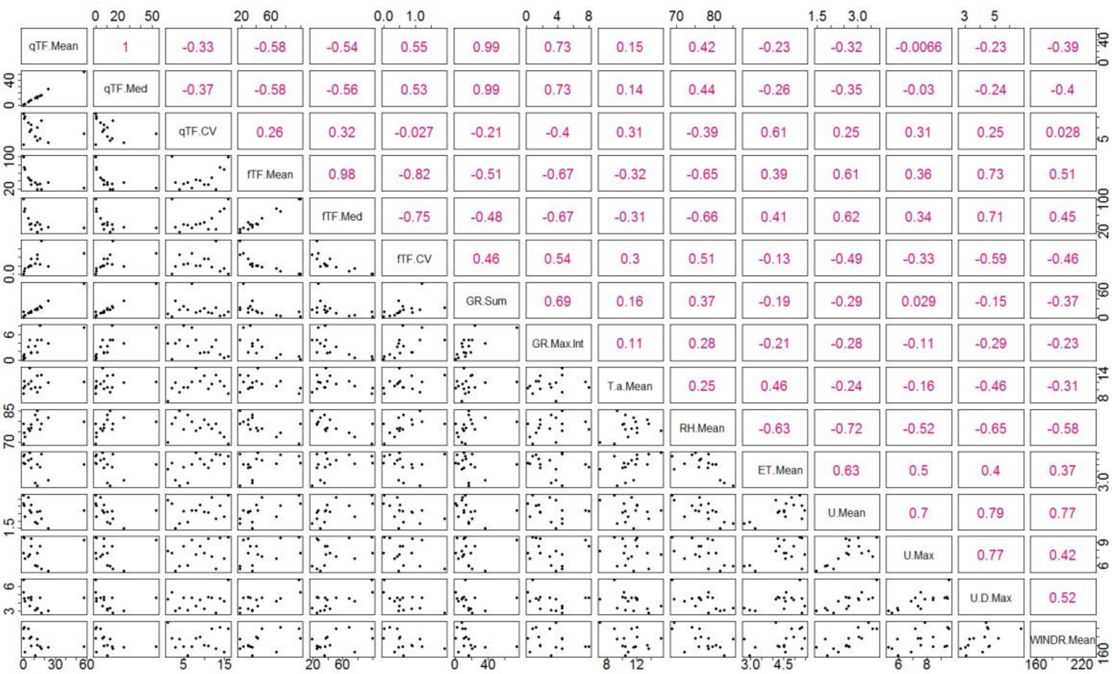

Figure Appendix A-5: Pearson correlation and Scatterplot for TF quantity (qTF.Mean, qTF.Median and qTF.CV) and TF fraction (fTF.Mean [mm], fTF.Median [mm] and fTF.CV [mm]) values for the south facing heather and some hydroclimatic variables like GR.Sum [mm], GR.M.Int. [mmh^{-1}], T.a.Mean [°C], RH.Mean [%], PETP.Mean [mm], U.Mean [ms^{-1}], U.Max [ms^{-1}], U.D.Max [ms^{-1}] and WINDR.Mean [°]. The pink numbers represent the correlation coefficient r.

APPENDIX B

Table Appendix B-1: Sample dates, days until next sampling date and Summarized Gross Rainfall (GR.Sum), maximum intensity of GR (GR.Max.Int) and mean SF for north- and south facing plantations ± standard deviation.

Sample Date	*Days*	*GR.Sum [mm]*	*GR.M.Int [mm h^{-1}]*	*SF north facing ± Std.Dev. [ml]*	*SF south facing ± Std.Dev. [ml]*
01/06/2015	11	7.6	3.8	36.4 ± 68.8	-
09/06/2015	8	12.2	0.8	2217 ± 2331.7	454 ± 783.8
17/06/2015	8	3.6	0.4	0 ± 0	0 ± 0
25/06/2015	8	10.4	1.8	352 ± 542.5	128 ± 214.7
02/07/2015	7	10.4	4.6	238 ± 372.1	0 ± 0
06/07/2015	4	20.8	4.6	4764 ± 4263.6	1924 ± 1210
20/07/2015	14	74.8	7.6	8456 ± 4171.3	6804 ± 4331.8
30/07/2015	10	23.6	8	10200 ± 5379.5	7734 ± 5163.8
06/08/2015	7	12.8	1.6	563 ± 430.1	55 ± 66.3
13/08/2015	7	2.2	1.2	0 ± 0	0 ± 0
19/08/2015	6	36.2	3.8	6004 ± 4349.4	3104 ± 2863.7
28/08/2015	9	18.8	1.8	1290 ± 1116.3	1086 ± 832.6
03/09/2015	6	8.8	3	336 ± 349.1	126 ± 227
10/09/2015	7	0.8	0.2	0 ± 0	0 ± 0
18/09/2015	8	16.8	3.2	2268 ± 1507.7	806 ± 489.5
24/09/2015	6	16	4.6	3160 ± 2092.1	1742 ± 1152.8

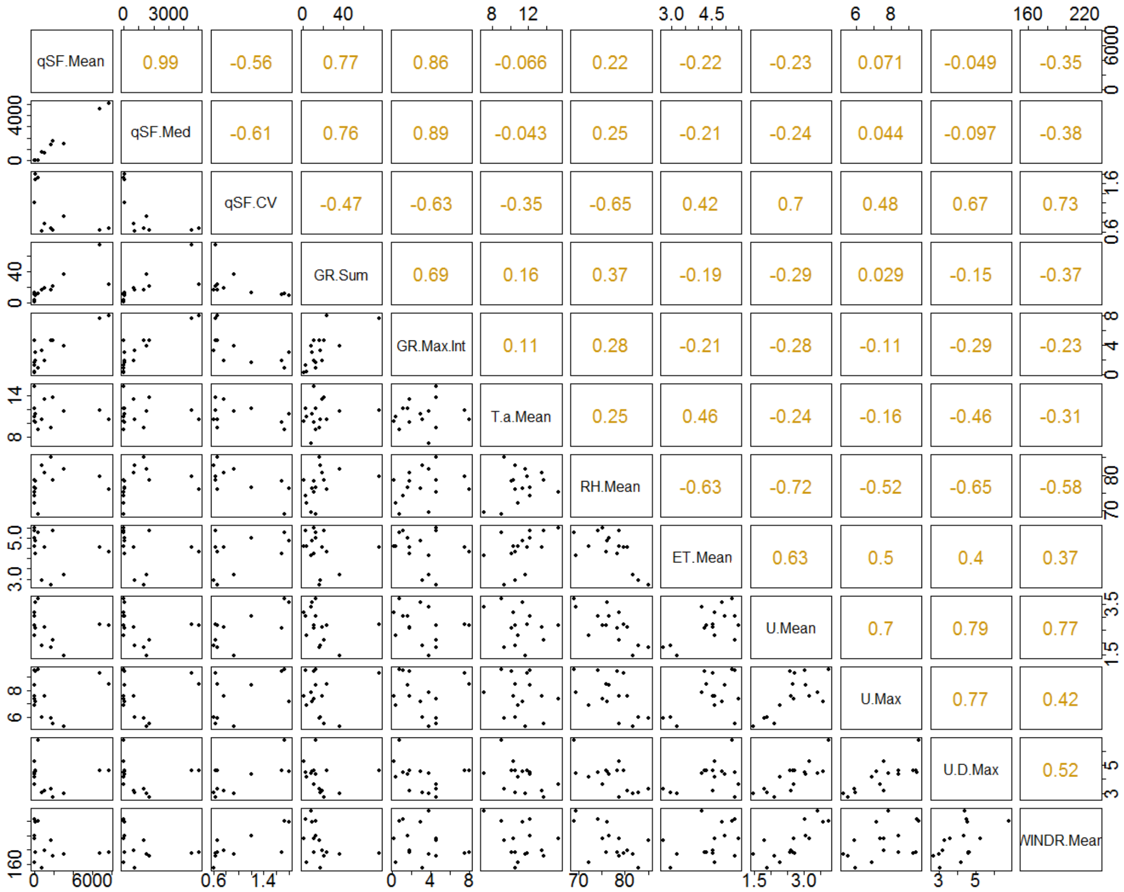

Figure Appendix B-1: Pearson correlation and Scatterplot for SF quantity (qSF.Mean, qSF.Median and qSF.CV) values for the north facing plantation and some hydroclimatic variables like GR.Sum [mm], GR.M.Int. [mm h^{-1}], T.a.Mean [°C], RH.Mean [%], PETP.Mean [mm], U.Mean [m s^{-1}], U.Max [m s^{-1}], U.D.Max [m s^{-1}] and WINDR.Mean [°]. The brown numbers represent the correlation coefficient r.

APPENDIX C

Table Appendix C-1: Amount, Intensity, weighted δ^2H and $\delta^{18}O$ values for the Gross Rainfall (GR) throughout the whole sampling period, averaged by sampling dates.

Gross rainfall (GR) – Mean values for each sample period

Date	*GR.Sum [mm]*	*GR.Hours [h]*	*GR.M.Int [mm h^{-1}]*	*T.a.Mean [°C]*	*$\delta^{18}O$ weighted [‰]*	*δ^2H weighted [‰]*	*lc-Excess weighted [‰]*
01/06/2015	7.6	14	3.8	7.04	-13.74	-105.12	-2.5 ± 1.2
09/06/2015	12.2	13	0.8	9.05	-10.36	-79.34	-3.24 ± 1.2
17/06/2015	3.6	13	0.4	10.89	-4.1	-23.99	2.83 ± 0.8
25/06/2015	10.4	26	1.8	10.15	-4.79	-38.68	-6.45 ± 2.3
02/07/2015	10.4	23	4.6	15.40	-2.99	-28.9	-10.81 ± 2.5
06/07/2015	20.8	12	4.6	13.75	-4.75	-40.47	-8.49 ± 4.2
20/07/2015	74.8	79	7.6	11.89	-8.01	-57.92	-0.33 ± 1.6
30/07/2015	23.6	31	8	10.53	-6.39	-47.48	-2.6 ± 1.5
06/08/2015	12.8	28	1.6	12.17	-4.16	-26.91	0.42 ± 1.3
13/08/2015	2.2	4	1.2	12.16	-5.67	-41.34	-2.19 ± 2
19/08/2015	36.2	37	3.8	11.69	-8.87	-64.24	0.13 ± 1.2
28/08/2015	18.8	27	1.8	13.56	-6.74	-46.55	1.06 ± 1.8
03/09/2015	8.8	19	3	11.40	-5.82	-45.15	-4.82 ± 0.6
10/09/2015	0.8	3	0.2	10.31	-	-	-
18/09/2015	16.8	21	3.2	10.50	-8.03	-56.26	1.49 ± 5.4
24/09/2015	16	19	4.6	9.37	-7.75	-55.98	-0.44 ± 0.9

Table Appendix C-2: Standards used for the isotope calibration to encompass the range of waters naturally experienced in the catchment.

Name	δ^2H	$\delta^{18}O$
LGR1A	-154.3	-19.5
LGR2A	-123.6	-16.1
LGR3A	-96.4	-13.1
LGR4A	-51.0	-7.7
LGR5A	-9.5	-2.8

Table Appendix C-3: $\delta^{18}O$, $\delta^{18}O$ Std.Dev., $\delta^{2}H$, $\delta^{2}H$ Std.Dev., dExcess, dExcess Std.Dev. of TF throughout the whole sampling period, averaged by sampling dates. No samples could be taken for the 10th of September due to very little precipitation the previous week and hence very small amounts of TF (~0.5mm).

Date	*GR ± Std.Dev. [mm]*	*$\delta^{18}O$ ± Std.Dev. [‰]*	*$\delta^{2}H$ ± Std.Dev. [‰]*	*lc-Excess ± Std.Dev. [‰]*
01/06/2015	2.55 ± 2.2	-12.08 ± 1.3	-93.09 ± 10.5	-3.53 ± 1
09/06/2015	5.35 ± 2.9	-9.82 ± 3.5	-76.48 ± 19.4	-4.63 ± 1.2
17/06/2015	1 ± 0.9	-4.58 ± 0.5	-106.18 ± 6.8	-7.58 ± 67.7
25/06/2015	5.11 ± 3	-5.01 ± 1.1	-37.09 ± 2.3	-3.13 ± 2.3
02/07/2015	3.95 ± 2.7	-2.95 ± 1.4	-25.44 ± 2.8	-7.67 ± 2.5
06/07/2015	15.76 ± 4.8	-5.56 ± 1.4	-40.62 ± 0.2	-2.28 ± 4.2
20/07/2015	51.1 ± 16.4	-8.17 ± 0.9	-57.48 ± 0.5	1.34 ± 1.6
30/07/2015	14.03 ± 5.4	-6.18 ± 1.3	-44.78 ± 3.6	-1.57 ± 1.5
06/08/2015	5.27 ± 3.2	-3.56 ± 1.3	-22.63 ± 5	0 ± 1.3
13/08/2015	0.35 ± 0.3	-5.29 ± 1.9	-41.27 ± 4	-5.11 ± 2
19/08/2015	21.99 ± 7.2	-8.53 ± 1.3	-61.84 ± 2.7	-0.2 ± 1.2
28/08/2015	10.5 ± 4.7	-6.02 ± 0.8	-40.91 ± 4	1.01 ± 1.8
03/09/2015	3.48 ± 2	-6.79 ± 0.7	-51.84 ± 4.6	-3.89 ± 0.6
10/09/2015	0.05 ± 0.1	-	-	-
18/09/2015	9.64 ± 3.7	-7.61 ± 0.4	-55.39 ± 2.2	-0.99 ± 5.4
24/09/2015	11.18 ± 3.6	-7.5 ± 0.2	-53 ± 2	0.58 ± 0.9

Table Appendix C-4: $\delta^{18}O$, $\delta^{18}O$Std.Dev., $\delta^{2}H$, $\delta^{2}H$ Std.Dev., dExcess Std.Dev., lc-excess, $\Delta\delta^{18}O$ and Δd-Excess of TF throughout the whole sampling period, averaged by sampling dates at the 4 different sites plantation and heather south- and north-facing.

Date	*Amount +Std.Dev. [mm]*	*δ¹⁸O + Std.Dev. [‰]*	*δ²H + Std.Dev. [‰]*	*dExcess + Std.Dev. [‰]*	*lc-Excess [‰]*	*Δδ¹⁸O [‰]*	*Δd-Excess [‰]*
Plantation North Facing							
01/06/2015	2.18 ± 0	-11.10 ± 0.8	-86.26 ± 5.0	2.52 ± 2.3	-4.39	1.38	-3.51
09/06/2015	6.51 ± 0.1	-11.90 ± 0.7	-92.47 ± 4.3	1.35 ± 2.7	-4.34	-2.07	-2.19
17/06/2015	0.71 ± 0	-4.80 ± 0.8	-79.13 ± 8.1	1.32 ± 7.1	-46.78	-1.38	-7.49
25/06/2015	3.4 ± 0	-5.46 ± 0.7	-38.46 ± 6.8	5.07 ± 2.2	-0.9	-0.46	5.43
02/07/2015	2.64 ± 0	-3.30 ± 0.6	-25.61 ± 4.5	0.71 ± 1.9	-5.08	-0.75	5.69
06/07/2015	15.56 ± 8.3	-5.81± 0.3	-40.50 ± 1.8	5.74 ± 1.2	-0.25	-1.00	8.21
20/07/2015	46.66 ± 17	-8.21 ± 0.3	-57.22 ± 1.5	8.2 ± 2.2	1.96	-0.17	2.04
30/07/2015	11.43 ± 4	-5.32 ± 0.5	-39.47 ± 3.4	3.53 ± 3.2	-3.01	-0.04	-0.11
06/08/2015	3.69 ± 0	-2.66 ± 0.6	-15.59 ± 4.3	4.4 ± 3.2	-0.08	1.06	-1.97
13/08/2015	0.23 ± 0	-4.90 ± 1	-38.89 ± 6.2	-0.38 ± 2.6	-5.76	0.17	-4.40
19/08/2015	20.71 ± 6	-8.19 ± 0.5	-59.53 ± 3.6	6.92 ± 1.6	0.62	0.68	0.20
28/08/2015	7.76 ± 0.5	-5.34 ± 0.7	-38.89 ± 5.6	4.75 ± 1.4	-0.95	1.51	-2.62
03/09/2015	2.66 ± 0	-7.20 ± 0.3	-54.71 ± 2.7	2.75 ± 0.9	-3.51	-1.37	1.34
10/09/2015	0.04 ± 0	-	-	-	-	-	-
18/09/2015	9.36 ± 1	-8.02 ± 0.6	-52.31 ± 4.7	9.74 ± 4.2	5.34	0.45	1.76
24/09/2015	9.72 ± 4	-7.26 ± 0.2	-51.76 ± 1.4	6.55 ± 1.1	0.03	0.50	0.53
Plantation South Facing							
01/06/2015	2.92 ± 2	-11.39 ± 0.7	-87.88 ± 4.4	2.9 ± 1.6	-3.71	1.50	-1.90
09/06/2015	6.08 ± 1.3	-6.06 ± 2.5	-48.46 ± 16.6	1.51 ± 3.1	-6.18	-3.07	-2.03
17/06/2015	0.88 ± 0.8	-5.05 ± 1	-87.87 ± 8.7	3.49 ± 3.5	-67.76	-1.20	-5.32
25/06/2015	5.27 ± 2.3	-4.66 ± 0.8	-33.64 ± 7.7	3.72 ± 2.9	-2.44	-0.48	4.08
02/07/2015	3.29 ± 2.2	-2.69 ± 0.7	-22.13± 3.9	-0.22 ± 3.4	-6.38	-0.52	4.76
06/07/2015	15.56 ± 3.5	-5.85 ± 0.4	-40.72 ± 1.7	6.09 ± 2	-0.15	-1.08	8.56
20/07/2015	51.16 ± 12.5	-8.34 ± 0.2	-56.96 ± 1.2	9.77 ± 1	3.22	-0.33	3.61
30/07/2015	14.92 ± 5.3	-6.55 ± 0.3	-45.93 ± 1.3	7.23 ± 2.6	0.18	-0.59	3.59
06/08/2015	4.46 ± 2.3	-3.72 ± 0.4	-22.46 ± 2.2	6.94 ± 2.3	1.4	0.55	0.57
13/08/2015	0.25 ± 0.2	-4.75 ± 0.8	-38.03 ± 5.4	0.73 ± 5	-6.18	0.19	-3.29
19/08/2015	21.79 ± 7.1	-8.01 ± 0.5	-59.48 ± 3.7	4.53 ± 1.5	-1.91	0.87	-2.19
28/08/2015	11.42 ± 3.9	-5.90 ± 0.5	-37.59 ± 3.5	9.73 ± 1.9	3.39	0.94	2.36
03/09/2015	3.32 ± 1.6	-6.88 ± 0.4	-52.37 ± 3.0	3.16 ± 0.9	-3.7	-1.85	1.75
10/09/2015	0.04 ± 0.1	-	-	-	-	-	-
18/09/2015	8.42 ± 2.6	-7.19 ± 0.7	-57.41 ± 5.3	7.52 ± 1.8	-6.3	0.05	-0.46
24/09/2015	11.64 ± 3.1	-7.45 ± 0.7	-52.03 ± 1.9	8.36 ± 6.4	1.43	0.24	2.34

Date	Amount [mm]	$\delta^{18}O$ [‰] weighted	$\delta^{2}H$ [‰] weighted	dExcess + Std.Dev. [‰]	lc-Excess [‰]	$\delta^{18}O$ [‰]	Δd-Excess [‰]
Heather South Facing							
01/06/2015	-	-	-	-	-	-	-
09/06/2015	6.8 ± 1.7	-10.97 ± 0.8	-85.64 ± 0.4	0.64 ± 0	-4.75	1.24	-1.41
17/06/2015	1.33 ± 0.8	-4.37 ± 0.4	-80.57 ± 2.6	3.78 ± 2.7	-51.63	-1.09	3.35
25/06/2015	5.2 ± 2	-5.11 ± 0.6	-37.57 ± 5.0	2.78 ± 1.9	-2.78	1.98	-5.23
02/07/2015	5.1 ± 1.5	-2.81 ± 0.5	-25.14 ± 2.5	7.98 ± 1.7	-8.43	-2.80	-1.94
06/07/2015	13.95 ± 4.1	-5.85 ± 0.4	-40.78 ± 2.0	9.8 ± 3.5	-0.21	-3.35	10.79
20/07/2015	45.9 ± 15.8	-8.11 ± 0.1	-57.82 ± 1.1	3.27 ± 1.2	0.53	1.53	9.40
30/07/2015	13.88 ± 3.8	-6.46 ± 0.2	-46.23 ± 1.7	1.09 ± 5.4	-0.8	2.69	-0.59
06/08/2015	6.65 ± 1.7	-3.71 ± 0.4	-25.54 ± 2.6	-0.47 ± 6.1	-1.73	-1.54	0.45
13/08/2015	0.53 ± 0.2	-5.84 ± 1.0	-46.81 ± 7.1	5.57 ± 1.4	-6.32	-3.20	-6.64
19/08/2015	20.5 ± 6.9	-8.89 ± 0.3	-64.11 ± 2	26.76 ± 19.2	0.38	2.83	2.98
28/08/2015	10.1 ± 2.9	-5.98 ± 0.5	-41.09 ± 3.8	4.1 ± 1	0.55	-0.52	0.04
03/09/2015	3.35 ± 1.1	-7.25 ± 0.4	-55.15 ± 3.3	-	-3.56	5.82	-4.64
10/09/2015	0.08 ± 0.1	-	-	0 ± 0	0	-	-
18/09/2015	9.98 ± 3.5	-7.19 ± 0.3	-55.57 ± 1.2	0 ± 0	-4.47	0.56	8.81
24/09/2015	9.9 ± 3	-7.50 ± 0.4	-52.31 ± 1.3	0.64 ± 0	1.29	7.75	-0.57
Heather North Facing							
01/06/2015	-	-13.74 ± 1.2	-105.12 ± 5.6	-	-2.48	-	-
09/06/2015	0.21 ± 0	-10.36 ± 1.5	-79.34 ± 0.25	2.16 ± 2.3	-3.28	-	-
17/06/2015	1.17 ± 0	-4.1 ± 0.4	-23.99 ± 4.4	6.89 ± 2.8	2.85	0.18	-8.17
25/06/2015	7.29 ± 0	-4.79 ± 0.4	-38.68 ± 1.9	3.58 ± 1.6	-6.42	-0.78	4.14
02/07/2015	5.96 ± 0	-2.99 ± 0.3	-28.90 ± 1.2	-2.3 ± 2.7	-10.79	-0.61	7.76
06/07/2015	17.02 ± 0	-4.75 ± 1.1	-40.47 ± 5.6	5.81 ± 1.1	-8.52	-1.48	10.45
20/07/2015	57.75 ± 0	-8.01 ± 0.3	-57.92 ± 1.2	6.93 ± 0.5	-0.34	-0.78	3.64
30/07/2015	15.92 ± 0	-6.39 ± 0.7	-47.48 ± 2.8	5.57 ± 0.7	-2.64	0.00	-0.37
06/08/2015	7.54 ± 0	-4.16 ± 0.6	-26.91 ± 4.4	4.09 ± 1.6	0.4	0.89	-5.28
13/08/2015	0.53 ± 0	-5.67 ± 0.4	-41.34 ± 2.1	-0.27 ± 1.6	-2.19	-0.31	-4.49
19/08/2015	23.5 ± 0	-8.87± 0.3	-64.24 ± 2.2	7.00 ± 1.3	0.1	0.32	-1.15
28/08/2015	13.21 ± 0	-6.74 ± 0.3	-46.55 ± 2.3	6.76 ± 1.3	1.05	0.72	19.39
03/09/2015	4.58 ± 0	-5.82 ± 0.3	-45.15 ± 2.7	2.73 ± 0.6	-4.79	-1.51	2.69
10/09/2015	0 ± 0	-	-	-	-	-	-
18/09/2015	10.94 ± 0	-8.03 ± 0.4	-56.26 ± 3.1	8.81 ± 3.1	1.48	-0.20	-7.98
24/09/2015	12.98 ± 0	-7.75 ± 0.5	-55.98 ± 1.4	7.41 ± 3.0	-0.44	0.42	-6.02

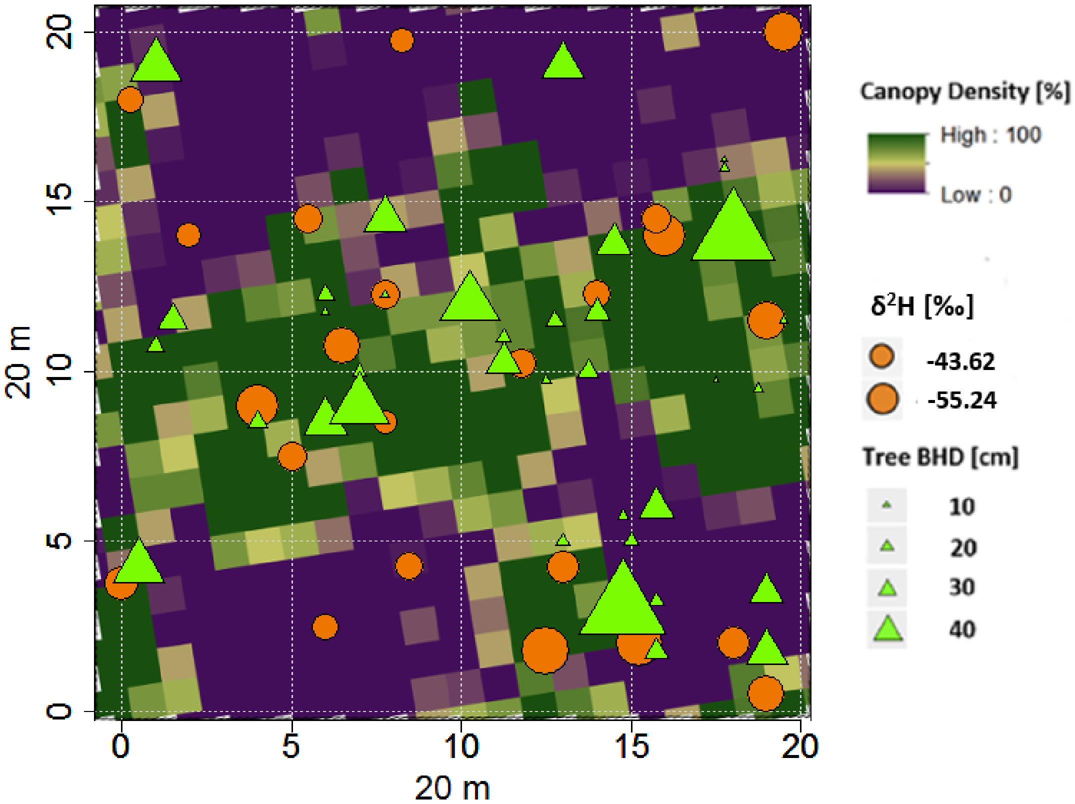

Figure Appendix C-1: 20 x 20m grid of the north facing plantation with 25 TF collectors (orange dots) and trees (green triangles). Orange points represent the δ^2H values. Bigger triangles represent trees with greater BHD [cm], smaller triangles represent trees with smaller BHD. Dark green squares indicate high canopy coverage [%], purple indicates no canopy coverage.

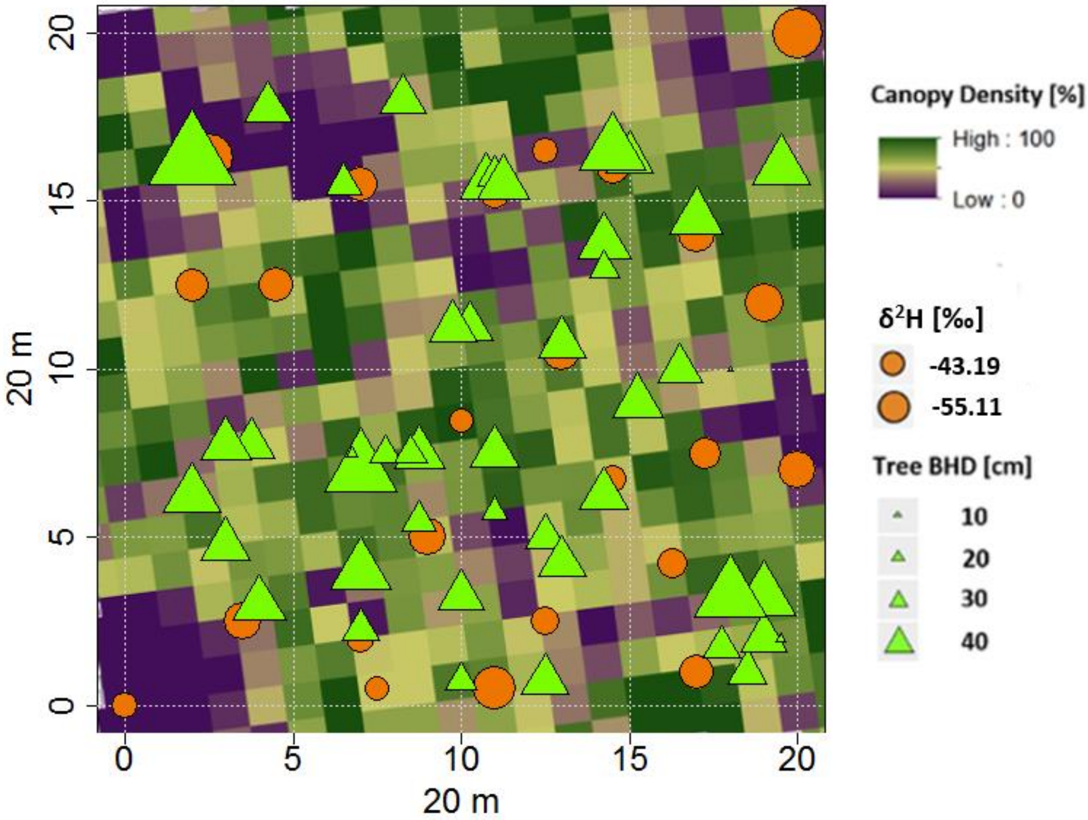

Figure Appendix C-2: 20 x 20m grid of the south facing plantation with 25 TF collectors (orange dots) and trees (green triangles). Orange points represent the δ^{2}H values. Bigger triangles represent trees with greater BHD [cm], smaller triangles represent trees with smaller BHD. Dark green squares indicate high canopy coverage [%], purple indicates no canopy coverage.

Table Appendix C-5: Multiple linear regression model (MLRM) for the south facing plantation. Y-variables are mean, median and CV of δ^{2}H and δ^{18}O, X-variables are the meteorological parameters derived by the weather station and calculated ET [mm]. R^2 values show the fit of the model. P-values show the importance of the parameter.

Y	*R^2*	*GR δ^{18}O/ δ^{2}H [‰] p- value*	*GR M.Int [mm h^{-1}] p-value*	*Ta. Mean [°C] p-value*	*U.D.Max [mm s^{-1}] p-value*	*U.Mean [mm s^{-1}] p-value*	*PETP.Mean [mm] p-value*
Plantation south facing							
δ^{18}O.TF.Mean	0.85	0.002	0.07	0.14	0.05	-	-
δ^{18}O.TF.Median	0.87	<0.001	-	-	0.01	-	-
δ^{18}O.TF.CV	0.62	0.16	0.04	0.07	0.01	0.01	-
δ^{2}H.TF.Mean	0.89	<0.001	0.06	-	0.07	0.10	0.08
δ^{2}H.TF.Median	0.88	<0.001	-	-	0.01	-	-
δ^{2}H.TF.CV	0.80	0.20	0.004	-	0.001	0.01	0.04

Table Appendix C-6: Multiple linear regression model (MLRM) for the south facing heather. Y-variables are mean, median and CV of δ^{2}H and δ^{18}O, X-variables are the meteorological parameters derived by the weather station and calculated ET [mm]. R^2 values show the fit of the model. P-values show the importance of the parameter.

Y	*R^2*	*GR δ^{18}O/ δ^{2}H [‰] p- value*	*Ta. Mean [°C] p-value*	*PETP.Mean [mm] p-value*	*U.D.Max [mm s^{-1}] p-value*	*GR M.Int [mm h^{-1}] p-value*	*U.Mean [mm s^{-1}] p-value*
Heather south facing							
δ^{18}O.TF.Mean	0.92	<0.001	0.11	0.06	0.19	-	-
δ^{18}O.TF.Median	0.91	<0.001	0.07	0.01	0.17	0.04	-
δ^{18}O.TF.CV	0.35	0.13	0.07	-	-	-	-
δ^{2}H.TF.Mean	0.96	<0.001	-	-	-	-	0.02
δ^{2}H.TF.Median	0.93	<0.001	0.07	0.002	-	0.2	-
δ^{2}H.TF.CV	0.25	0.14	-	-	0.06	-	-

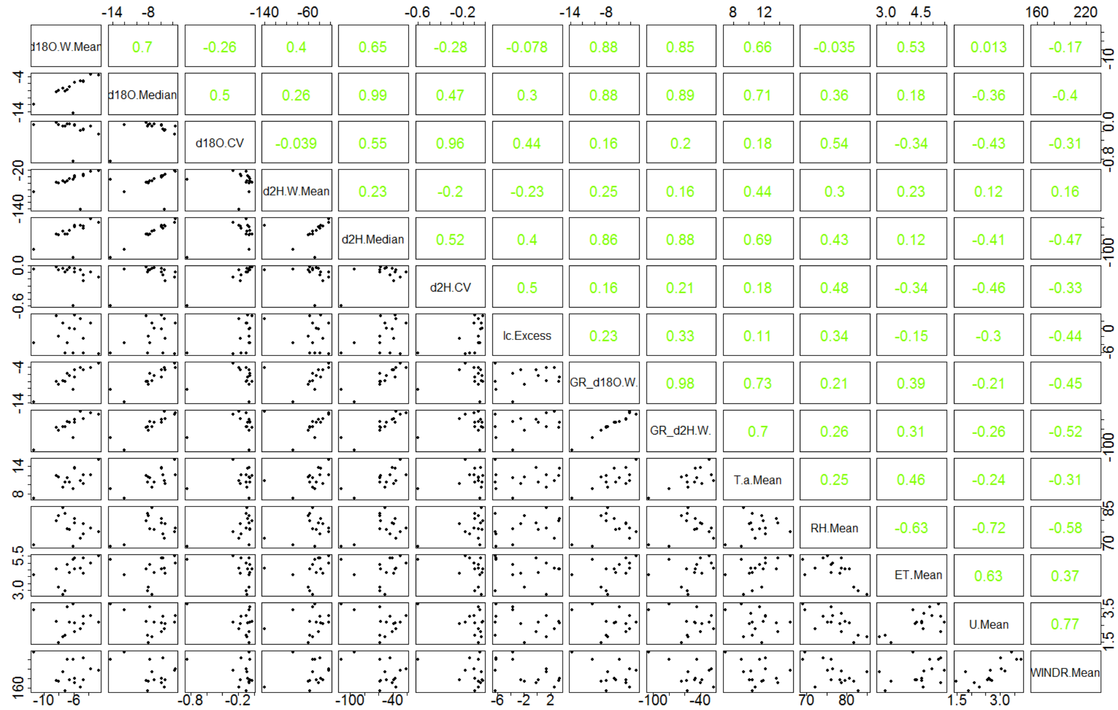

Figure Appendix C-3: Pearson correlation and Scatterplot for TF isotopic compositions (d18O.W.Mean, d18O.W.Median and d18O.W.CV) values for the south facing plantation and isotopic signatures for the GR (GR_d18.W, GR2H.W), lc-excess and hydroclimatic variables like T.a.Mean [°C], RH.Mean [%], ET.Mean [mm], U.Mean [ms^{-1}] and WINDR.Mean [°]. The green numbers represent the correlation coefficient r.

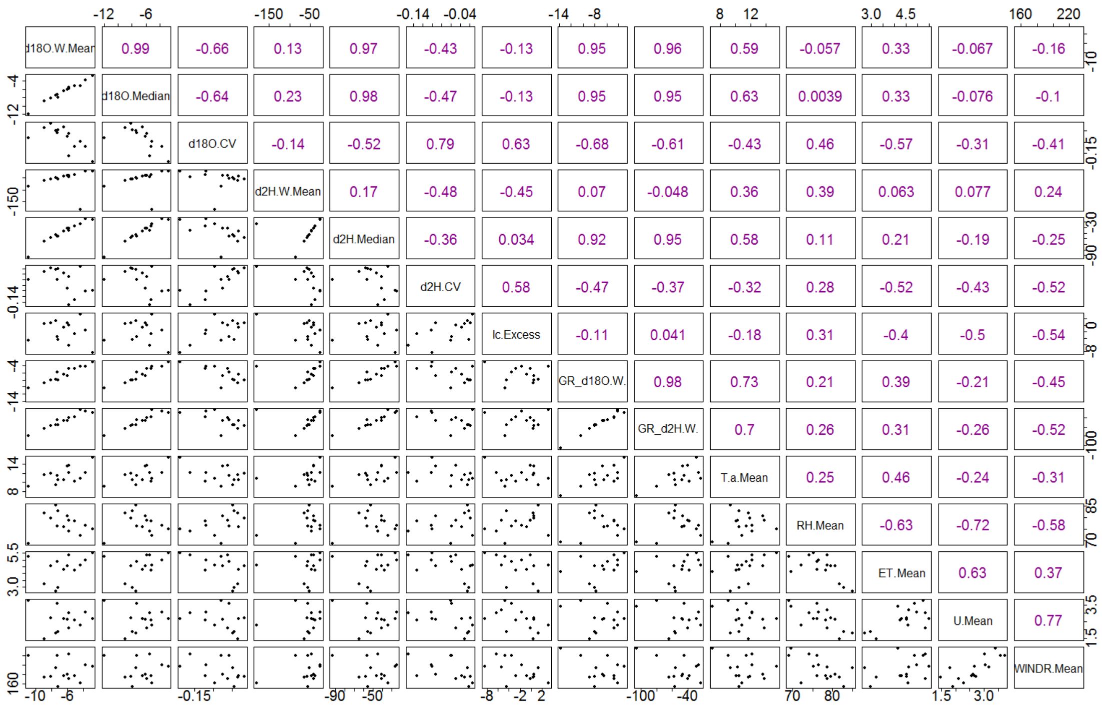

Figure Appendix C-4: Pearson correlation and Scatterplot for TF isotopic compositions (d18O.W.Mean, d18O.W.Median and d18O.W.CV) values for the north facing heather and isotopic signatures for the GR (GR_d18.W, GR2H.W), lc-excess and hydroclimatic variables like T.a.Mean [°C], RH.Mean [%], ET.Mean [mm], U.Mean [ms^{-1}] and WINDR.Mean [°]. The green numbers represent the correlation coefficient r.

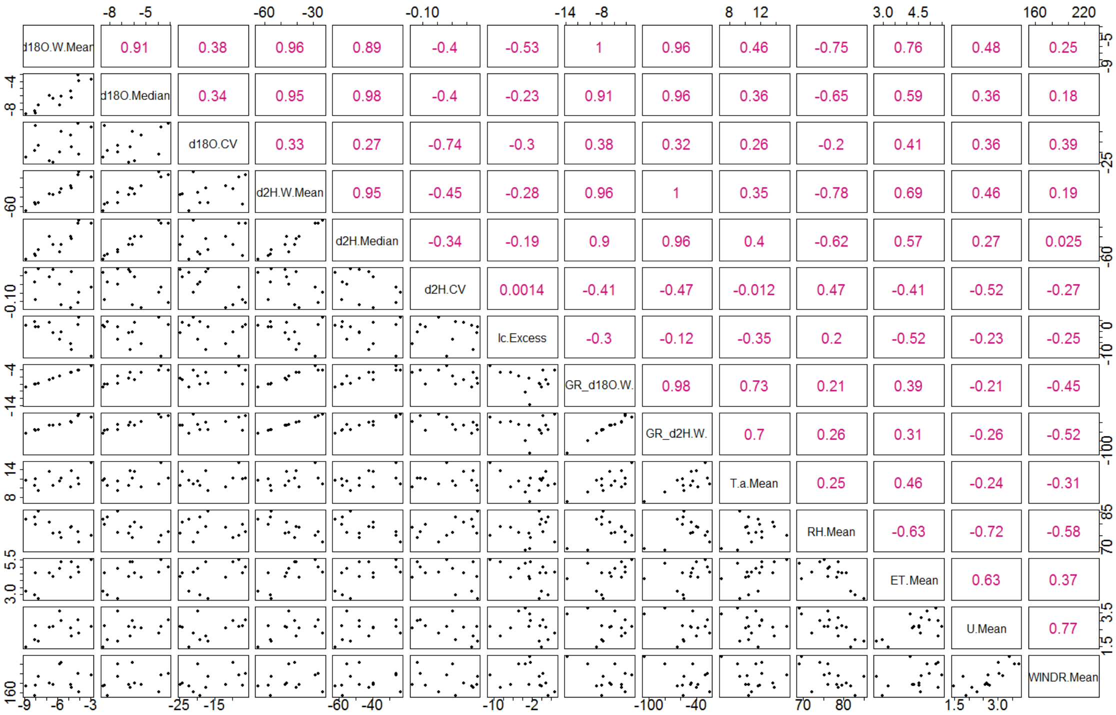

Figure Appendix C-5: Pearson correlation and Scatterplot for TF isotopic compositions (d18O.W.Mean, d18O.W.Median and d18O.W.CV) values for the south facing heather and isotopic signatures for the GR (GR_d18.W, GR2H.W), lc-excess and hydroclimatic variables like T.a.Mean [°C], RH.Mean [%], ET.Mean [mm], U.Mean [ms^{-1}] and WINDR.Mean [°]. The green numbers represent the correlation coefficient r.

APPENDIX D

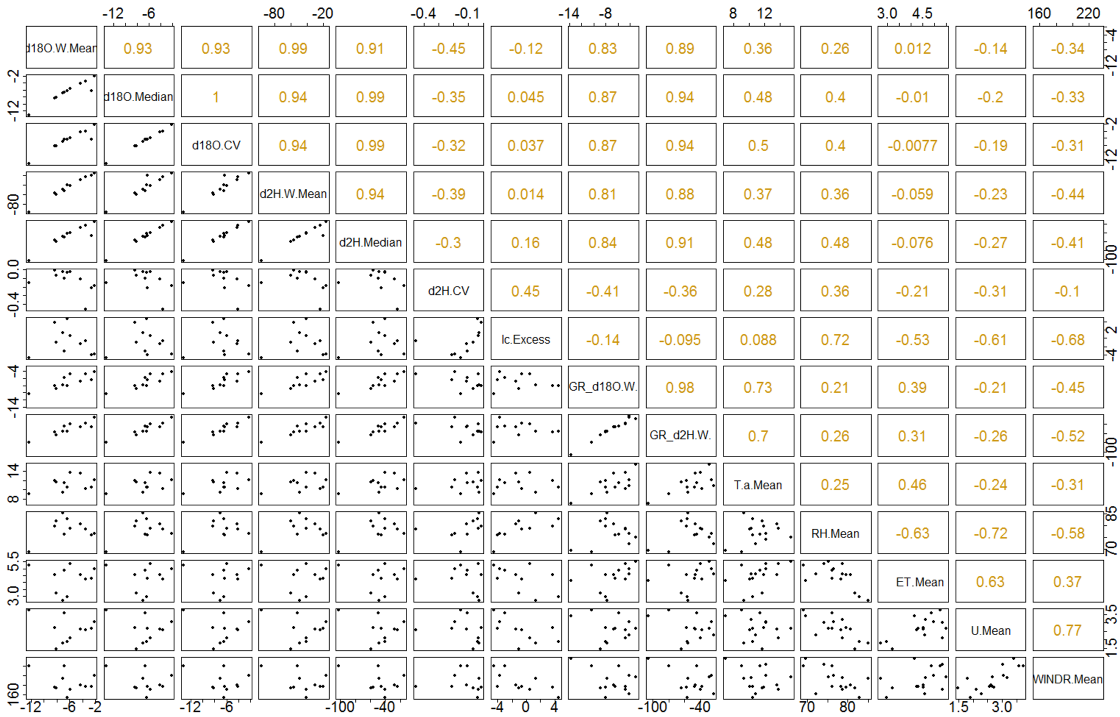

Figure Appendix D-1: Pearson correlation and Scatterplot for TF isotopic compositions (d18O.W.Mean, d18O.W.Median and d18O.W.CV) values for the south facing stemflow and isotopic signatures for the GR (GR_d18.W, GR2H.W), lc-excess and hydroclimatic variables like T.a.Mean [°C], RH.Mean [%], ET.Mean [mm], U.Mean [ms^{-1}] and WINDR.Mean [°]. The green numbers represent the correlation coefficient r.

Table Appendix D-1: Stemflow parameters for the north facing Plantation. Amount of GR ± Std.Dev. [mm], $\delta^{18}O$ ± Std.Dev. [‰], δ2H ± Std.Dev. [‰] and lc-Excess [‰], weighted and averaged per sampling date for the field season.

Stemflow (SF) North Facing Plantation

Date	*GR_{sum}[mm]*	*$\delta^{18}O$ ± Std.Dev. [‰]*	*$\delta^{2}H$ ± Std.Dev. [‰]*	*lc-Excess [‰]*
01/06/2015	7.6	-7.05 ± 0	-62.42 ± 0	-12.42
09/06/2015	12.2	-13.74 ± 2	-106.69 ± 2	-4.04
17/06/2015	3.6	-	-	-
25/06/2015	10.4	-4.64 ± 0.6	-32.15 ± 1.3	-1.06
02/07/2015	10.4	-3.41 ± 1.8	-32.02 ± 0	-10.59
06/07/2015	20.8	-6.49 ± 0.6	-39.3 ± 0.5	6.32
20/07/2015	74.8	-8.19 ± 1.5	-56.42 ± 0.1	2.57
30/07/2015	23.6	-7.89 ± 0.4	-54.6 ± 0.3	2.05
06/08/2015	12.8	-1.98 ± 0.5	-14.14 ± 0.5	-3.98
13/08/2015	2.2	-	-	-
19/08/2015	36.2	-8.39 ± 0.7	-60.78 ± 0.5	-0.24
28/08/2015	18.8	-4.39 ± 0.7	-32.72 ± 0.5	-3.64
03/09/2015	8.8	-6.88 ± 0.2	-52.64 ± 0.7	-3.93
10/09/2015	0.8	-	-	-
18/09/2015	16.8	-6.59 ± 0.2	-44.04 ± 0.2	2.4
24/09/2015	16	-7.01 ± 0.1	-50.32 ± 0.2	-0.61

Table Appendix D-2: Stemflow parameters for the south facing Plantation. Amount of GR ± Std.Dev. [mm], $\delta^{18}O$ ± Std.Dev. [‰], $\delta^{2}H$ ± Std.Dev. [‰] and lc-Excess [‰], weighted and averaged per sampling date for the field season.

Stemflow (SF) South Facing Plantation

Date	*GR_{sum}[mm]*	*$\delta^{18}O$ ± Std.Dev. [‰]*	*$\delta^{2}H$ ± Std.Dev. [‰]*	*Lc-Excess [‰]*
01/06/2015	7.6	-	-	-
09/06/2015	12.2	-12.36 ± 11.6	-102.5 ± 14.7	-10.73
17/06/2015	3.6	-	-	-
25/06/2015	10.4	-3.53 ± 4	-27.93 ± 10.4	-5.58
02/07/2015	10.4	0 ± 11.7	0 ± 0	-5.41
06/07/2015	20.8	-5.95 ± 1.6	-40.27 ± 1.3	1.09
20/07/2015	74.8	-8.33 ± 7.7	-56.47 ± 0.8	3.64
30/07/2015	23.6	-2.67 ± 1.9	-45.51 ± 4.2	-29.96
06/08/2015	12.8	-2.21 ± 0.9	-16.39 ± 3	-4.4
13/08/2015	2.2	-	-	-
19/08/2015	36.2	-8.1 ± 4.6	-59.82 ± 3.9	-1.52
28/08/2015	18.8	-4.29 ± 4.1	-28.78 ± 3.3	-0.43
03/09/2015	8.8	-6.85 ± 1.3	-47.95 ± 5.5	0.49
10/09/2015	0.8	-	-	-
18/09/2015	16.8	-6.4 ± 3	-40.82 ± 1.5	4.13
24/09/2015	16	-7.05 ± 0.9	-48.83 ± 1.3	1.18